ASSESSING THE DOSE RECEIVED BY THE VICTIMS OF A RADIOLOGICAL DISPERSAL DEVICE WITH GEIGER-MUELLER DETECTORS

A Thesis
Presented to
The Academic Faculty

By

Ryan Paul Manger

In Partial Fulfillment
Of the Requirements for the Degree
Master of Science in the
School of Nuclear and Radiological Engineering

Georgia Institute of Technology

August 2008

ASSESSING THE DOSE RECEIVED BY THE VICTIMS OF A RADIOLOGICAL DISPERSAL DEVICE WITH GEIGER-MUELLER DETECTORS

Approved by:

Dr. Nolan E. Hertel, Advisor
School of Nuclear and Radiological Engineering
Georgia Institute of Technology

Dr. Chris Wang
School of Nuclear and Radiological Engineering
Georgia Institute of Technology

Dr. Armin Ansari
Radiation Studies Branch
Centers for Disease Control and Prevention

Date Approved: June 13, 2008

ACKNOWLEDGEMENTS

First I want to thank God for guiding me throughout my entire life. Without God I would not even have the privilege of being in this great place and surrounded by such great people. I would like to extend a heartfelt thank you to my fiancé, Caitlin, my parents, Ruben and Cindy, and my sister, Erica. Each one of you has helped me in a special way. You are the core of my support system, without which, I would have been unable to accomplish half of what I have been able to accomplish.

I would like to extend a deep gratitude to Dr. Nolan Hertel for giving me the opportunity to work for him as a researcher; I have learned more than I could have imagined in the past two years. I would like to thank the members of my thesis committee: Dr. Chris Wang and Dr. Armin Ansari. I have learned many things in the classes that Dr. Wang has taught and I have received some great insight from Dr. Ansari on this work. I would like to thank all members of Team Hertel who have helped me in some way, without your assistance in matters concerning research and matters outside of research, I would have had a much more difficult time accomplishing this thesis. I would like to thank Clint Alday for understanding my decision to go to graduate school and supporting me in my decision. I would also like to thank Craig Robinson for always being there for me. Once again thanks to my family, you are always by my side encouraging me and supporting me in all that I do.

TABLE OF CONTENTS

LIST OF TABLES

LIST OF FIGURES

SUMMARY

This research investigates the use of Geiger-Mueller detectors to triage the individuals who have been exposed to a Radiological Dispersal Device (RDD). Upon exposure to an RDD, inhalation of the airborne radionuclide is a method by which someone can receive dose. Bioassay via analysis of excreta is a commonly used method of determining the amount of uptake, yet it would be cumbersome and time consuming if there are a large number of people needing to be screened.

An *in vivo* method must be considered so that a non-intrusive and more efficient triaging method can be implemented. Whole body counters are commonly used in counting facilities as an *in vivo* bioassay method, yet they are limited in number and not easily portable. Therefore, a more portable and more common detection device should be considered. Geiger-Mueller (GM) survey meters are common devices that are highly portable and widely available, making them ideal candidates to fulfill this necessity. The ease of use contributes to the viability of the device as a portable, *in vivo* screening device.

To analyze this detector, a Monte Carlo model of the detector was created to be used in simulations with the Medical Internal Radiation Dose (MIRD) phantoms [8]. Once the model was validated against experimental data using a PMMA slab phantom, the detector was placed in a few locations on the anthropomorphic phantoms. Four locations were strategically chosen for detector placement: the posterior upper right torso, the anterior upper right torso, the lateral upper thigh, and the anterior of the neck. Six phantoms were considered: Reference Male, Female, Adipose Male, Adipose Female, Post Menopausal Adipose Female, and a Child.

Six radionuclides were investigated: Am-241, Co-60, Cs-137, I-131, Ir-192, and Sr-90. The nuclides were distributed throughout the phantoms according to Dose and Risk Calculation Software (DCAL), a code that determines how a radionuclide is distributed over time upon inhalation, ingestion, or injection [10]. Monte Carlo simulations were performed to determine the count rate per Bq of each detector location, radionuclide type, and phantom type over a time period of 30 days. A decision level was determined as a threshold, above which further medical attention would be required. This decision level was named a Clinical Decision Level (CDL) [2] and was equivalent to 0.25 Sv of dose.

A set of count rates per CDL were determined for each detector location on each phantom for up to 30 days after inhalation. The optimal detector location was chosen and the data were used to compile a set of procedure sheets to be used when triaging the victims of an RDD. The procedure sheets are detailed to minimize the operational error of the first responders. Each procedure sheet included information on how to properly use the detector, how to determine background, how to apply the decision levels, and how to determine if someone is in need of additional screening. The procedure sheets for each body type were condensed into one procedure sheet that contained a set of decision levels for adults and children. This condensed procedure sheet can be used by a first responder to determine if an individual needs further medical attention.

CHAPTER 1: INTRODUCTION

In the 21st century, the threat of a terrorist attack is rising and becoming increasingly imminent. The method of attack cannot be predicted; therefore preparation for the most probable modes of attack is necessary.

One possible mode of attack is a radiological dispersal device (RDD). An RDD is any device used for the deliberate dissemination of radioactive material to create terror or harm without nuclear detonation [11]. The most commonly cited type of RDD is a "Dirty Bomb." A dirty bomb uses an explosive to create radioactive dust that will contaminate the surrounding areas and potentially lead to radiation exposure. RDDs may also be dispersed in a passive manner such as releasing an aerosol or gas form an airborne device such as an aircraft [32].

The focus of this research is to determine if a victim of an RDD has received a significant amount of internal contamination. Typically whole body counters and *in vitro* bioassay are the methods used to determine the dose due to internal contamination. The facilities housing these technologies are not designed to promptly handle a large population of individuals, as may be necessary after an RDD. Therefore a method must be developed to provide rapid initial screening and triage of a large influx of individuals [14, 34].

Handheld detectors are a prime choice for their portability, ease of use, and widespread availability in the radiation safety community. A count rate meter rather than a spectrometer is more advantageous because the output is scalar and its operation is relatively intuitive. Based on these facts, a couple of Geiger-Mueller count rate meters were investigated in this study.

The radiation type associated with the radionuclides of an RDD can be beta, alpha, or gamma. In this research, a number of well known common radionuclides were investigated: Am-

241, Ir-192, Co-60, Cs-137, I-131, and Sr-90. Am-241, Co-60, Cs-137, and Ir-192 are considered to be of the highest risk for use in an RDD due to their availability in industrial applications [7]. Food preservation irradiators, industrial radiography, teletherapy, radionuclide thermoelectric generators, well logging, thickness/density gauges, and moisture/density detectors are some examples of industrial applications that may be a source for RDD radionuclides.

After an RDD event, the radionuclides can be in an airborne form that can be deposited in the lungs. In this work, all of the radionuclides were assumed to be deposited internally through inhalation. Only internal contamination was considered; this assumes that the individuals have had any external contamination removed. As with any bioassay problem, the time of intake must be known to accurately determine the dose. The inhalation of the radionuclides and the changing distribution throughout the body over time were modeled with a Monte Carlo simulation using five Medical Internal Radiation Dose (MIRD) based phantoms [8] and one child phantom created with BodyBuilder [37].

Ultimately, a triaging method will be created whereby those who are exposed to an RDD will be screened to determine if they received a medically-significant amount of dose. The system will be conservative, minimizing false-negatives, and it should be easy to implement, minimizing operational error.

CHAPTER 2: BACKGROUND

A large amount of research has been performed to study radiological dispersal devices. In an April 2004 report by GAO (U.S. Government Accountability Office), it was disclosed that there is an unknown number of unwanted greater-than-Class-C sealed sources in the United States, but the Department of Energy would recover an estimated 14,300 greater-than-Class-C sources by 2010 [12]. A source that is greater than Class C is a cause for concern because they may be used by terrorists to make dirty bombs. In another GAO report, it was stated that nearly 10 million sealed sources exist in the U.S. and 49 other countries, and that there is limited information about the thousands of lost, stolen, or abandoned sealed sources [13]. A large number of the most vulnerable sealed sources that would pose a security risk are located in the countries of the former Soviet Union. So the materials for an RDD attack are potentially available to terrorists or other evildoers who may consider an attack against the U.S.

As a result of the RDD threat, research has been performed in the area of portable *in vivo* counting methods to determine the committed effective dose received by an individual. A well known instance of mass triaging of individuals following a radiological accident is the Cs-137 Goiania, Brazil incident. Over 300 individuals were assayed with a Whole Body Counter (WBC) constructed of a 20-cm diameter NaI(Tl) detector installed 2.05 m above the person being contaminated[31]. The distance between the detector and the subject was large because of the great amount of activity contaminating the actual victims of the radiological accident. Studies have been conducted by Kramer et al. on using a field deployable, high resolution HPGe WBC to successfully determine the activity in the lungs at a given time [22]. The use of portal monitors for emergency response has also been investigated by Kramer [21]. These

technologies, although effective, are not commonly available in every city. The G-M detector being considered in this work are more likely to be available.

The use of the NaI detectors in a thyroid uptake counter to triage RDD victims was determined to be feasible by Lorio at Georgia Tech [26]. This type of instrument was further analyzed by Scarboro [33], and a set of decision levels to be used when triaging the victims of an RDD were developed for the inhaled nuclides being considered in this research. The fact that a detector may be used to assess the dose received by an individual after inhaling the radiation emitted by RDDs is well documented in Scarboro's research. A similar analysis that utilized the same detector as Scarboro in addition to other meters including a Ludlum Survey Meter, was performed by Anigstein et al. [1]. As opposed to the G-M meters being considered in this research, the meter considered by Anigstein et al. had an output in μR/hr. The research performed by Anigstein used Monte Carlo simulation with the NORMAN phantoms as opposed to the MIRD phantoms being used in this research.

A common problem encountered while performing lung counts is the amount of uncertainty due to varying chest wall thickness and varying lung volumes [19]. Kramer et al. have studied the amount of uncertainty in activity estimates that is introduced by varying chest wall profiles in working males. An underestimate or overestimate of a factor of 1.07 is introduced by the varying chest wall thicknesses in working males [24]. Biases in activity estimates from -21% to 63% were discovered by Kramer et al. in their analyses of how lung volumes vary from the volume found in the reference male [20]. These uncertainties must be considered in the analyses of the handheld G-M detectors by introducing a level of conservatism allowing for more false-positives and less false-negatives when screening individuals.

CHAPTER 3: METHODOLOGY

Two G-M counters were evaluated in this work to determine if they can be used for the triaging potential RDD victims. Modeling the inhalation and time-dependent distribution of radionuclides in the human body cannot be performed in a laboratory and therefore required modeling. Models of the G-M counters were created for use in Monte Carlo simulations. The detector models were validated by comparing experimental data from a polymethyl methacryclate (PMMA) slab phantom experiment to the Monte Carlo simulation of the experiment. Upon verification of the Monte Carlo detector model, MIRD phantoms were modeled with sources distributed in its organs for each radionuclide being considered. After simulation, the data were analyzed to create a set of guidelines in the form of threshold values above which a candidate would be considered to have received a medically significant amount of dose.

3.1 G-M Pancake Probe with Ludlum 2 and 3 Scalers

The G-M Probes and scalers being considered are the HP-260 Pancake Probe with the Ludlum 2 Scaler and the Model 44-9 Pancake Probe with the Ludlum 2 Scaler [27]. These detectors were chosen because they are commonly found in radiation safety departments and other emergency facilities across the United States. The HP-260 and the Model 44-9 pancake probes are essentially the same so they are assumed to be identical in this research. A visual representation of these probes is presented in Figure 3.1.1.

Figure 3.1.1 Ludlum Model 44-9 Pancake Probe

Each pancake probe contains a model 7311 G-M tube from LND [25] consisting of a mica window and filled with a neon gas and a halogen gas. The fill gas and fill pressures are proprietary information of LND, and estimates of the composition and gas density were selected.

The outputs of both scalers are in units of counts per minute. Two modes of data collection are available: Slow and Fast. All data were taken in slow mode, which is a 3-second rolling average of the instantaneous count rate. The Ludlum 3 scaler has an upgradeable option to allow reading of the number of counts over a period of time. But this mode of data collection was ignored in this analysis because it may not be available in detectors used for triaging. Data collection with these two scalers is intuitive, making it a prime candidate for an emergency situation. A picture of a Ludlum 3 scaler is displayed in Figure 3.1.2.

Figure 3.1.2 Ludlum Model 3 Survey Meter

3.2 PMMA Slab Phantom Measurements

A PMMA slab phantom was constructed with which to perform benchmark experiments with point sources to validate the computational model of the detector. A picture of the PMMA (lucite) slab phantom experimental set-up is shown in Figure 3.2.1. The phantom consisted of varying thicknesses of PMMA, a backscattering medium of Virtual Water™, and a source holder to fix the location of the radionuclide being analyzed. PMMA was chosen since its attenuation properties are comparable to human tissue. The backscatter medium was constructed of 100mm of Virtual Water to simulate the backscattering of gamma rays that would occur while taking measurements on a human. The source holder was constructed out of a 6 mm sheet of PMMA, with a section that was carved out to hold the sources being used.

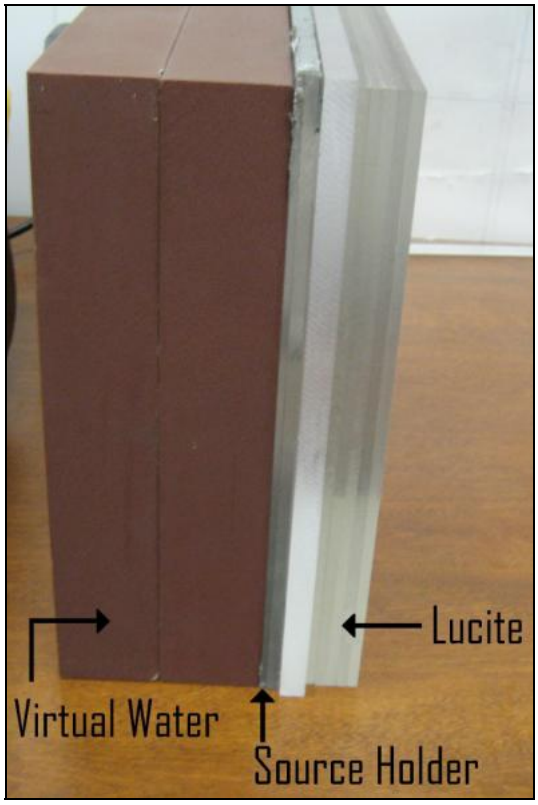

Figure 3.2.1 PMMA Slab Phantom Set-up

A source was placed in the source holder and measurements were taken from thicknesses of bare to 144mm in 6mm and 12mm increments. The sources used the slab measurements were Am-241, Ba-133, Co-60, Cs-137, Mn-54, and Na-22. These radionuclides were chosen because of their availability and range of energies that they cover. The energies and intensities of these sources are shown in Table 3.2.1 for all gammas greater than 1% emission.

Table 3.2.1 Slab Phantom Source Gamma Energy-Intensity Data

Nuclide	Energy (keV)	Intensity
Am-241	59.5, 13.9, 17.8, 16.8, 20.8, 13.8, 26.3, 17.1, 18	0.357, 0.219, 0.188, 0.0582, 0.0457, 0.0245, 0.024, 0.0222, 0.0196
Co-60	1173, 1332	0.9985, 0.9998
Cs-137	662, 33.2, 31.8	0.898, 0.039, 0.021
Ba-133	30.9, 356, 30.6, 81.0, 302, 34.987, 383.8, 276.4, 34.9	0.63072, 0.6215, 0.3412, 0.337, 0.184, 0.1217, 0.0891, 0.0708, 0.0627
Mn-54	0.835	1
Na-22	511, 1270	1.80, .999

The detector was placed on the front surface of the PMMA at the same location for each measurement. An additional $1/R^2$ attenuation factor was introduced as a result of placing the detector on the surface of the PMMA, varying the distance between the detector and the source [35]. Measurements were taken at PMMA thicknesses of 0 mm, 6 mm, 12 mm, and 12 mm increments up to 144 mm. The data were collected in the slow mode. The count rate would be recorded when the needle on the counter settled on a value. Count rates were taken three times

to ensure that no erroneous data have been registered. A sample plot of the attenuation of Co-60 is displayed in Figure 3.2.2.

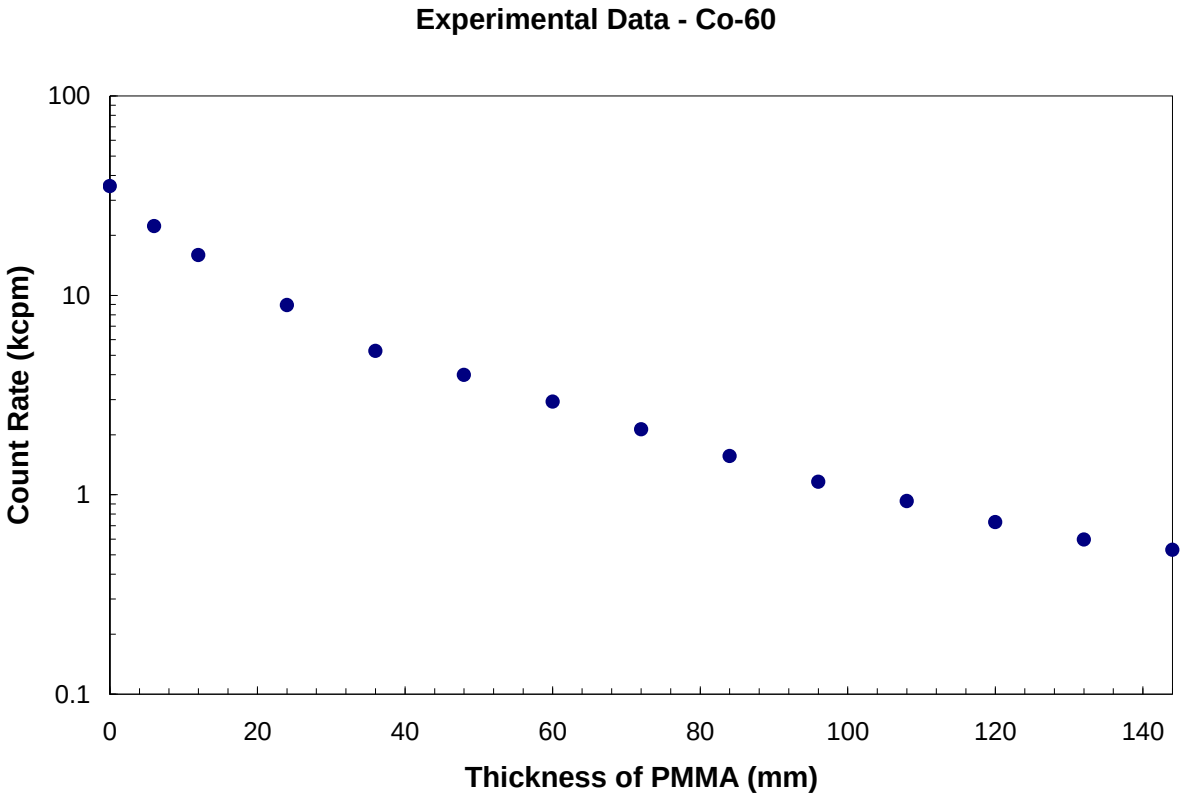

Figure 3.2.2 Experimental Slab Phantom Data for Co-60

3.3 MCNP Model Validation

The code used for the Monte Carlo simulation was MCNP version 5 [39]. The MCNP model of the detector would be used with a corresponding MCNP phantom simulation the inhalation of a radionuclide. Validation of the detector Monte Carlo model is important to assure that the anthropomorphic data, which can only be determined by simulation, are acceptable. Comparison between the PMMA slab experiment and an MCNP modeled version of the same experiment were used to validate the modeled detector and arrive at a scaling factor.

3.4 MIRD Phantoms and Biokinetics

In total, six anthropomorphic phantoms were used for simulation: Male, Female, Adipose Male, Adipose Female, Post-Menopausal Adipose Female, and a 10-year-old Child. The reference male and reference female were Medical Internal Radiation Dose (MIRD) [8] phantoms and the 10-year-old Child was a BodyBuilder [36] phantom. The distribution of a given radionuclide over time was determined using Dose and Risk Calculation Software (DCAL) [10], a code developed by Eckerman et al. at Oak Ridge National Laboratory (ORNL). The retention factors for a given radionuclide with a given inhalation class were determined using DCAL, which implements the ICRP 66 respiratory tract kinetics [15].

When screening the individuals, the goal is to find detector placement location that will produce the most counts per unit activity inhaled. Four strategic detector locations were evaluated to determine where the optimal count rate occurred for a given phantom-radionuclide-time post-inhalation combination. The four locations used were the anterior right upper torso, the posterior right upper torso, the anterior of the neck, and the lateral location of the left thigh. The anterior right upper torso position was not considered for the female, adipose male, adipose female and post menopausal adipose female because of the breast tissue that would cause greater attenuation. A visual representation of these detector placement locations is displayed in Figure 3.4.1.

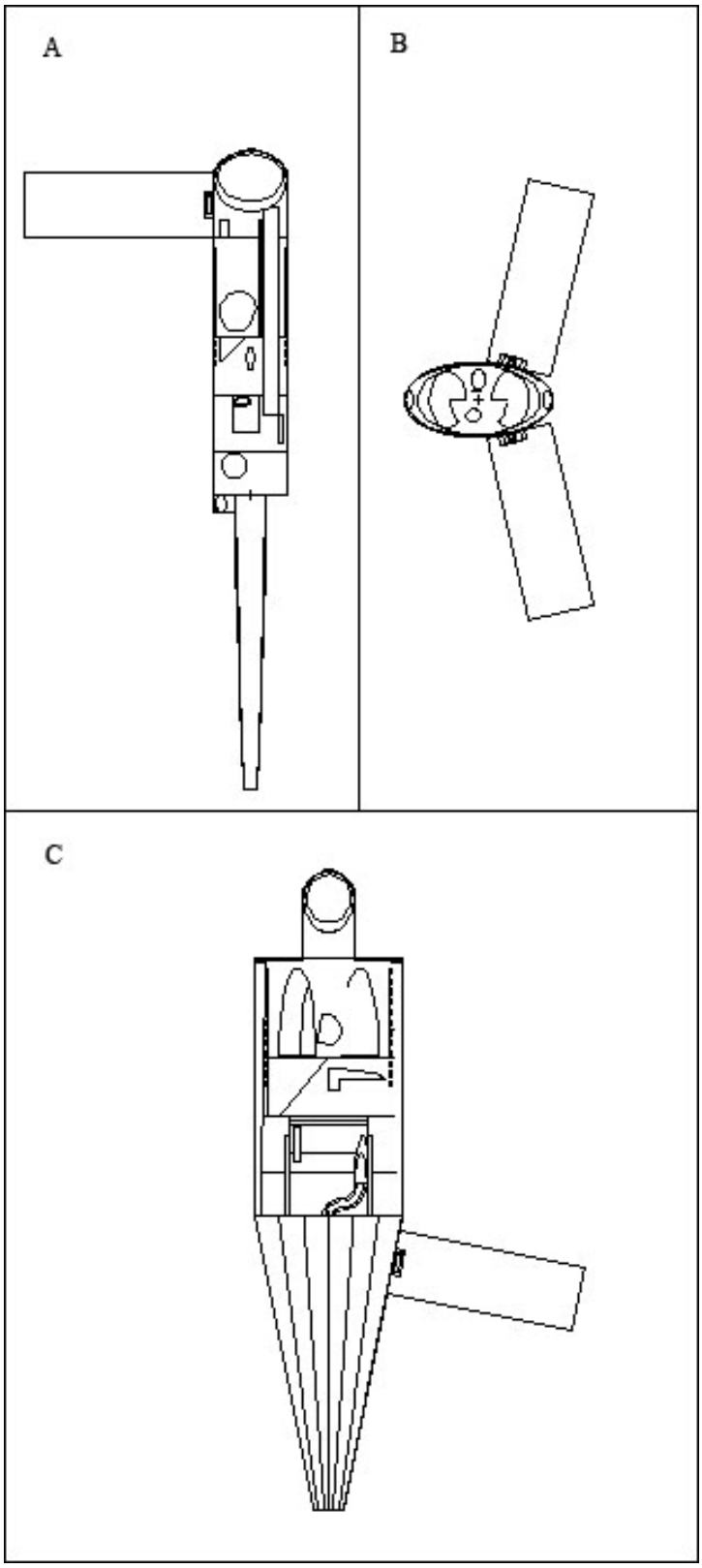

Figure 3.4.1 Detector Placement Locations: A is the anterior neck position, B is the anterior and posterior upper right torso positions, and C is the lateral left thigh position.

The upper torso locations were chosen because inhalation initially deposits a large amount of radioactivity in the lungs, and more radiation will be detected if the detector is placed over the lungs. The right lung location was chosen because according to previous research, the right lung yields a higher count rate than the left lung [26]. The neck location was chosen to read thyroid counts from a thyroid seeker such as I-131.

3.5 Clinical Decision Levels and Triaging Protocol

After the all the MIRD phantoms were simulated with the four detector locations, a count rate per unit activity inhaled was developed. These data were used to develop a set of decision levels which were used to determine if someone needs further medical attention. The decision level to be used in an emergency situation is a committed effective dose of 0.25 Sv. This quantity is termed a Clinical Decision Level (CDL) [2]. The detector locations yielding the highest count rate per CDL for a given radionuclide-phantom pairing were chosen to be used during the screening for that radionuclide-phantom pairing. A procedure sheet showing the first responders how to operate the detector and a set of count rate decision levels were assembled from these data. This type of procedure sheet was made for each phantom-nuclide pairing, giving the first responder a count rate decision level for multiple time periods following the radiological event.

CHAPTER 4: COMPUTATIONAL MODELS

The crux of this research relies on computational modeling. MCNP models of the detector, the PMMA slab phantoms, and the MIRD phantoms were created to simulate the in vivo counting after an RDD.

4.1 G-M Probe Model

The G-M probes that are being considered in this project were assumed to be identical due to their similarity. One MCNP model was created and compared to two sets of PMMA slab experimental data. Ludlum and LND specifications were used to model the geometry and materials of the detector models. The composition and fill pressure is proprietary to LND, Inc.; therefore, neon was the only gas used. The density of the gas was chosen in accordance to a typical G-M fill pressure according to Knoll [18]. Material compositions were obtained from the National Institute of Standards and Technology (NIST) [29]. A two-dimensional VisEd [37] rendering of the detector is presented in Figure 4.1.1.

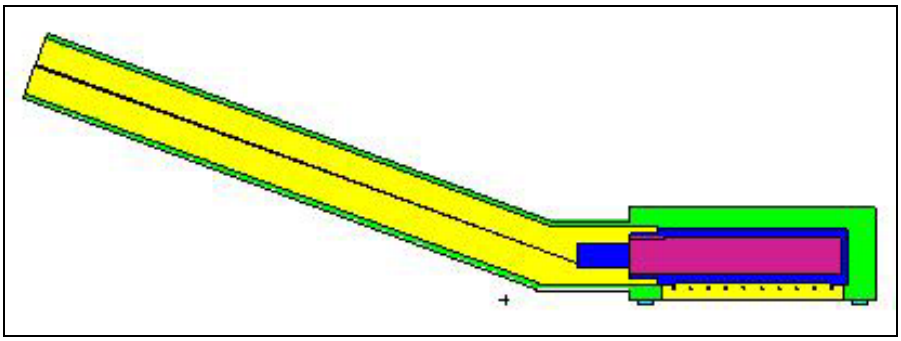

Figure 4.1.1 VisEd rendering of Model 44-9 Pancake Probe

The detector was modeled with attention to detail to ensure proper modeling and transport. The detailed input file for this detector is presented in Appendix A. A three-dimensional visualization of the model is shown in Figure 4.1.2 to display the detail of the modeling.

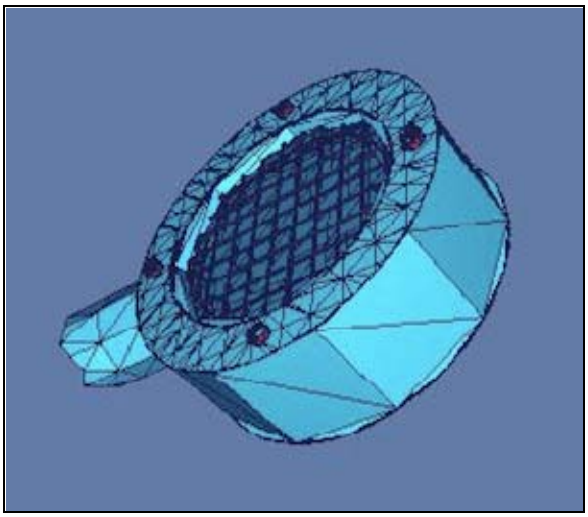

Figure 4.1.2 Three-dimensional VisEd rendering of pancake probe head

4.2 Slab Phantom Model

The slab attenuation measurements were simulated to compare against the experimental data as a validation mechanism. The geometries of the slab phantom model were the same as the experimental model and the material properties were obtained from NIST [29]. The cylindrically shaped sources that were used in the experiment were modeled with the same dimensions and of the same material, polyester.

Table 4.2.1 Composition of Slab Model

Component	Material	Composition (w/o)	Density
Backscatter Medium	Virtual Water	8.02% H 67.03% C 2.14% N 19.91% O 0.14% Cl 2.31% Ca	1.03 g/cm^3
Attenuation Material	PMMA	55.6% C 29.6% O 14.8% H	1.19 g/cm^3
Source Medium	Polyester	85.6% C 14.4%H	0.94 g/cm^3

Photons and secondary electrons were transported in the simulation, and a pulse height tally (F8 in MCNP) was performed over the fill gas volume [28]. The tally output was multiplied by the source activity and the number of particles emitted per decay to determine the count rate. This count rate was compared to the experimental count rate for all PMMA thicknesses to ensure that their ratios are constant over all thicknesses, showing no thickness dependence. The tally cutoff energy, 10keV, was adjusted to simulate the unknown detection threshold. A VisEd representation of the slab model with the detector is presented in Figure 4.2.1. The dots signify collisions of the particles.

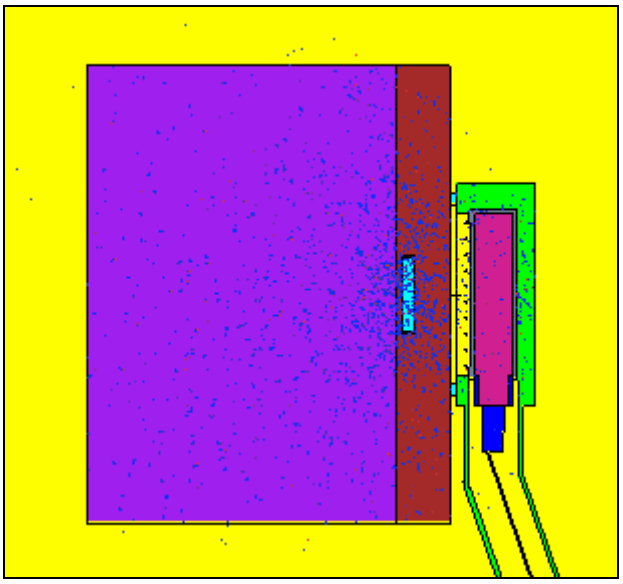

Figure 4.2.1 Vised representation of the slab phantom model

4.3 MIRD Phantom Models and Biokinetic Modeling

The following phantoms were used: for the anthropomorphic phantom simulation: Reference Male, Reference Female, Adipose Male, Adipose Female, Post-Menopausal Adipose Female, and a 10-year-old androgynous child. An MCNP input file for the reference male phantom with Co-60 is presented in Appendix B. The height, weight, and BMI of each phantom are listed in Table 4.3.1.

Table 4.3.1 MCNP phantom data

	Height (cm)	Weight (kg)	BMI (kg/m^2)
Reference Male	179	73.1	23
Reference Female	168	56.5	20
Adipose Male	179	93.7	30
Adipose Female	168	73.9	26
Post-Menopausal Adipose Female	168	85.9	30
10-year Child	140	32.7	17

The sources were distributed according to DCAL; therefore sources were only generated in organs to which the radionuclides would migrate. The organs, or compartments, that contained sources are displayed in Table 4.3.2 for each nuclide.

Table 4.3.2 Compartments of Interest for each Nuclide being modeled

Nuclide	Compartments of Interest
Am-241	Lungs, Stomach Contents, Small Intestines Contents, Upper Large Intestines Contents, Lower Large Intestines Contents, Blood, Body Tissue, Cortical Bone, Trabecular Bone, Liver, Kidneys, Testes/Ovaries, Red Marrow, Urinary Bladder Contents
Co-60	Lungs, Stomach Contents, Small Intestines Contents, Upper Large Intestines Contents, Lower Large Intestines Contents, Blood, Body Tissue, Liver, Urinary Bladder Contents
Cs-137	Lungs, Stomach Contents, Small Intestines Contents, Upper Large Intestines Contents, Lower Large Intestines Contents, Blood, Body Tissue, Urinary Bladder Contents
I-131	Lungs, Stomach Contents, Small Intestines Contents, Upper Large Intestines Contents, Lower Large Intestines Contents, Blood, Body Tissue, Thyroid, Urinary Bladder Contents
Ir-192	Lungs, Stomach Contents, Small Intestines Contents, Upper Large Intestines Contents, Lower Large Intestines Contents, Blood, Body Tissue, Liver, Kidneys, Spleen, Urinary Bladder Contents
Sr/Y-90	Lungs, Stomach Contents, Small Intestines Contents, Upper Large Intestines Contents, Lower Large Intestines Contents, Blood, Body Tissue, Cortical Bone, Trabecular Bone, Urinary Bladder Contents

An SCX tally modifier was used to determine the organ of origin for each source particle that scored in the detector. The output of an MCNP models was a collection of count rates per Bq for each possible "source organ"-"detector location" pairing. DCAL was used to determine how much of a given radionuclide was in a given organ at a given time. The ICRP default inhalation classes were used [16] and the particle size activity median aerodynamic diameter (AMAD) was chosen to be 1μm. The inhalations classes are Fast (F), Moderate (M), and Slow (S), and they correspond to how rapidly a radionuclide is absorbed through the lungs. The radionuclides considered were Co-60, Sr/Y-90, I-131, Cs-137, Ir-192, and Am-241. A table of the default inhalation classes is displayed in Table 4.3.3.

Table 4.3.3 Default Inhalation Classes for Nuclides Used

Nuclide	Inhalation Class
Am-241	M
Co-60	M
Cs-137	F
I-131	F
Ir-192	M
Sr-90/Y-90	M

DCAL outputs for the six sources of interested are displayed in Figures 4.3.1 – 4.3.6. Only the significant compartments are displayed. A common trend among the M class nuclides is dominant saturation in the lungs. For the F class nuclides, the lungs are more promptly depleted of radionuclides and other compartments become saturated. In the case of Cs-137, the body tissue becomes the most highly effected compartment, and in the case of I-131, the thyroid is the most highly saturated compartment.

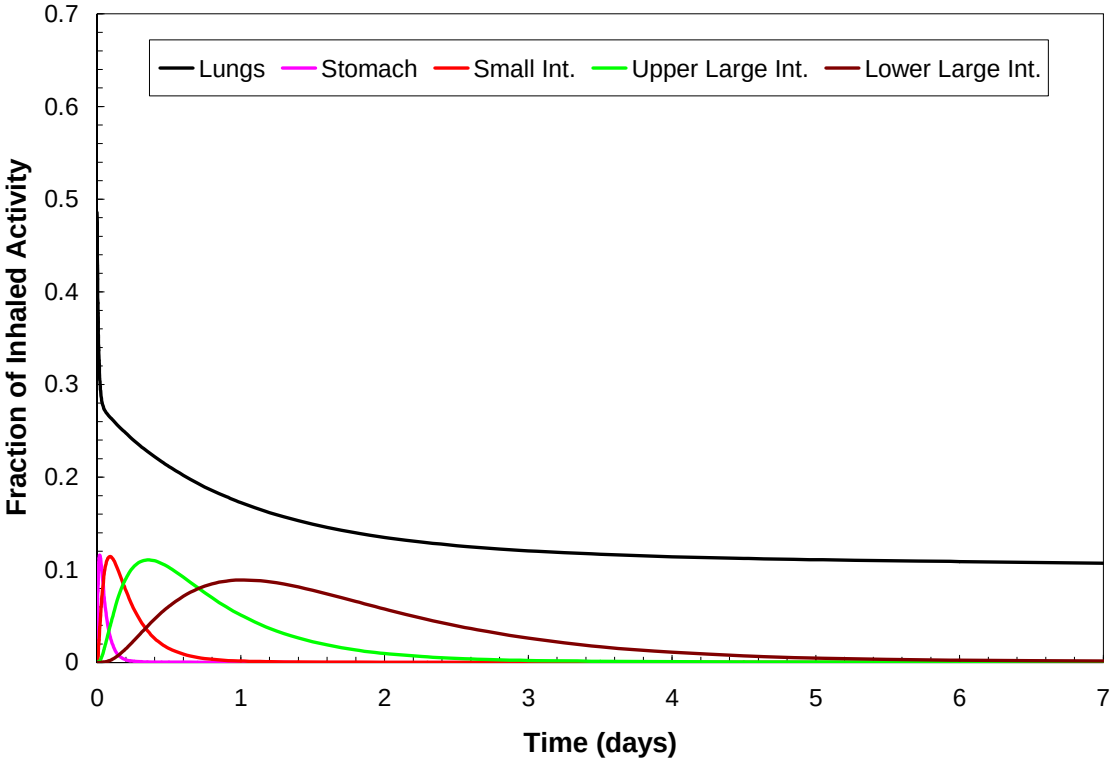

Figure 4.3.1 Am-241 M Distribution Over Time

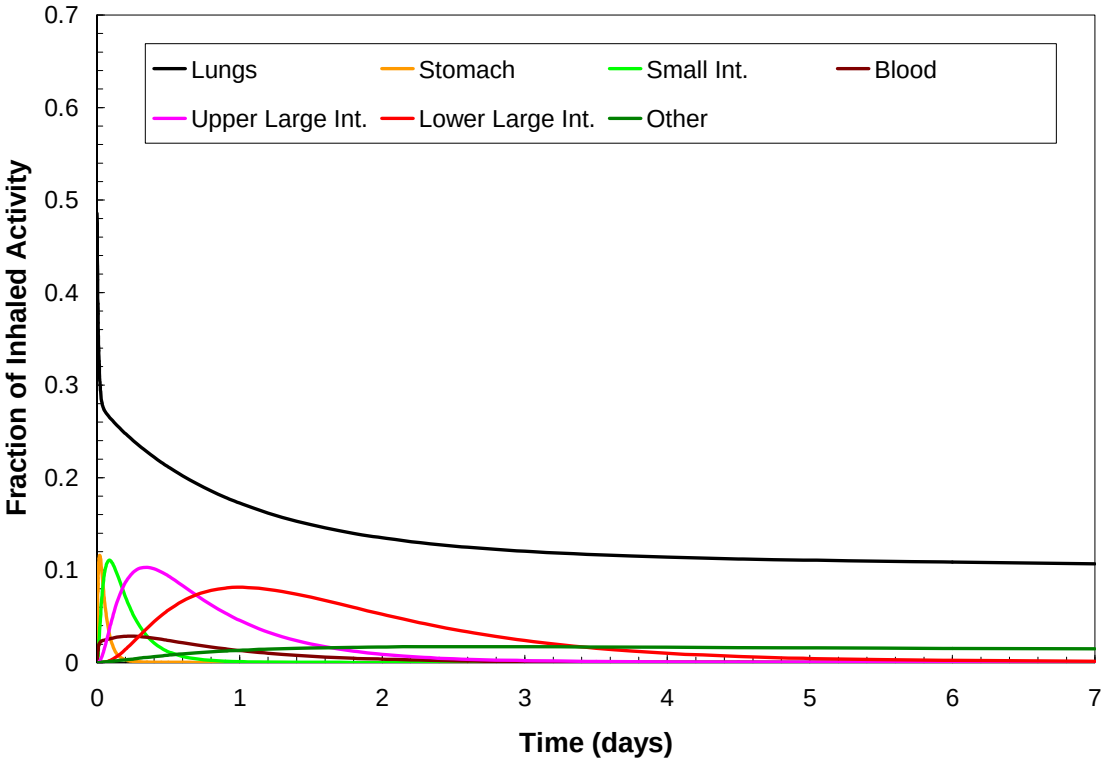

Figure 4.3.2 Co-60 M Distribution Over Time

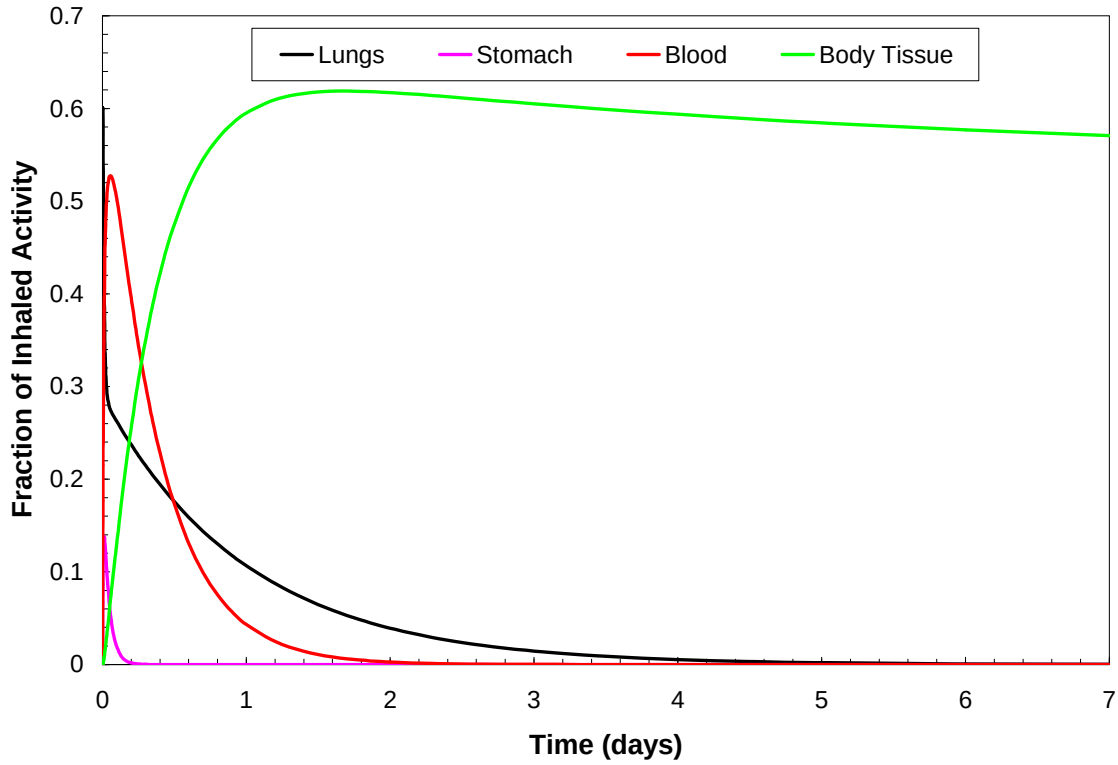

Figure 4.3.3 Cs-137 F Distribution Over Time

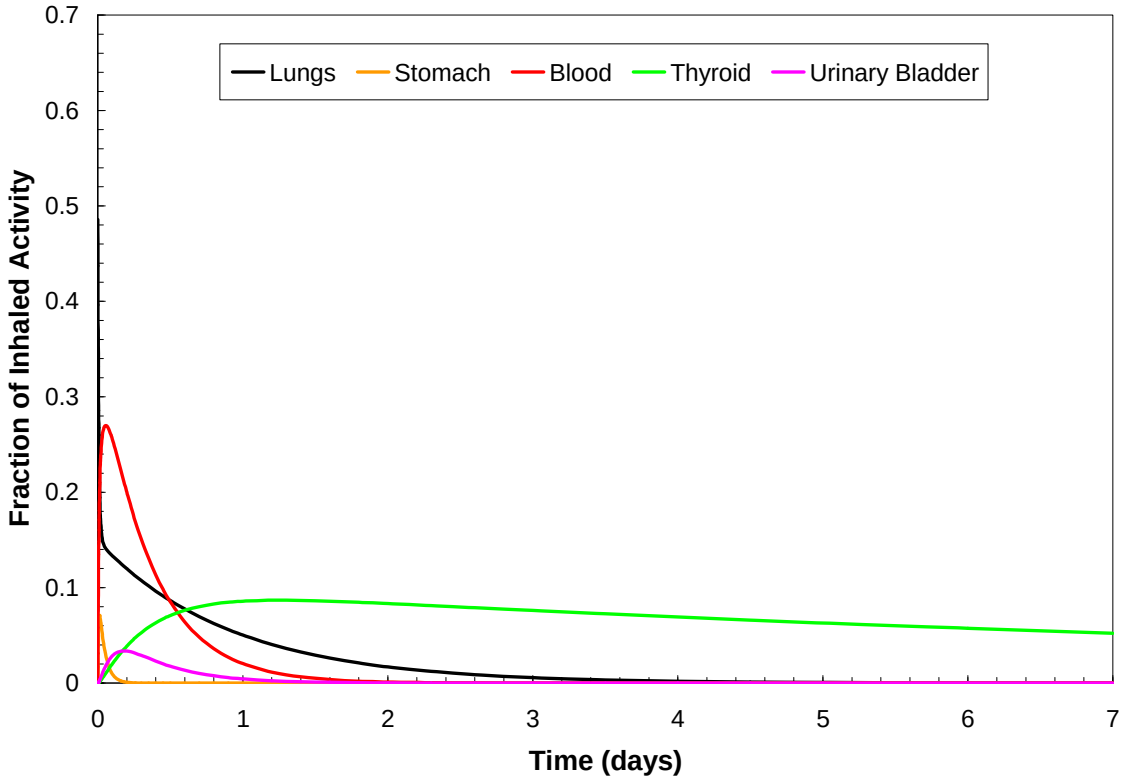

Figure 4.3.4 I-131 F Distribution Over Time

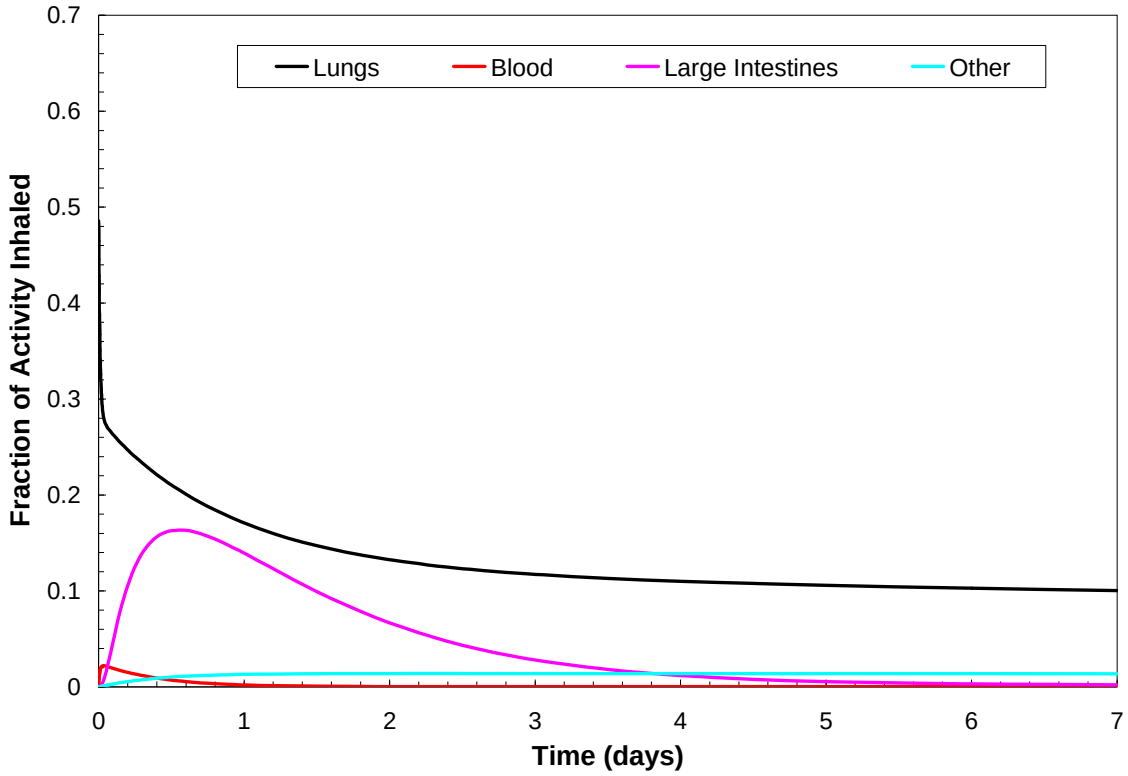

Figure 4.3.5 Ir-192 M Distribution Over Time

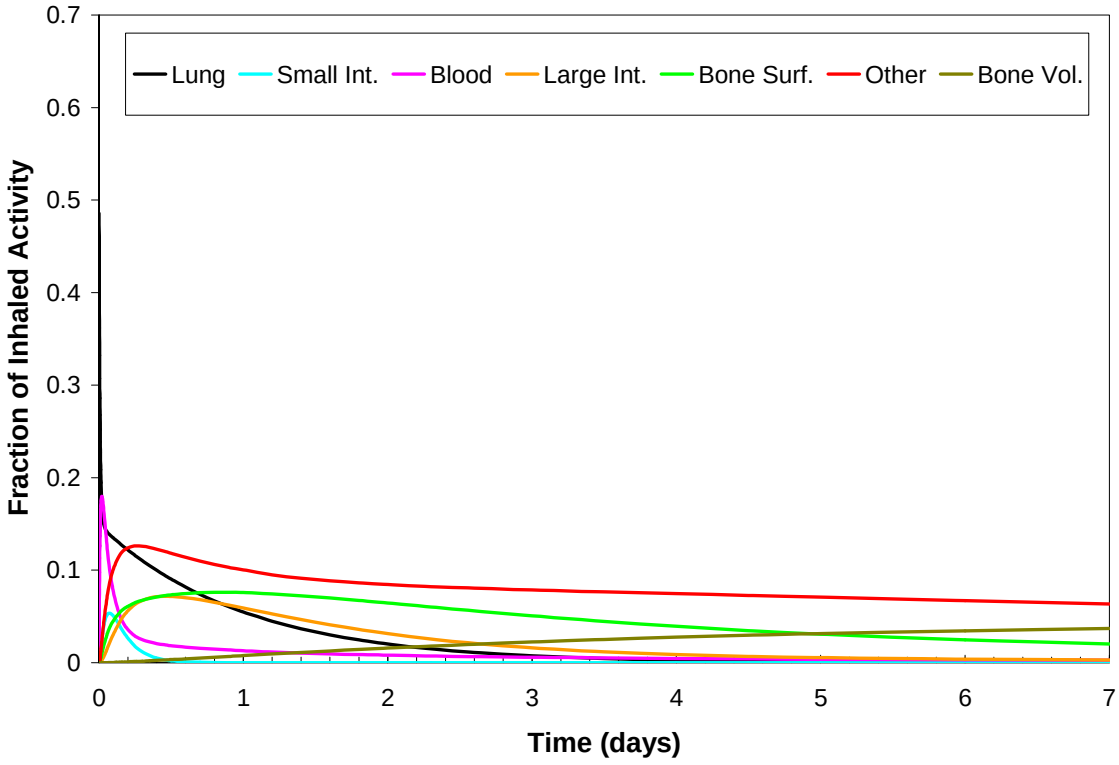

Figure 4.3.6 Sr-90/Y-90 M Over Time

The DCAL data sets were combined with MCNP output to determine the total count rate per Bq over time. Environment Inhalation Dose Coefficients were obtained from Radiological Toolbox [9] which used the ICRP recommendations [16]. The inhalation dose coefficients were in the units of Bq/Sv, which was conveniently used to determine the amount of activity to yield a particular dose. A table of the dose coefficients is presented in Table 4.3.4.

Table 4.3.4 Environmental Inhalation Dose Coefficients

Nuclide	**Adult Inhalation Coefficient** (Bq/CDL)	**Child Inhalation Coefficient** (Bq/CDL)
Co-60 M	2.50E+07	1.67E+07
Cs-137 F	5.43E+07	1.25E+08
I-131 F	3.38E+07	1.32E+07
Ir-192 M	4.81E+07	3.29E+07
Am-241 M	5.95E+03	6.25E+03

The MCNP output was multiplied by the appropriate intake activity (Bq) associated with a CDL (0.25 Sv). The final data were standardized to units of count rate per CDL. These data were calculated for a time period of 30 days after the incident. An individual count rate per CDL would correspond to a particular phantom-nuclide-"detector location" pairing, therefore a total of 144 sets of screening levels existed over a time period of 30 days. To further condense the data, the location that yielded the highest count rate of a given phantom-nuclide pair was chosen as the optimum location for that phantom-nuclide pair. Ultimately, Sr-90/Y-90 did not yield any counts on the MCNP simulation, reducing the number of screening level sets to 120.

CHAPTER 5: RESULTS

The first step in determining the screening guidelines was to create a valid MCNP model. After a valid model is created, the detector was used in conjunction with the MIRD phantoms to determine the count rate for a CDL. Once the count rate per CDL is determined for each radionuclide-phantom combination, the data must be processed in to an easy-to-comprehend form so that the first responds can implement the data in an efficient, accurate manner.

5.1 Model Validation and Scaling Factors

To validate the model, the ratio between the MCNP model of the slab phantom and the experimental data from the slab phantom experiment must be constant over all thicknesses. The ratios should fluctuate about a mean value, with the error bars of each data point overlapping a mean value. The results for each of the nuclides used are displayed as graphs in Figures 5.1.1 through 5.1.6. The figures feature the ratio of MCNP to experiment fluctuating about a line that represents the mean value. Figures 5.1.1 through 5.1.6 are the ratios corresponding to the Ludlum 2 and HP-260 pancake probe.

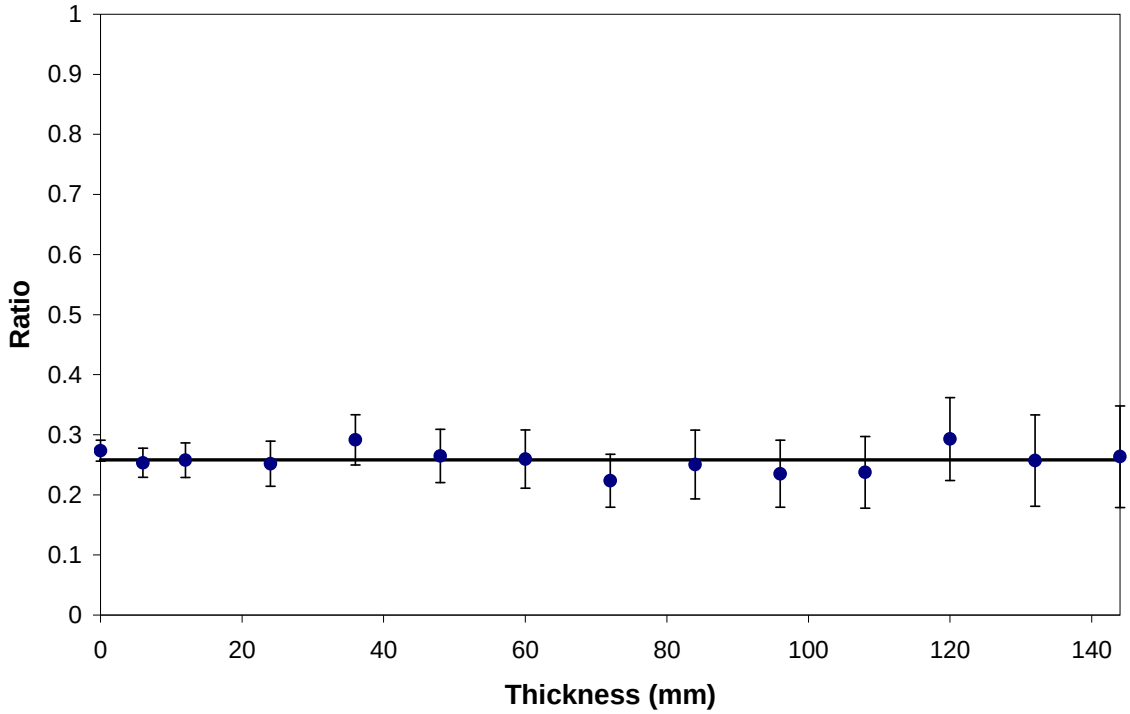

Figure 5.1.1 Am-241 Scaling Factor Chart

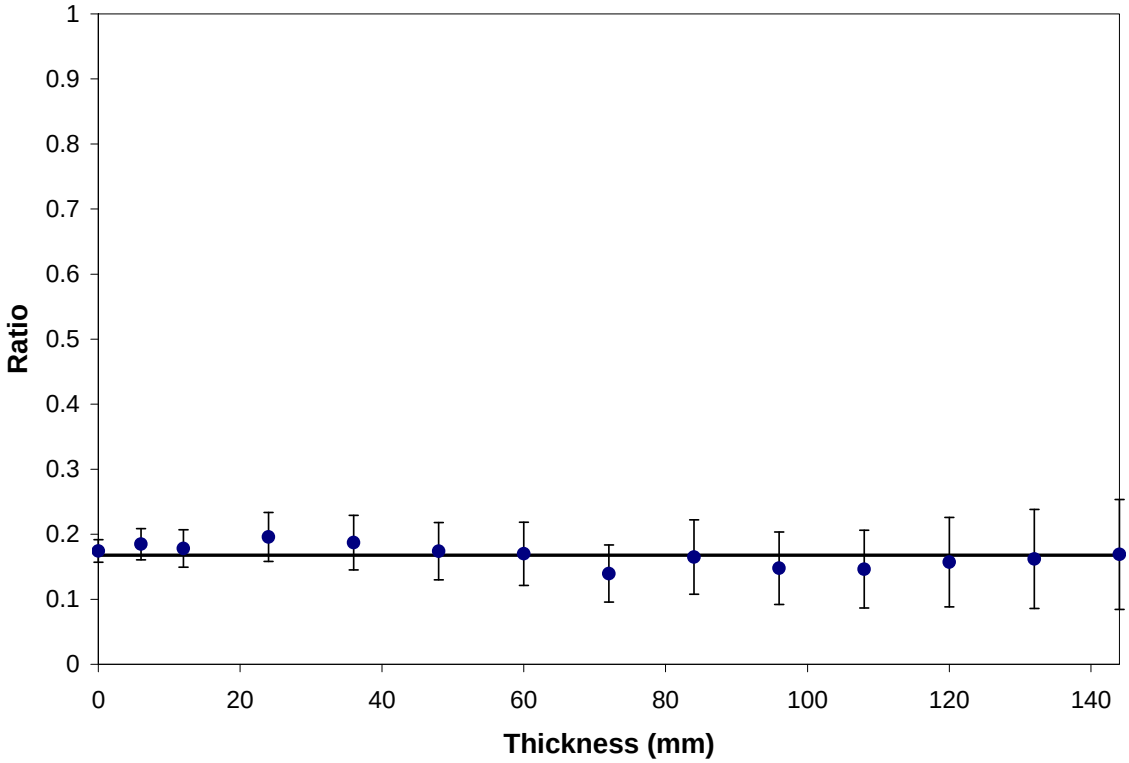

Figure 5.1.2 Co-60 Scaling Factor Chart

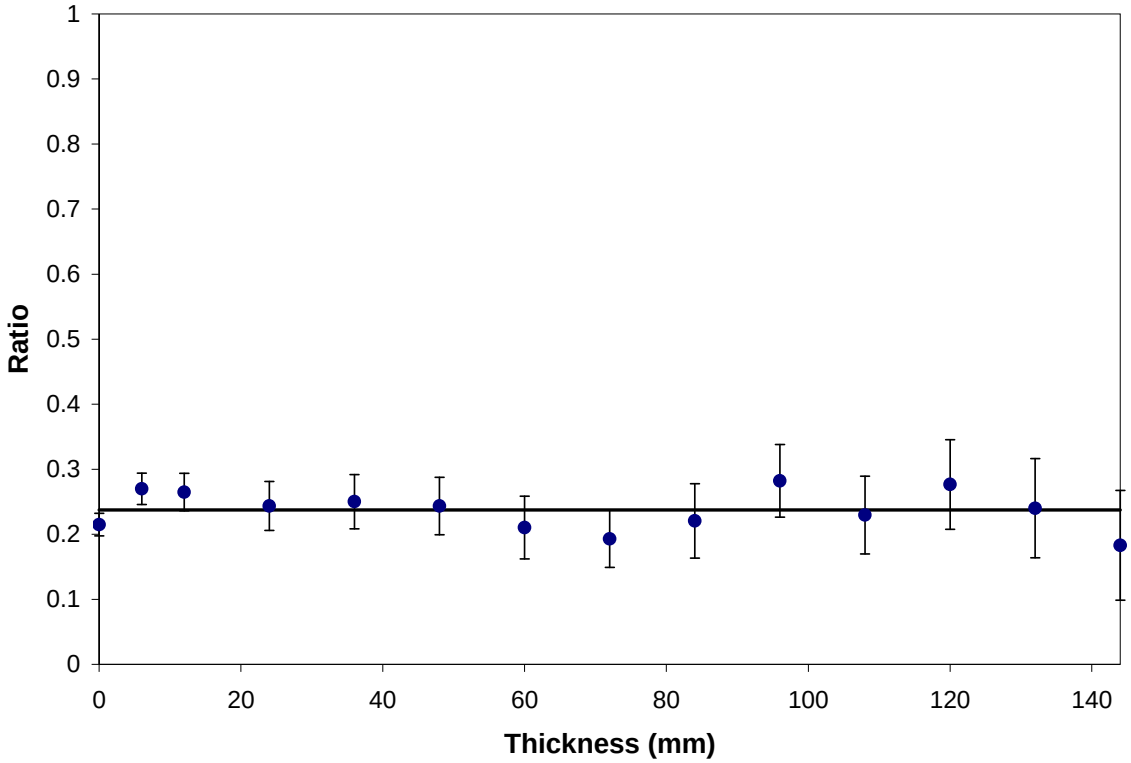

Figure 5.1.3 Cs-137 Scaling Factor Chart

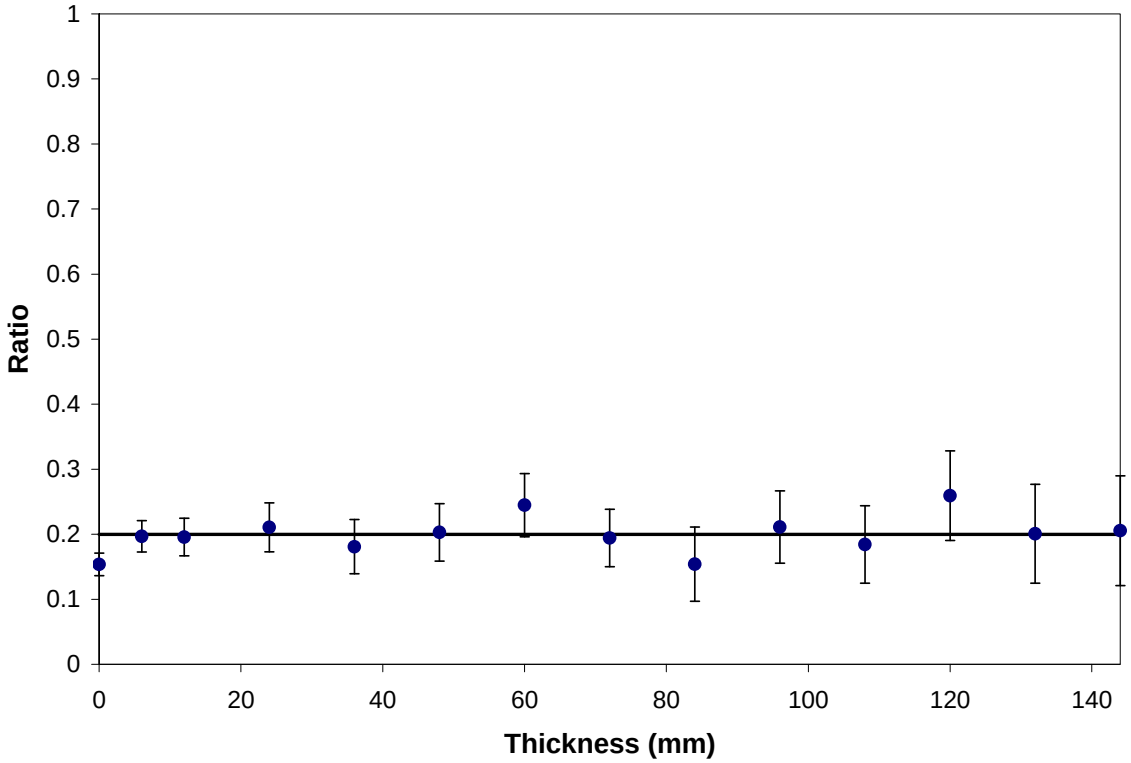

Figure 5.2.4 Mn-54 Scaling Factor Chart

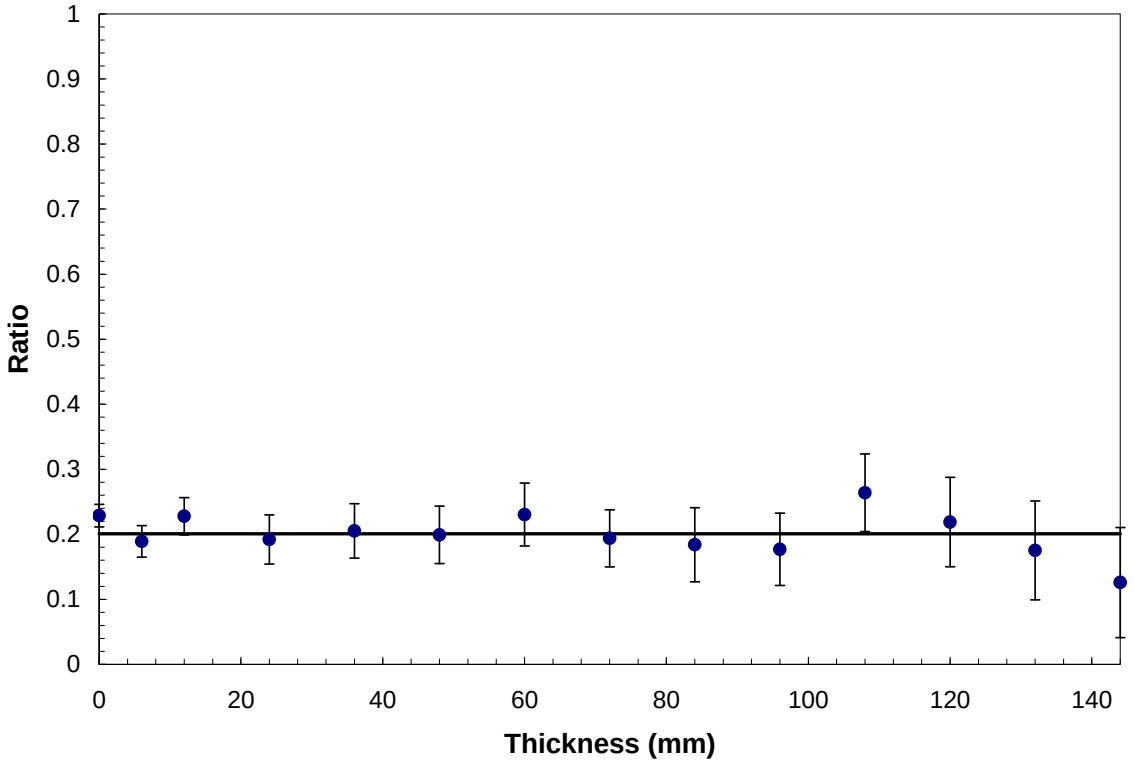

Figure 5.1.5 Na-22 Scaling Factor Chart

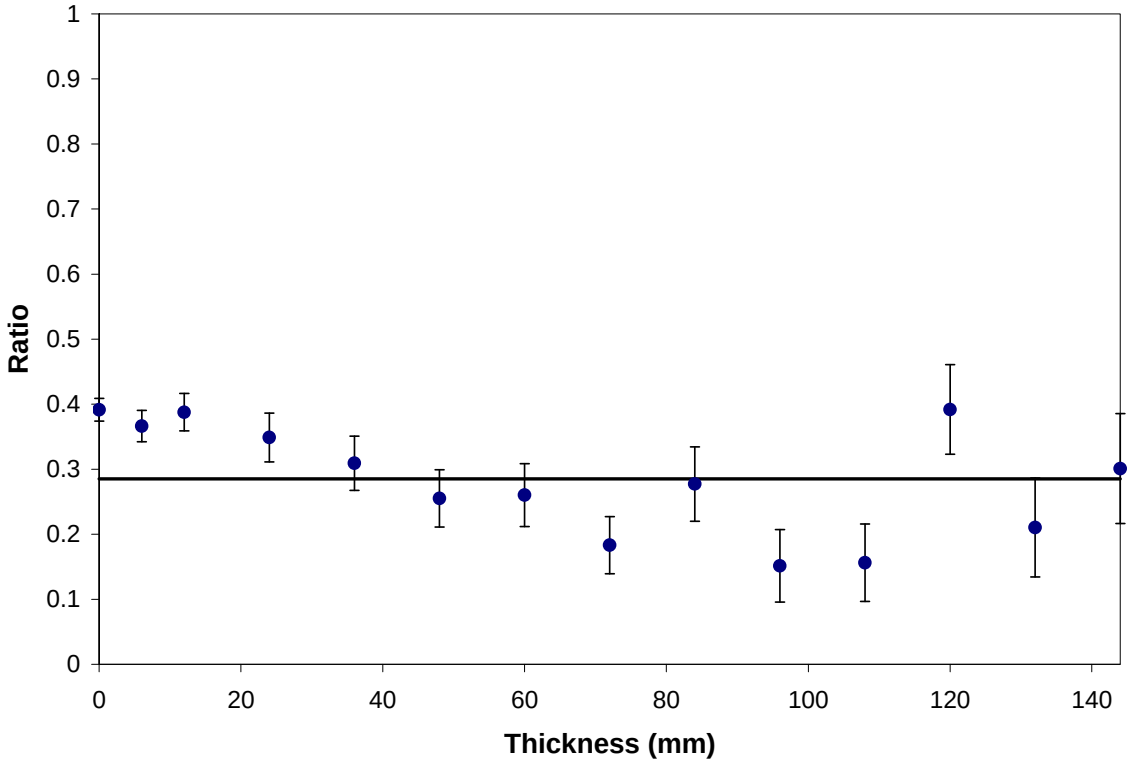

Figure 5.1.6 Ba-133 Scaling Factor Chart

The charts show that the ratios fluctuate normally about a mean value. The mean value is not unity because the fill gas and its density were not identical to the fill gas used by LND due to its proprietary nature. The mean value that the ratios fluctuate about will be termed the "scaling factor." The scaling factors are not the same for each individual nuclide; therefore, energy dependence must be considered when using the scaling factors. Once the scaling factor is applied to MCNP data, the detector output matches the MCNP output. An example of the preceding is shown in Figure 5.1.7.

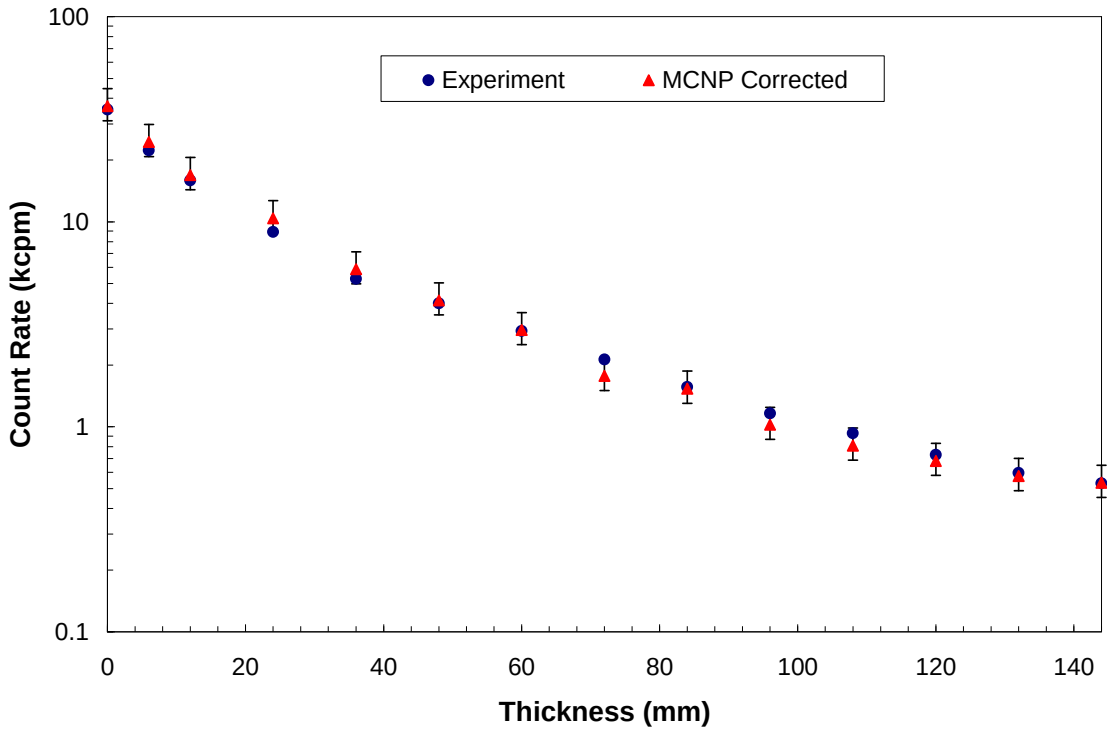

Figure 5.1.7 Co-60 Slab Phantom MCNP-to-Experiment Comparison After Scaling

A similar scaling factor analysis was performed on the Ludlum 3 with the Model 44-9 pancake probe. The scaling factor for the Ludlum 3 set-up was nearly identical to that of the

Ludlum 2 set-up. By applying a constant of proportionality, 1.1, to the Ludlum 2 scaling factors, the Ludlum 3 scaling factors can be determined. This signifies that the output on the Ludlum 2 detector is directly proportional to the output on the Ludlum 3 detector.

5.2 MIRD Phantom Results

The MIRD-based phantoms were used in this project along with the BodyBuilder-generated child phantom. The sources were generated in the organs of interest and were tallied in the four detector locations with an SCX tally modifier to signify where the tallied particles originated. A chart showing the data resulting from an SCX tally modifier for the male inhaling I-131 is displayed in Figure 5.2.1. Note that the values on the y-axis correspond to the number of tallies per source particle generated.

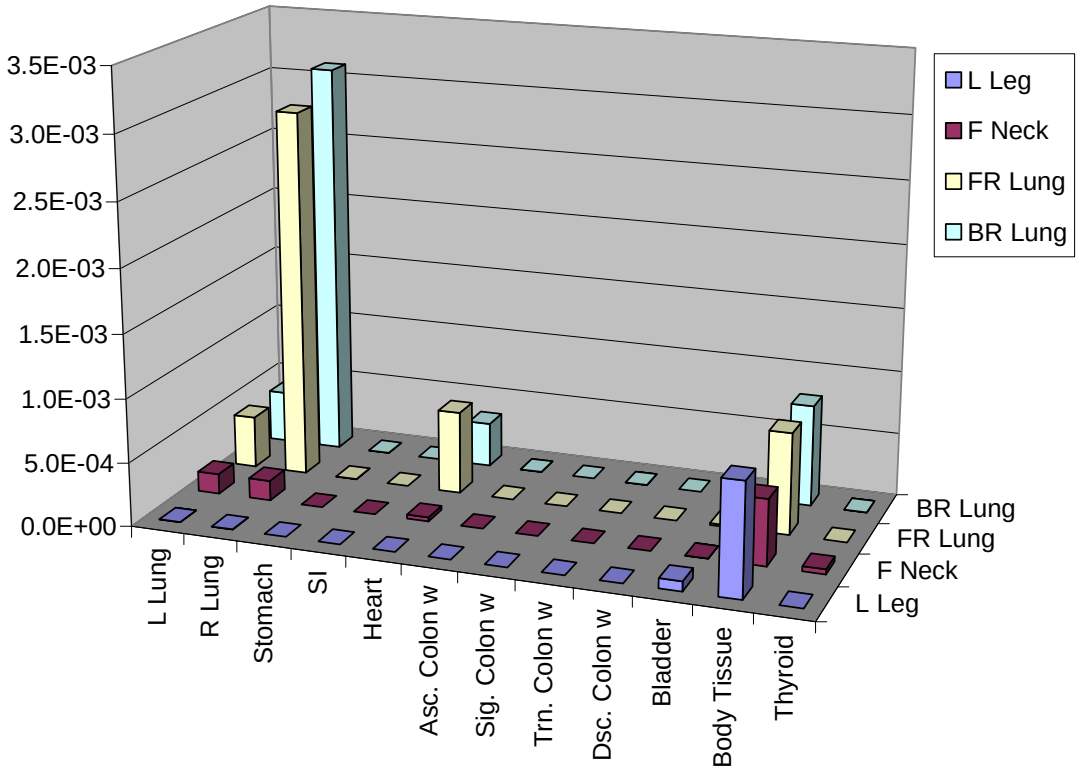

Figure 5.2.1 SCX Unit Tally for I-131

A unit source was generated in each organ to produce the data in Figure 5.2.1. Therefore it does not represent the actual distribution of activity. As expected, the lung locations result in a larger number of counts from the lungs and heart than the neck and leg locations. The thyroid source particles only scored counts with the detector in the neck location, and the urinary bladder source particles only scored in the leg location. The body tissue compartment contributed a considerable amount of counts to all detector locations. Any activity that was to be distributed to the body tissue was uniformly distributed among all regions of the body that were not compartments in the DCAL model. Examples of regions that were not compartments in the DCAL model are the brain, areas in the torso not occupied by organs, and the muscles in the arms and legs.

Sr-90 was undetectable by any of the detector locations. The source was generated with the proper electron distribution of Sr-90/Y-90 and electrons were transported along with bremmsstrahlung. The inability to detect Sr-90 is expected because the range of electrons from Sr-90 is only 1cm for the maximum energy electron; and the bremmsstrahlung yield in tissue for electrons corresponding to the peak energy of 2.28 MeV is rather low [3]. A bremmsstrahlung yield chart is displayed in Figure 5.2.2 [9] for electrons of varying energy in ICRP soft tissue [4,5,17]. The bremmsstrahlung yield for bone was also investigated and shown to have small radiation yield.

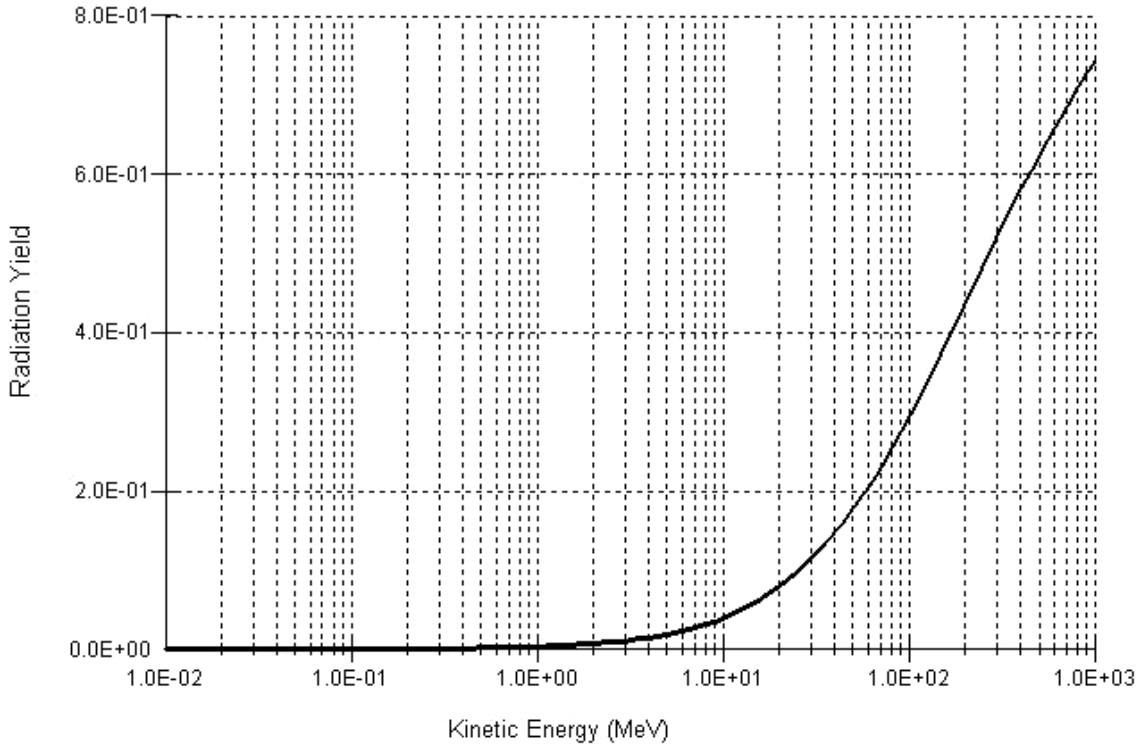

Figure 5.2.2 Bremmsstrahlung Yield for ICRP Soft Tissue

Am-241 was not able to be sufficiently detected in any of the detector locations investigated. This is expected because the low energy gamma rays emitted by Am-241 are easily

attenuated, and Am-241 also requires a relatively low activity to yield a high dose (Table 4.3.4). According to calculations, the amount of Am-241 required to be detectable would deliver a dose of 55 Sv. A dose of this amount would cause death, far exceeding the upper limit of the LD_{50} value with medical intervention, ~10 Sv [30]. Therefore, Am-241 was considered undetectable by the Geiger-Mueller meters.

I-131, Ir-192, Co-60, and Cs-137 have proven to be detectable over at time period of 10 days. The optimal location for detector placement was over the posterior upper right torso. Although the neck location for I-131 receives a large amount of counts from the thyroid, the posterior upper right torso received a higher count rate for a portion of time and comparable count rates otherwise. A table of the count rate per Bq for each of the nuclides with the detector in the posterior upper right torso location is presented in Table 5.2.1. The table is displayed for the Ludlum 2 detector on a reference male phantom, yet each of the phantoms behaves in similar manner for each of the nuclides. Similar tables are presented for each phantom and isotope pairing in Appendix C.

Table 5.2.1 Count Rate per Bq for Ludlum 2 on Male Phantom

	Count rate per Bq (cpm)			
Time (days)	**Co-60**	**Cs-137**	**I-131**	**Ir-192**
0.00	4.99E-6	1.11E-6	5.98E-6	3.13E-6
0.25	2.92E-6	9.29E-7	1.78E-6	1.76E-6
0.50	2.70E-6	1.04E-6	1.27E-6	1.62E-6
1.00	2.33E-6	1.09E-6	6.68E-7	1.39E-6
2.00	1.94E-6	1.02E-6	2.15E-7	1.13E-6
3.00	1.76E-6	9.75E-7	7.55E-8	1.02E-6
4.00	1.67E-6	9.46E-7	2.97E-8	9.68E-7
5.00	1.62E-6	9.28E-7	1.46E-8	9.38E-7
6.00	1.58E-6	9.15E-7	9.82E-9	9.17E-7
7.00	1.54E-6	9.04E-7	8.33E-9	8.99E-7
8.00	1.51E-6	8.95E-7	7.88E-9	8.83E-7
9.00	1.48E-6	8.87E-7	7.70E-9	8.68E-7
10.00	1.46E-6	8.80E-7	7.56E-9	8.53E-7

To illustrate the source of the counts that are being tallied by the detector, three dimensional charts are presented in Figures 5.2.3 through 5.2.6 showing the count rate per source organ at 2 days.

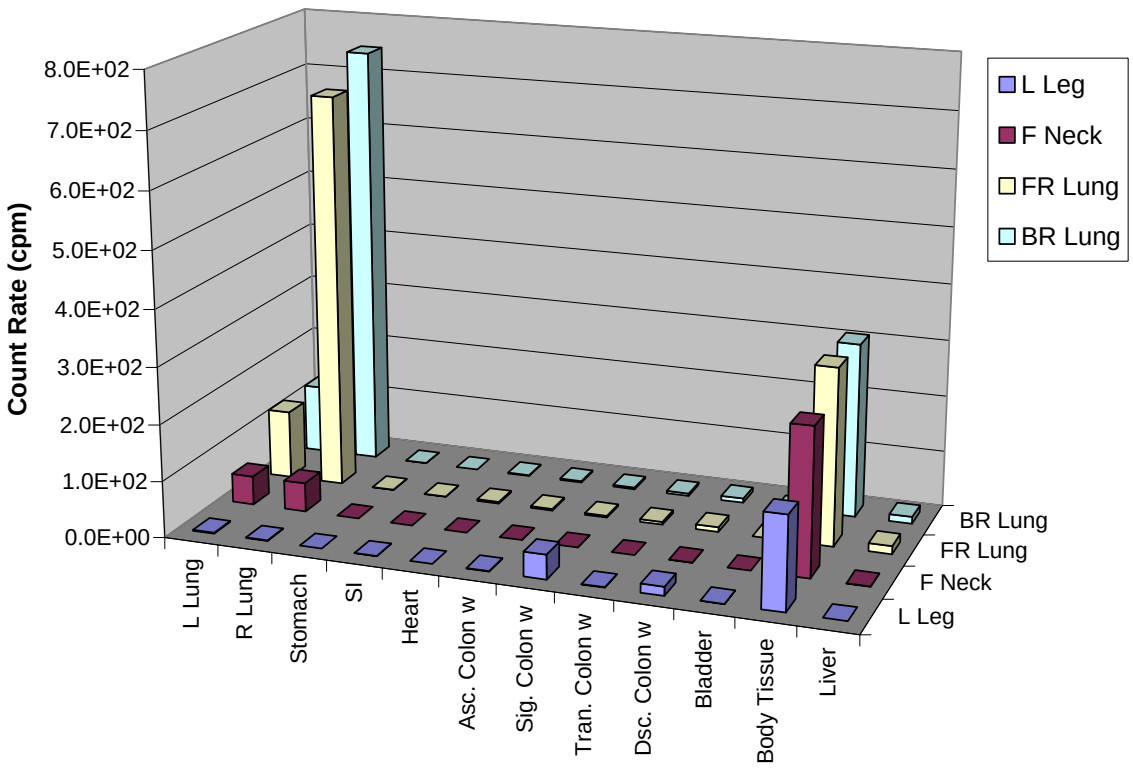

Figure 5.2.3 Male Co-60 Count Rate per Source Organ at 2 days

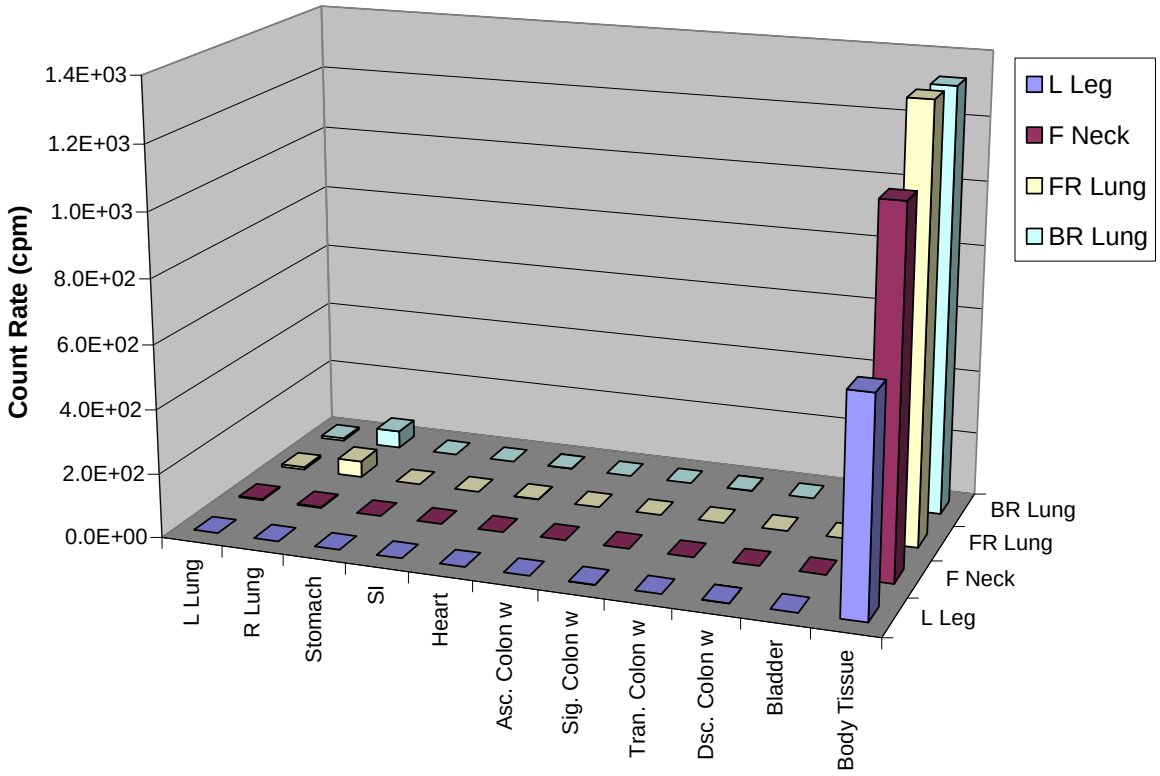

Figure 5.2.4 Male Cs-137 Count Rate per Source Organ at 2 days

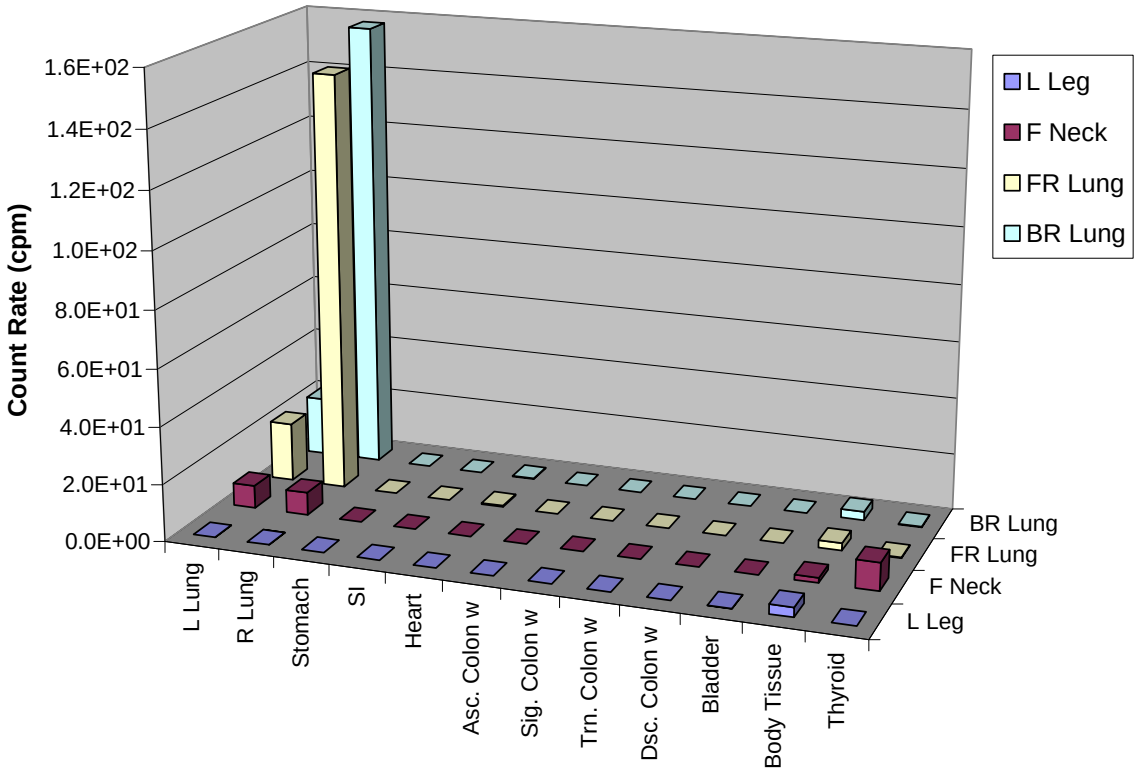

Figure 5.2.5 Male I-131 Count Rate per Source Organ at 2 days

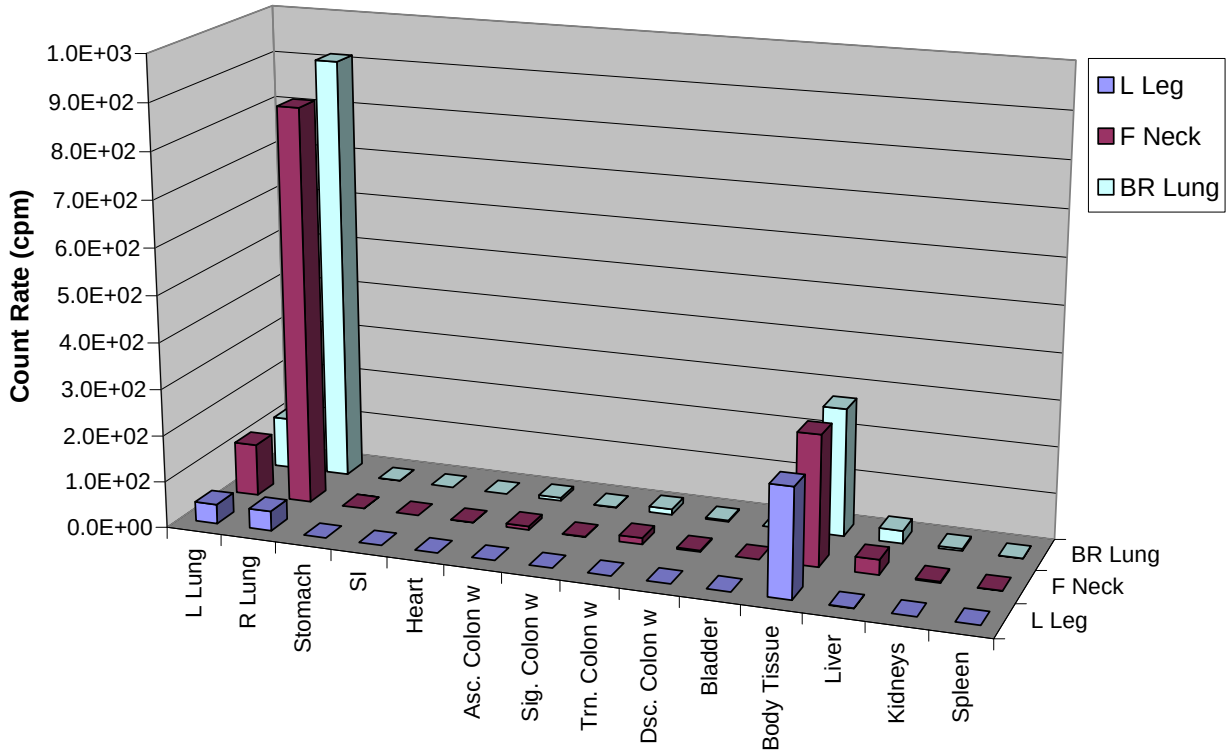

Figure 5.2.6 Male Ir-192 Count Rate per Source Organ at 2 days

It is apparent that most of the counts are originating in either the body tissue or the lungs. Cs-137 produced the majority of the counts from the body tissue, while Ir-192, I-131, and Co-60 produced the majority of the counts from the lungs.

5.3 Phantom Nuclide Decision Levels

The goal of this research is to develop a set of decision levels that can be used by first responders in a way that will minimize error and maximize efficiency. The decision level suggested by Dr. Ansari should be the count rate corresponding to 0.25 Sv of committed

effective dose [2]. A Clinical Decision Level (CDL) is defined as 0.25 Sv of dose; therefore all results were formatted as the count rate per CDL.

The location that yielded the highest count rate per CDL in most cases was the posterior upper right torso. The only case when it was not the most efficient location was for a period of time for the inhalation of I-131. During this period of time, the count rate form the posterior upper right torso was comparable to the anterior neck location; therefore the posterior upper right torso was considered optimal for simplicity.

The location chosen for triaging victims was the posterior upper right torso location. By having one location of detector placement regardless of the individual being screened or the radionuclide of concert, operation error will be minimized. Also, the location chosen yielded a high enough count rate to be able to detect a CDL of radiation over nearly all time periods.

Another area of concern for the detector is the minimum detectable activity. Being a count rate meter, the traditional minimum detectable activity formulas cannot be properly applied. Therefore a hybrid formula was developed to gain a decent estimate of the minimum detectable activity. The minimum detectable counts can be represented by the Currie Equation [6]:

$$N_D = 4.653\sigma_{N_B} + 1.645, \qquad \text{[Equation 5.3.1]}$$

where N_D is the number of counts required to have a false-negative rate less than 5%, given a background count standard deviation of σ_{N_B}. To determine the standard deviation of the background counts, the detector was allowed to fluctuate in count rate with no sources in the vicinity. The fluctuation of the detector was considered to be σ_{N_B} and the count rate was

determined using Equation 5.3.1. Knowing the minimum detectable count rate, the activity was calculated using Equation 5.3.2 [18].

$$A = \frac{N_D}{f\varepsilon}, \qquad \text{[Equation 5.3.2]}$$

where f is the number of gamma rays emitted per decay and ε is the absolute detection efficiency. Knowing the activity, the dose could also be calculated, using the retention factors given by DCAL. Another concern is the background count rate limit, because the data will not be taken in a controlled environment and contamination from those waiting in a queue may create a larger than average background count rate [23]. The background count rate cannot exceed a certain value, or else the decision levels cannot be used.

The amount of data corresponding to the decision levels is large and is reported in Appendix C. An example of the count rate per CDL over time for Co-60 in the reference male is presented in a tabular form in Table 5.3.1 and a graphical form in Figure 5.3.1.

Table 5.3.1 Count Rate per CDL for Male with Co-60

Co-60 M	Total Count Rate above BG (kcpm)		MDA (μCi)		Background Limit (kcpm)	
Time (days)	Ludlum 2	Ludlum 3	Ludlum 2	Ludlum 3	Ludlum 2	Ludlum 3
0.00	3.1	3.6	11	9.5	4.4	5.0
0.25	1.8	2.1	18	16	2.6	2.9
0.50	1.7	1.9	20	18	2.4	2.7
1.00	1.5	1.7	23	20	2.0	2.3
2.00	1.2	1.4	28	24	1.7	1.9
3.00	1.1	1.3	31	27	1.5	1.8
4.00	1.0	1.2	32	28	1.5	1.7
5.00	1.0	1.2	33	29	1.4	1.6
6.00	1.0	1.1	34	30	1.4	1.6
7.00	1.0	1.1	35	31	1.3	1.5
8.00	0.9	1.1	36	31	1.3	1.5
9.00	0.9	1.1	36	32	1.3	1.5
10.00	0.9	1.0	37	33	1.3	1.5
20.00	0.8	0.9	43	37	1.1	1.3
30.00	0.7	0.8	47	42	1.0	1.1

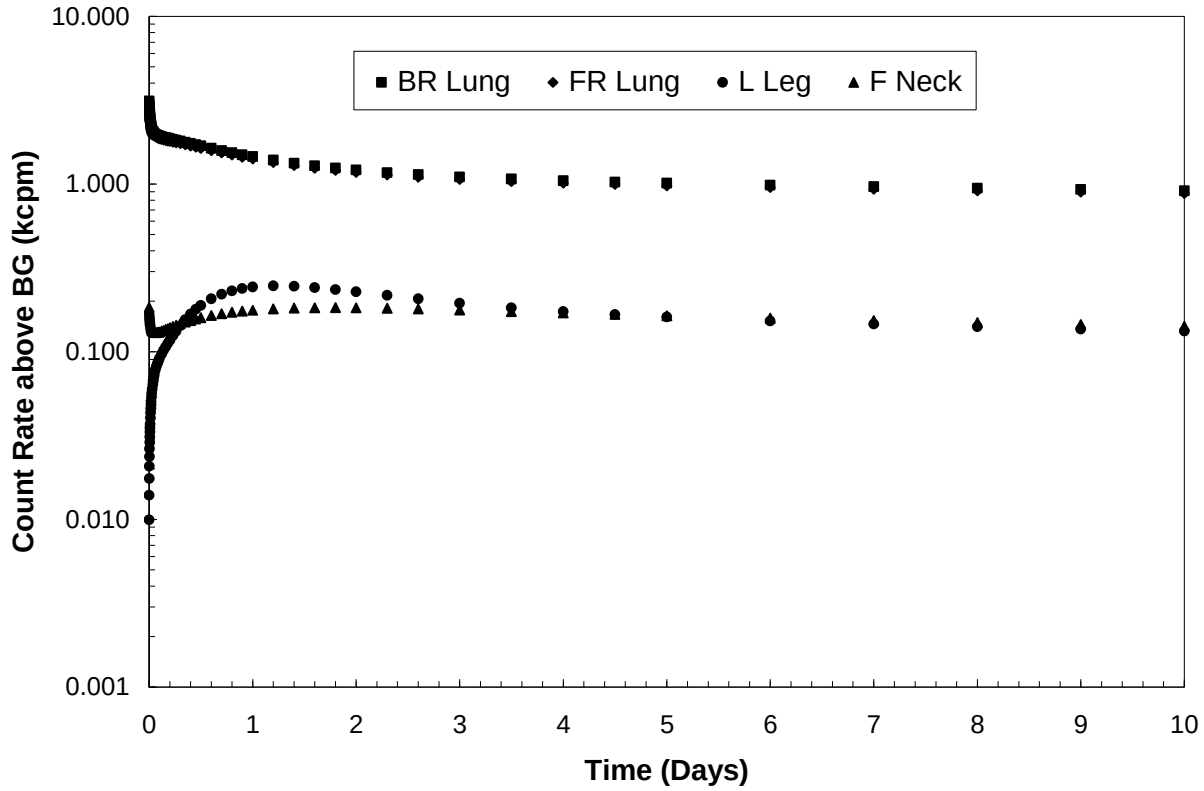

Figure 5.3.1 Count Rate per CDL for Male with Co-60

Comparing all six phantoms for any of the nuclides shows that the child will produce the highest count rate per CDL and the adipose phantoms produce the lowest count rate per CDL. An example of this is displayed in Figure 5.3.2 for the inhalation of Co-60 and Figure 5.3.3 for the inhalation of Cs-137..

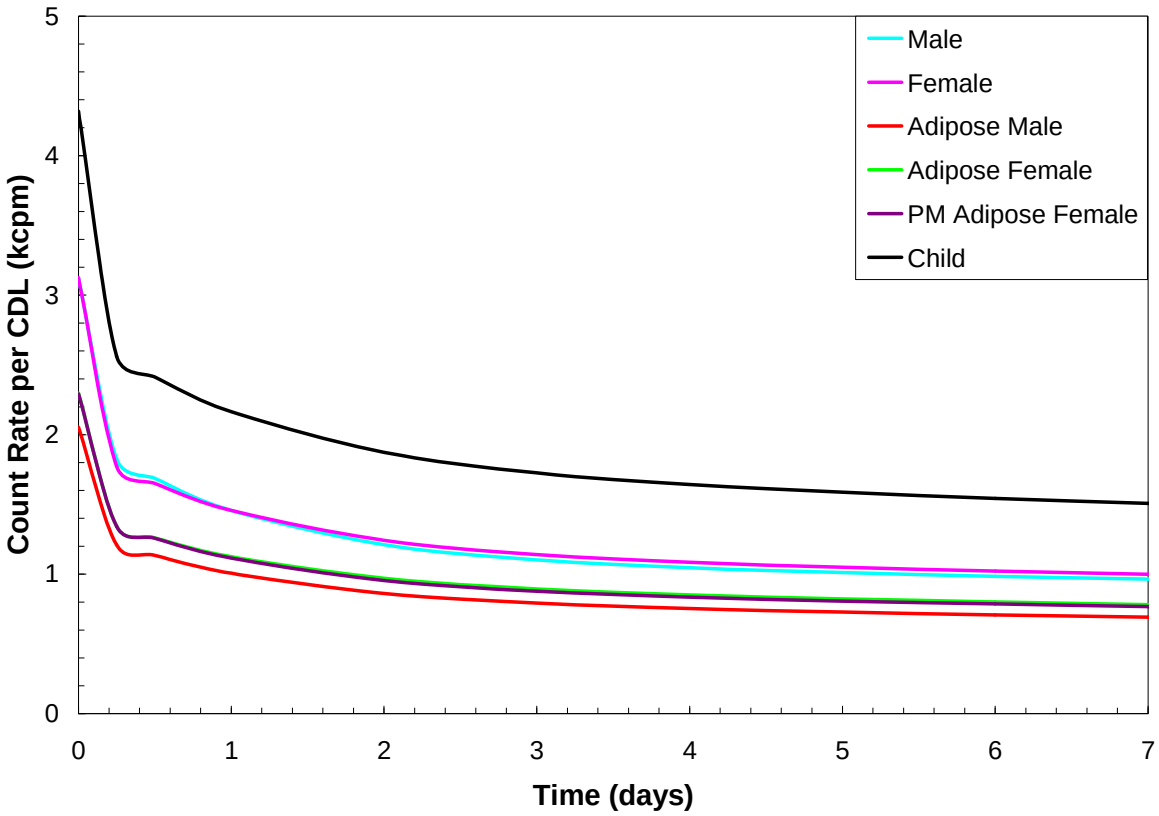

Figure 5.3.2 Comparing Phantom Count Rate per CDL for Co-60

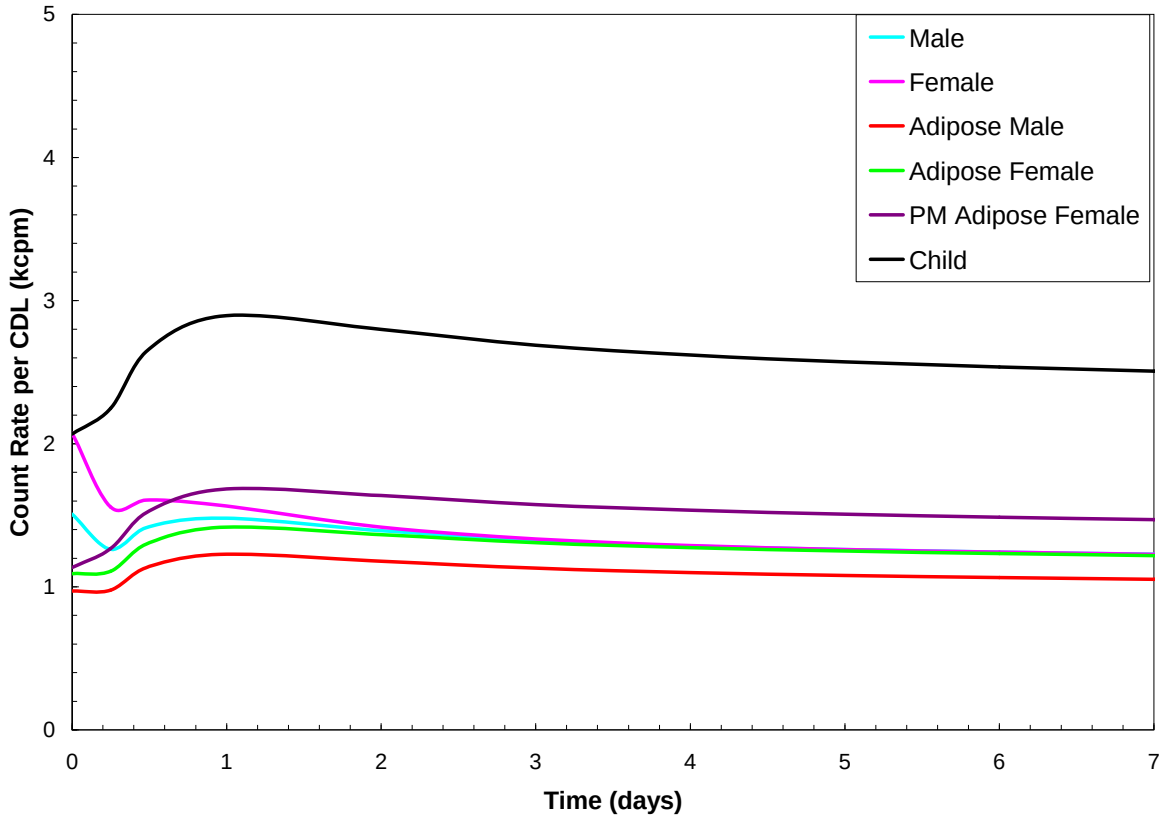

Figure 5.3.3 Comparing Phantom Count Rate per CDL for Cs-137

5.4 Triaging Procedure Sheets

After the decision levels were determined, a set of procedure sheets were developed in order to make the information usable. The procedure sheets are meant to be a method of communicating how to properly use the detector and how to determine if someone is in need of further medical attention. A few sample triaging instructional sheets are presented in Appendix D. Each procedure sheet contains five main sections. The first section is a picture of the detector to ensure that the operator has selected the correct instrument. A detailed description of basic operation is included in the next section. The basic operation was as detailed as possible, to make certain that the operator is properly using the detector. The details of how to take a

background measurement is explained in the third section, because the decision levels are presented in count rates above background. The "warning levels," or decision levels, are described in the fourth section to clarify how to properly read the table of decision levels. The final section of the procedure sheets consists of the decision level tables. The data were presented in counts per minute corresponding to a CDL.

A procedure sheet has been crafted for each detector-phantom combination. But to further simplify the triaging material, a condensed procedure sheet was also produced. This triage sheet is the same as each of the other sheets in terms of the first four sections, but the decision level tables have been condensed to allow for the need of only one set of guidelines. Using the previous method with a sheet for each detector-phantom combination would force the operator to make a decision as to whether an individual were adipose, not adipose, post menopausal, or pre menopausal. With the condensed method, the tables have been condensed into two tables, one for the adult and one for the child. Therefore, an operator would only have to determine if the individual was an adult or a child.

In order to combine the phantoms, the lowest count rate per CDL was chosen for each phantom-nuclide-time pairing. This is the most conservative estimate, allowing for the least false negatives. Having more false positives is preferred over the former because there is a lower chance of contaminated people not receiving additional medical attention. The phantoms yielding the lowest count rate on average was the adipose male, therefore most of the data corresponding to the adult were the adipose male data. To determine whether someone is an adult or a child can be accomplished via BMI requirements or height requirements. The height, weight, and BMI of the child phantom may be used as a reference (Table 4.3.1).

The count rate difference among the phantoms varied as much as a 100% difference. For example, the male may have required 2 kcpm at one day after inhalation, but the adipose male may have required just 1 kcpm at one day after inhalation. By choosing 1 kcpm as the decision level, more false positives will be introduced, yet this is preferred to the alternative. Also, the detectors were combined into one set of decision levels because of their proportional and nearly identical response. The same method was used when combining the detector types: the set of data with the lowest response for a given stimulus was chosen as the decision level. The condensed triage procedure sheet is presented in Appendix E.

CHAPTER 6: CONCLUSIONS

Geiger Mueller detectors are ideal for triaging the individuals exposed to an RDD if the radionuclide of concern is Co-60, Cs-137, I-131, or Ir-192. Am-241 and Sr-90 could not be detected by the G-M meters because of the ease of attenuation for the lower energy gammas of Am-241 and the betas of Sr-90. The availability of a G-M surveying meter and ease of use are the two most attractive traits of this option. The count rates output by the detector allow for detection of a CDL, 0.25 Sv, any of the four radionuclides mentioned within 30 days of inhalation.

A procedure sheet containing decision levels allows for straightforward implementation by a first responder in an emergency situation. All of the possible types of adults can be combined into one set of decision levels by choosing the phantom that provided the lowest response for a given stimulus. The most simplified implementation has two classes, adult and child, which results in a smaller probability of error by the operator. The two detectors were also combined into one set of decision levels because their output was proportional and nearly identical. The primary concern in an emergency situation is having an efficient system that minimizes operator error.

CHAPTER 7: FUTURE WORK

Future work can be performed for the ingestion of the radionuclides. After an RDD, the most common method of uptake is inhalation, yet some form of ingestion will also occur.

It may be possible to determine the time of inhalation and/or ingestion by taking a ratio of counts from two different detector locations. The distribution of a radionuclide throughout the body varies over time; therefore the time of inhalation may be determined by the distribution of the radionuclide. Potentially a detector could be placed on the abdomen and over the chest and the ratio of the counts could determine when the radionuclide was inhaled. Upon discovery of the time of inhalation, the amount of radioactivity inhaled/ingested could be determined with the data presented in this work.

Another topic of concern is the inhalation of more than one type of radionuclide. If an RDD contains two or more radionuclides, it would be prudent to have a system of decision levels to implement after this scenario.

Not being able to detect Am-241 and Sr-90 creates a weakness in the triaging plan developed by this research. Some other method of detecting these two radionuclides should be investigated in order that a system is in place to determine how much intake someone has received following exposure to these radionuclides.

APPENDIX A: MCNP INPUT FILE FOR SLAB PHANTOM

```
HP-260 Pancake Probe
c  Thickness = 12 mm
c  Cell Cards
1  1  -0.000165 -1:-15  $ fill gas
2  2  -7.8 -16 1 15:-17:-18 19 $ steel casing
3  3  -0.0012 -3 :-6 20 21 22 23 24 25 26 27 28 29 30 31 32 33 34
     35 36 37 38 39:-7 2 15 16 17 18 19:-9 19 $ surrounding air
4  4  -2.6989 -5 2 3 6 7 20 21 22 23 24 25 26 27 28 29 30 31 32 33 34 35
     36 37 38 39 16: -8 7 9:-10 9 7 $ aluminum mesh
5  5  -0.94 -11:-12:-13:-14:-44 $ Poly
6  6  -8.96 -19 $ Copper Wire
7  7  -2.6989 -20:-21:-22:-23:-24:-25:-26:-27:-28:-29:-30:-31
     :-32:-33:-34:-35:-36:-37:-38:-39 $ aluminum mesh
8  8  -1.03 -40 $ Virtual Water
9  9  -1.19 -41 43:-42 $ Lucite Sheets
10 10 -0.017 -2 1 3 15 16 $ Mica Window
28 3 -0.0012 -43 44 $ surrounding air
29 3  -0.0012 -99 5 6 8 10 11 12 13 14 19 40 41 42 44 $ surrounding air
30 0    99 $ vacuum

c  surface cards
c  gas in detector
1  RCC 0.6 0 0 1.19 0 0 2.5297
c  inner detector casing
2  RCC 0.4175 0 0 1.5494 0 0 2.6797
c  air cutout in the inner casing
3  RCC 0.4175 0 0 0.05 0 0 2.2225
c  outer detector head
5  RCC 0 0 0      2.54   0 0 3.4925
c  air cutout in outer casing
6  RCC 0 0 0      0.4175 0 0 2.54
c detector arm extension
7  RCC 1.1922 -2.66  0 0 -3.40995 0 0.8025
8  RCC 1.1922 -2.91465 0 0 -3.175   0 0.9525
9  RCC 1.12 -5.6 0 5.3427 -14.6789 0 0.8025
10 RCC 1.12 -5.6 0 5.3427 -14.6789 0 0.9525
c nubs on outside of detector head
11 RCC 0 3.016  0      -0.17 0 0 0.2
12 RCC 0 -3.016 0      -0.17 0 0 0.2
13 RCC 0 0      3.016  -0.17 0 0 0.2
14 RCC 0 0      -3.016 -0.17 0 0 0.2
c extension of inner detector
15 RCC 1.1922 -2.5296 0 0   -0.9629  0 0.485
16 RCC 1.1922 -2.5296 0 0   -0.9629  0 0.635
17 RCC 1.1922 -3.4925 0 0   -0.8128  0 0.35
18 RCC 1.1922 -4.3053 0 0   -0.635   0 0.3175
c wire inside the handle
19 RCC 1      -4.9403 0 5.5 -15.3386 0 0.01
c wire mesh
20 RCC 0.3 -2.52 0.25 0 5.04 0 0.03
21 RCC 0.3 -2.45 0.75 0 4.9  0 0.03
22 RCC 0.3 -2.2  1.25 0 4.4  0 0.03
23 RCC 0.3 -1.85 1.75 0 3.7  0 0.03
24 RCC 0.3 -1.15 2.25 0 2.3 0 0.03
25 RCC 0.3 -2.52 -0.25 0 5.04 0 0.03
26 RCC 0.3 -2.44 -0.75 0 4.88 0 0.03
```

```
27 RCC 0.3 -2.2 -1.25 0 4.4  0 0.03
28 RCC 0.3 -1.85 -1.75 0 3.7 0 0.03
29 RCC 0.3 -1.15 -2.25 0 2.3 0 0.03
30 RCC 0.3 0.25 -2.52 0 0 5.04 0.03
31 RCC 0.3 0.75 -2.45 0 0 4.9 0.03
32 RCC 0.3 1.25 -2.2 0 0 4.4 0.03
33 RCC 0.3 1.75 -1.85 0 0 3.7 0.03
34 RCC 0.3 2.25 -1.15 0 0 2.3 0.03
35 RCC 0.3 -0.25 -2.52 0 0 5.04 0.03
36 RCC 0.3 -0.75 -2.45 0 0 4.9 0.03
37 RCC 0.3 -1.25 -2.2 0 0 4.4 0.03
38 RCC 0.3 -1.75 -1.85 0 0 3.7 0.03
39 RCC 0.3 -2.25 -1.15 0 0 2.3 0.03
c water
40 RPP -11.97 -1.97 -7.2 7.2 -7.2 7.2
c lucite
41 RPP -1.97 -1.37 -7.2 7.2 -7.2 7.2
42 RPP -1.37 -0.17 -7.2 7.2 -7.2 7.2
c source holder
43 RCC -1.37 0 0 -.4 0 0 1.2
c source medium
44 RCC -1.57 -1.15 0 0 2.3 0 0.1999
c surroundings
99 SO 30

IMP:P 1 1 1 1 1 1 1 1 1 1 1 0
IMP:E 1 1 1 1 1 1 1 1 1 1 1 0
mode p e
c Cs-137 Source
SDEF ERG=D1 POS= -1.5699 -1.1499 0 RAD=D2 EXT=D3 AXS=0 1 0
     VEC= 1 0 0
SI1 L 0.662 0.0332 0.0318
SP1 0.898 0.0392 0.0213
SI2= 0 0.1998
SI3= 0 2.298
C Tally over the gas
F8:P,E 1
E8 0 1E-5 1000I 1
c Material Cards
M1  10000.04p 1 $ Neon Fill Gas
M2  26000.04p .75 24000.04p .25 $ 446 SS
M3  7000.04p .78 8000.04p .21 18000.04p .01 $ AIR
M4  13000.04p 1 $ Aluminum
M5  6000.04p .856 1000.04p .144 $ Polyethylene
M6  29000.04p 1 $ Copper
M7  13000.04p 1 $ Aluminum
M8  1000.04p 0.0802 6000.04p 0.6748 7000.04p 0.0214 8000.04p 0.1991
     17000.04p 0.0014 20000.04p 0.0231$ V-Water
M9  6000.04p .556 8000.04p 0.296 1000.04p 0.148 $ Lucite
M10 19000.04p .043 13000.04p .087 14000.04p .174 8000.04p .522
     1000.04p .087 9000.04p .087 $ Mica
phys:p 4j 1
nps 5e6
```

APPENDIX B: MCNP INPUT FILE FOR MIRD PHANTOM

```
Male with Co-60
1    1 -.001293    -1 (607:-37:606) (-606:601:35) (600:-35) &
                   (-615:37:-43:44:4:-616) (37:-608:609) &
                   (37:-608:610) 900 901 902 903
2    2 -0.2958     ((-2 -4 3):(-2 4)) 5                    $ left lung
3    3 -0.9869     -7 51 -6 (-8:32) 84 101 #2 #24 #28 #58 #59
                   (113:115) (114:115) #62 #700            $ torso insd ribs/lvrtop-shldr
4    3 -0.9869     -7 8 -32 117 113 114 #15 #16 #17 #18 #19 #20 #700
                   (-4:-9:116:118:-119) (-4:-9:116:120:-121)    $torso
5    3 -0.9869     -7 8 -117 51 113 114 #9 #13 #14 #700        $ torso
6    3 -0.9869     -7 50 -51 56 84 96 105 106 113 114 #10 #11 #12
                   #27 #32 #43 #44 #47 #700                $ torso
7    3 -0.9869     -7 97 -50 (83:-86:87:-88) 113 114 #30 #33 #38 #39
                   #63 #64 #65 #700                        $ torso abdoman
8    3 -0.9869     -7 37 -97 95 113 114 #31 #33 #38 #65 #66 #700    $ torso abdoman
9    4 -1.4862     8 -9 5 -10                              $ rib
10   4 -1.4862     8 -9 11 -12                             $ rib
11   4 -1.4862     8 -9 13 -14                             $ rib
12   4 -1.4862     8 -9 15 -16                             $ rib
13   4 -1.4862     8 -9 17 -18                             $ rib
14   4 -1.4862     8 -9 19 -20                             $ rib
15   4 -1.4862     8 -9 21 -22                             $ rib
16   4 -1.4862     8 -9 23 -24                             $ rib
17   4 -1.4862     8 -9 25 -26                             $ rib
18   4 -1.4862     8 -9 27 -28                             $ rib
19   4 -1.4862     8 -9 29 -30                             $ rib
20   4 -1.4862     8 -9 31 -32                             $ rib
21   3 -0.9869     ((35 -34):(-33 6 -35)) 102 (84:85)
                   #37 #60 #61 #62 #700                    $ head
22   3 -0.9869     -37 38 -39 103 #700                     $ left leg
23   3 -0.9869     -37 38 -40 104 #22 #700                 $ right leg
24   2 -0.2958     ((-41 -4 42):(-41 4)) 5                 $ right lung
25   3 -0.9869     715 -37 43 -44 -4 716 39 40 72 73 #700 #600    $ genitalia
26   3 -0.9869     -47                                     $ brain
27   3 -0.9869     50 -51 -48 -49 #10 #11 #12              $ liver
28   3 -0.9869     (-52 54):(-53 -54 55)                   $ heart
29   3 -0.9869     -56                                     $ stomach
30   3 -0.9869     138 -57 58 -59                          $ Ascending Colon Wall
31   3 -0.9869     (-63 141 65 -61):(-64 142 37 -65)       $ Sigmoid Colon Wall
32   3 -0.9869     -62 139 66 -67 59                       $ Transverse Colon Wall
33   3 -0.9869     -60 140 61 -59 -83                      $ Descending Colon Wall
35   3 -0.9869     -72                                     $ testicle
36   3 -0.9869     -73                                     $ testicle
37   3 -0.9869     -74 75 -76 6 -77                        $ thyroid
38   4 -1.4862     -82 83 37 -78 80 (79:-81)               $ pelvis
39   4 -1.4862     -84 78 -85 102                          $ spine
40   3 -0.9869     -83 86 -50 88 -87 #30 #32 #33 #63 #64 #65    $ small int.
41   1 -0.001293   -107 606 -4                             $ air
42   1 -0.001293   -108 606 -4                             $ air
43   3 -0.9869     -92 65                                  $ kidney
44   3 -0.9869     -93 -94                                 $ kidney
45   3 -0.9869     -95                                     $ bladder
46   3 -0.9869     -96                                     $ spleen
47   3 -0.9869     -98 99 (-65:100)                        $ pancreas
48   3 -0.9869     -101                                    $ thymus
49   4 -1.4862     47 -102 #60 #61                         $ skull
```

```
50    4 -1.4862     -103 38 -37                          $ leg bone
51    4 -1.4862     -104 38 -37                          $ leg bone
52    3 -0.9869     -105 92                             $ adrenal
53    3 -0.9869     -106 93                             $ adrenal
54    4 -1.4862     37 -115 -113                         $ arm bone
55    4 -1.4862     37 -115 -114                         $ arm bone
56    4 -1.4862     4 9 -32 -116 117 -118 119                  $ scapulae
57    4 -1.4862     4 9 -32 -116 117 -120 121                  $ scapulae
58    4 -1.4862     -4 -122 -123 124                      $ clavicle
59    4 -1.4862     -4 -122 -125 126                      $ clavicle
60    3 -0.9869     -33 128 129 -130 133 -134 -4 #700           $ eye lense
61    3 -0.9869     -33 128 -131 132 133 -134 -4 #700           $ eye lense
62    3 -0.9869     -77 -137 51                         $ oesophagus
63    3 -0.9869     -138 58 -59                         $ Ascending Colon Interior
64    3 -0.9869     -139 66 -67                         $ Transvers Colon Interior
65    3 -0.9869     -140 61 -59 -83                      $ Decending Colon Interior
66    3 -0.9869     (-141 65 -61) : (-142 37 -65)              $ Sigmoid Colon Interior
600   0          -600 35 34 902 : -601 33 -35 606 902 : &          $ Head & Neck
                 -606 6 33 -607 902: -607 7 -6 37 900 901 902 : &   $ Shoulders & Torso
  (((-46 616) (43 -44) (615 -37)):((615 -45)(610 609)(46 -4)(43 -44))): & $ Genitalia
                 -610 40 -37 38 : -609 39 -37 38 903: &          $ Legs
                 -708 608 -609 : -708 608 -610 : &            $ Feet
                 -38 708 -610 40 : -38 708 -609 39
700   5 -1.04       700 35 102 -34 : 701 -33 -35 6 : &           $ Head & Neck
                 706 -6 701 -707 : 707 -7 -6 37 114 113 : &      $ Shoulders & Torso
  (((46 -716)(43 -44)(609 610)(715 -37)):((-715 45)(610 609)(46 -4)(43 -44))): & $ Genitalia
                 -40 710 -37 38 : -39 709 -37 38 : &           $ Legs
                 -38 708 -39 : -38 708 -40                  $ Feet
900   1 -.001293    -900 7 507
901   1 -.001293    -901 7 517
902   1 -.001293    -902 6 33 34 527
903   1 -.001293    -903 39 537
c Detector in box 900
501  501  -0.000165 -501
502  502  -0.0012 -503 :-506
503  503  -2.6989 -505 502 503 506
504  504  -0.017 -502 501 503
c Detector
505  502  -0.0012 -507 505 506
c Detector in box 901
511  501  -0.000165 -511
512  502  -0.0012 -513 :-516
513  503  -2.6989 -515 512 513 516
514  504  -0.017 -512 511 513
c Detector
515  502  -0.0012 -517 515 516
c Detector in box 902
521  501  -0.000165 -521
522  502  -0.0012 -523 :-526
523  503  -2.6989 -525 522 523 526
524  504  -0.017 -522 521 523
c Detector
525  502  -0.0012 -527 525 526
c Detector in box 903
531  501  -0.000165 -531
532  502  -0.0012 -533 :-536
```

```
533  503  -2.6989 -535 532 533 536
534  504  -0.017 -532 531 533
c Detector
535  502  -0.0012 -537 535 536
67    0          1

1     SO  200
2     SQ  23.04 10.24 1 0 0 0 -576 8.5 0 43.5
3     SQ  23.04 10.24 1 0 0 0 -576 2.5 0 43.5
4     PY  0.0
5     PZ  43.5
6     PZ  70
706   PZ  69.8
606   PZ  70.2
7     SQ  1 4.0 0 0 0 0 -400.0 0 0 0
707   SQ  0.002551 0.010412 0 0 0 0 -1 0 0 0
607   SQ  0.002451 0.00961  0 0 0 0 -1 0 0 0
8     SQ  1 3.15 0 0 0 0 -272.25 0 0 0
9     SQ  1 3.01 0 0 0 0 -289.0 0 0 0
10    PZ  44.9
11    PZ  35.1
12    PZ  36.5
13    PZ  37.9
14    PZ  39.3
15    PZ  40.7
16    PZ  42.1
17    PZ  46.3
18    PZ  47.7
19    PZ  49.1
20    PZ  50.5
21    PZ  51.9
22    PZ  53.3
23    PZ  54.7
24    PZ  56.1
25    PZ  57.5
26    PZ  58.9
27    PZ  60.3
28    PZ  61.7
29    PZ  63.1
30    PZ  64.5
31    PZ  65.9
32    PZ  67.3
33    SQ  100 49 0 0 0 0 -4900 0 0 0
701   SQ  0.021626 0.010412 0 0 0 0 -1 0 0 0
601   SQ  0.01929 0.009612 0 0 0 0 -1 0 0 0
34    SQ  7225 3540.25 4900 0 0 0 -354025 0 0 85.5
700   SQ  0.021626 0.010412 0.014516 0 0 0 -1 0 0 85.5
600   SQ  0.01929 0.009612 0.013212 0 0 0 -1 0 0 85.5
35    PZ  85.5
36    PZ  94
37    PZ  0
38    PZ  -80
708   PZ  -80.215
608   PZ  -80.415
39  601  GQ  5.025 5 0 0 0 -1 -100 0 0 0
709 603  GQ  5.05 5 0 0 0 -1 -100 0 0 0
```

```
609 605  GQ  4.963 5 0 0 0 -1 -100 0 0 0
40  600  GQ  5.025 5 0 0 0 1 100 0 0 0
710 602  GQ  5.089 5 0 0 0 1 100 0 0 0
610 604  GQ  4.963 5 0 0 0 1 100 0 0 0
41    SQ  23.04 10.24 1 0 0 0 -576 -8.5 0 43.5
42    SQ  23.04 10.24 1 0 0 0 -576 -2.5 0 43.5
43    P   10 0 1 -100
44    P   10 0 -1 100
45    PZ  -4.8
715   PZ  -4.6
615   PZ  -5.0
46    P   0 10 1 -100
716   P   0 10.2 1 -100
616   P   0 9.8 1 -100
47    SQ  2.25 1 1.91716 0 0 0 -81 0 0 86.5
48    SQ  64 272.25 0 0 0 0 -17424 0 0 0
49    P   9 7 -7.3256 -315
50    PZ  27
51    PZ  43
52    GQ  45.2 59.9 47.9 17.5 -16.2 34.8 -1632.1 1204.8 -4898.2 124295.2
53    SQ  1 1 1 0 0 0 -25 -1 -3 51
54    P   .6943 -.3237 -.6428 -32.506
55    P   5.2193 -2.4336 -0.916 -59.6345
56    SQ  4 7.11 1 0 0 0 -64 8 -4 35
57    SQ  1 1 0 0 0 0 -6.25 -8.5 -2.36 0
58    PZ  14.45
59    PZ  24
60    GQ  4.54 3.53 .096 0 1.16 -0.166 -77.68 -10.08 -.223 323.52
61    PZ  8.72
62    SQ  0 2.25 6.25 0 0 0 -14.0625 0 -2.36 25.5
63    TY  3 0 8.72 5.72 1.57 1.57
64    TY  3 0 0 3 1.57 1.57
65    PX  3
66    PX  -10.5
67    PX  10.5
68    PX  -20
69    PX  20
70    PY  -30
71    PY  -29
72    SQ  11.9025 8.9401 3.8025 0 0 0 -20.115225 1.3 -8 -2.3
73    SQ  11.9025 8.9401 3.8025 0 0 0 -20.115225 -1.3 -8 -2.3
74    C/Z 0 -6 2.2
75    C/Z 0 -6 1
76    PY  -6
77    PZ  75
78    PZ  22
79    PZ  14
80    PY  -3
81    PY  5
82    C/Z 0 -3 12
83    C/Z 0 -3.8 11.3
84    SQ  6.25 4 0 0 0 0 -25 0 5.5 0
85    PZ  78.5
86    PZ  17
87    PY  2.2
88    PY  -4.86
```

```
89   C/Z 0 -11. 0.6350
90   C/Z 0 -11. 0.8636
91   PZ  56.335
92   SQ  1.49 13.44 1 0 0 0 -30.25 6 6 32.5
93   SQ  1.49 13.44 1 0 0 0 -30.25 -6 6 32.5
94   PX  -3
95   SQ  1 2.0557 2.0557 0 0 0 -24.5818 0 -4.5 8
96   SQ  2.94 9 1 0 0 0 -36 11 3 37
97   PZ  12
98   SQ  1 225 25 0 0 0 -225 0 0 37
99   PX  0
100  PZ  37
101  SQ  1.78 64 1 0 0 0 -16 -2 -6 60.5
102  SQ  2.08 1 1.39 0 0 0 -96.04 0 0 85.5
103  GQ  1 1 .0091 0 0 -.2005 -20 0 1.7857 87.75
104  GQ  1 1 .0091 0 0 .2005 20 0 1.7857 87.75
105  SQ  100 900 9 0 0 0 -225 4.5 6.5 38
106  SQ  100 900 9 0 0 0 -225 -4.5 6.5 38
107  SQ  1.39 .5 2 0 0 0 -70 -6.5 -3 50
108  SQ  1.39 .5 2 0 0 0 -70 6.5 -3 50
109  PX  17
110  PX  6
111  PX  -6
112  PX  -17
113  GQ  503.01 135.24 0 0 0 10.206 -19215 0 -202.0788 183257
114  GQ  503.01 135.24 0 0 0 -10.206 19215 0 -202.0788 183257
115  PZ  69
116  SQ  1 3.7589 0 0 0 0 -361 0 0 0
117  PZ  50.9
118  P   0.25 -1 0 0
119  P   0.8 -1 0 0
120  P   -0.25 -1 0 0
121  P   -0.8 -1 0 0
122  TZ  0 11.1 68.25 20 0.7883 0.7883
123  P   0.89415 1 0 11.1
124  P   7.0342 1 0 11.1
125  P   -0.89415 1 0 11.1
126  P   -7.0342 1 0 11.1
C    2 concentric elliptical cylinders and planes to define eye lenses
127  SQ  100 64 0 0 0 0 -6400 0 0 0
128  SQ  88.36 40.96 0 0 0 0 -3619.2256 0 0 0
129  PX  2
130  PX  4
131  PX  -2
132  PX  -4
133  PZ  82.5
134  PZ  84.5
C    segmenting planes for RBM regions in leg and arm bones
135  PZ  -22.8
136  PZ  52.6
C    Oesophagus
137  SQ 0.16 1.0 0 0 0 0 0 -0.16 0.5 2.5 0                    $ Oesophagus Exterior
C    Colon Wall
138  SQ 1 1 0 0 0 0 0 -3.209 -8.5 -2.36 0                    $ Ascending Colon Interior
139  SQ 0 0.9467 3.8927 0 0 0 -3.6854 0 -2.36 25.5
140  GQ 1.796 2.496 0.0674 0 0.818 -0.066 -30.75 -7.12 -0.602 132.2
```

```
141   TY 3 0 8.72 5.72 0.91 0.91                    $ Upper Sigmoid Interior
142   TY 3 0 0 3 0.91 0.91                          $ Lower Sigmoid Interior
C Boxes for Detectors
900 900 BOX 0.39 10.9607 38.36   -17.78 0 0 &
      0 50.8 0      0 0 17.78
901 901 BOX 0.39 -10.9609 38.35  -17.78 0 0 &
      0 -50.8 0     0 0 17.80
902 BOX -8.89 -10 70.01  17.78 0 0  0 -50.8 0   0 0 17.78
903 903 BOX 19.98 -8.89 0  50.8 0 0  0 17.78 0  0 0 -17.78
c
c c
c Detector in Box 900
c c
c
501  501 RCC 0.6 0 0 1.19 0 0 2.5297
c  inner detector casing
502  501 RCC 0.4175 0 0 1.5494 0 0 2.6797
c  air cutout in the inner casing
503  501 RCC 0.4175 0 0 0.05 0 0 2.2225
c  outer detector head
505  501 RCC 0 0 0      2.54   0 0 3.4925
c  air cutout in outer casing
506  501 RCC 0 0 0      0.4175 0 0 2.54
c detector casing
507  501 RPP -0.01 2.55 -3.5 3.5 -3.5 3.5
c
c c
c Detector in Box 901
c c
c
511  502 RCC 0.6 0 0 1.19 0 0 2.5297
c  inner detector casing
512  502 RCC 0.4175 0 0 1.5494 0 0 2.6797
c  air cutout in the inner casing
513  502 RCC 0.4175 0 0 0.05 0 0 2.2225
c  outer detector head
515  502 RCC 0 0 0      2.54   0 0 3.4925
c  air cutout in outer casing
516  502 RCC 0 0 0      0.4175 0 0 2.54
c detector casing
517  502 RPP -0.01 2.55 -3.5 3.5 -3.5 3.5
c
c c
c Detector in Box 902
c c
c
521  503 RCC 0.6 0 0 1.19 0 0 2.5297
c  inner detector casing
522  503 RCC 0.4175 0 0 1.5494 0 0 2.6797
c  air cutout in the inner casing
523  503 RCC 0.4175 0 0 0.05 0 0 2.2225
c  outer detector head
525  503 RCC 0 0 0      2.54   0 0 3.4925
c  air cutout in outer casing
526  503 RCC 0 0 0      0.4175 0 0 2.54
c detector casing
```

```
527  503 RPP -0.01 2.55 -3.5 3.5 -3.5 3.5
c
c c
c Detector in Box 903
c c
c
531  504 RCC 0.6 0 0 1.19 0 0 2.5297
c  inner detector casing
532  504 RCC 0.4175 0 0 1.5494 0 0 2.6797
c  air cutout in the inner casing
533  504 RCC 0.4175 0 0 0.05 0 0 2.2225
c  outer detector head
535  504 RCC 0 0 0      2.54   0 0 3.4925
c  air cutout in outer casing
536  504 RCC 0 0 0      0.4175 0 0 2.54
c detector casing
537  504 RPP -0.01 2.55 -3.5 3.5 -3.5 3.5

C Data Cards
tr600 -0.1
tr601 0.1
tr602 -0.15
tr603 0.15
tr604 -0.051
tr605 0.051
tr900 0 -0.2 0 0.973527 0.228573 0 -0.228573 0.973527 0 0 0 1
tr901 0 0.2 0 0.973527 -0.228573 0 0.228573 0.973527 0 0 0 1
tr903 -0.35 0 0 0.979903 0 -0.199474 0 1 0 0.199474 0 0.979903
tr501 -8.7 9.05 47.5 -0.229 0.973 0 -0.973 -0.229 0 0 0 1
tr502 -8.7 -9.05 47.5 -0.229 -0.973 0 0.973 -0.229 0 0 0 1
tr503 0 -10.03 78.88 0 -1 0 1 0 0 0 0 1
tr504 17.55 0 -12.5 .982 0 -.191 0 1 0 .191 0 .982
IMP:P 1 90R 0
IMP:E 0 64R 1 1 0 0 0 0 1 19R 0
C
C Sources
SDEF  PAR=2  ERG=D1  CEL=D2  RAD=fcel=D3  &
     POS=fcel=D4  EXT=fcel=D5  AXS=fcel=D6
SI1 L 1.173 1.332
SP1 0.9985 0.999826
C Left Lung, Right Lung, Stomach, Small Int., Heart, Ascending Colon,
C Sigmoid Colon, Transvers Colon, Descending Colon, Bladder,
C Body Tissue (3, 4, 5, 6, 7, 8, 21, 22, 23, 25), Liver
SI2 L 2 24 29 40 28 30 31 32 33 45 3 4 5 6 7 8 21 22 23 25 27
SP2 D 1 1  1  1  1  1  1  1  1  1  1 1 1 1 1 1 1 1  1  1  1  1
DS3 S 7 8 9 10 11 12 13 14 15 16 17 18 19 20 21 22 23 24 25 26 27
DS4 L 8.5 0 43.4   -8.5 0 43.4   8 -4 35   0 -3.8 11.3   -1 -3 51   &
     -8.5 -2.36 14.35   5 0 -0.1   -10.6 -2.36 25.5   8.72 0 8.52  &
     0 -4.5 8   0 0 42.9   0 0 50.8   0 0 42.9   0 0 26.9          &
     0 0 11.9   0 0 -0.1   0 0 69.9   10.5 0 -80.1   -10.5 0 -80.1 &
     0 -8 -4.9   0 0 26.9
DS5 S 30 31 0 32 0 33 34 35 36 0 37 38 39 40 41 42 43 44 45 46 47
DS6 L 0 0 1   0 0 1   0 0 0   0 0 1   0 0 0   0 0 1   0 0 1 &
     1 0 0   0 0 1   0 0 0   0 0 1   0 0 1   0 0 1   0 0 1 &
     0 0 1   0 0 1   0 0 1   0 0 1   0 0 1   0 0 1   0 0 1
SI7  0 7.6
```

```
SP7  -21 1
SI8  0 7.6
SP8  -21 1
SI9  0 8.2
SP9  -21 2
SI10 0 11.4
SP10 -21 1
SI11 0 8.2
SP11 -21 2
SI12 0 2.6
SP12 -21 1
SI13 0 7.1
SP13 -21 1
SI14 0 3.85
SP14 -21 1
SI15 0 4
SP15 -21 1
SI16 0 5.2
SP16 -21 2
SI17 0 20.2
SP17 -21 1
SI18 0 20.3
SP18 -21 1
SI19 0 20.3
SP19 -21 1
SI20 0 20.3
SP20 -21 1
SI21 0 20.3
SP21 -21 1
SI22 0 20.3
SP22 -21 1
SI23 0 10.1
SP23 -21 1
SI24 0 11
SP24 -21 1
SI25 0 11
SP25 -21 1
SI26 0 8.1
SP26 -21 1
SI27 0 16.6
SP27 -21 1
SI30 0 24.6
SP30 -21 0
SI31 0 24.6
SP31 -21 0
SI32 0 10.2
SP32 -21 0
SI33 0 9.75
SP33 -21 0
SI34 0 8.92
SP34 -21 0
SI35 0 21.2
SP35 -21 0
SI36 0 16
SP36 -21 0
SI37 0 27.2
```

```
SP37 -21 0
SI38 0 16.6
SP38 -21 0
SI39 0 8.1
SP39 -21 0
SI40 0 16.2
SP40 -21 0
SI41 0 15.2
SP41 -21 0
SI42 0 12.2
SP42 -21 0
SI43 0 24.2
SP43 -21 0
SI44 0 80.2
SP44 -21 0
SI45 0 80.2
SP45 -21 0
SI46 0 5
SP46 -21 0
SI47 0 16.2
SP47 -21 0
C
C Tally Cards
c Back Right Lung
F8:P,E 501
E8 0 10I 1.59E-3 1000I 1.3
FT8 SCX 2
c Front Right Lung
F18:P,E 511
E18 0 10I 1.59E-3 1000I 1.3
FT18 SCX 2
c Front Neck Under Chin
F28:P,E 521
E28 0 10I 1.59E-3 1000I 1.3
FT28 SCX 2
c Outer Left Leg
F38:P,E 531
E38 0 10I 1.59E-3 1000I 1.3
FT38 SCX 2
C
C Material Cards
C       THIS IS THE COMPOSITION FOR AIR
M1    7014 -.7558 8016 -.2314 18000 -.0128
C      THIS IS THE COMPOSITION FOR LUNG TISSUE
M2    1001 -.1021
      6012 -.1001
      7014 -.0280
      8016 -.7596
     11023 -.0019
     15031 -.0008
     16032 -.0023
     17000 -.0027
     19000 -.0020
     20000 -.0001
     26000 -.0004
C       THE COMPOSITION FOR TOTAL BODY MINUS SKELETON AND LUNGS
```

```
M3    1001 -.1047
      6012 -.2302
      7014 -.0234
      8016 -.6321
     11023 -.0013
     12000 -.0002
     15031 -.0024
     16032 -.0022
     17000 -.0014
     19000 -.0021
C     THE COMPOSITION FOR SKELETAL TISSUE
M4    1001 -.0704
      6012 -.2279
      8016 -.4856
      7014 -.0387
     11023 -.0032
     12000 -.0011
     15031 -.0694
     16032 -.0017
     17000 -.0014
     19000 -.0015
     20000 -.0991
c     Adult Tissues (Density = 1.04 g/cc)
M5       1001  -0.10454
         6012  -0.22663
         7014  -0.02490
         8016  -0.63525
        11023  -0.00112
        12000  -0.00013
        14000  -0.00030
        15031  -0.00134
        16032  -0.00204
        17000  -0.00133
        19000  -0.00208
        20000  -0.00024
        26000  -0.00005
        30000  -0.00003
        37085  -0.000007217
        37087  -0.000002783
        40000  -0.00001
c Detectors Materials
M501  10000.04p 1 $ Neon Fill Gas
M502  7000.04p .78 8000.04p .21 18000.04p .01 $ AIR
M503  13000.04p 1 $ Aluminum
M504  19000.04p .043 13000.04p .087 14000.04p .174 8000.04p .522
      1000.04p .087 9000.04p .087 $ Mica
c STOP NPS 1E8 F38 0.01
NPS 2E9
c RAND GEN=2 SEED=1561615651
PHYS:P 4J 1
PRINT
MODE P E
```

APPENDIX C: COUNT RATE PER CDL FOR MIRD PHANTOMS

Some notes on the data:

- Tabulated Data are for the Posterior Upper Right Torso location
- BR Lung – Back Right Lung (Posterior Upper Right Torso)
- FR Lung – Front Right Lung (Anterior Upper Right Torso)
- L Leg – Left Leg (Lateral Upper Thigh)
- F Neck – Front Neck (Posterior Neck)

CONTENTS OF APPENDIX C

Reference Male – Co-60

Co-60 M	Total Count Rate above BG (kcpm)		MDA (µCi)		Background Limit (kcpm)	
Time (days)	Ludlum 2	Ludlum 3	Ludlum 2	Ludlum 3	Ludlum 2	Ludlum 3
0.00	3.12	3.56	10.83	9.50	4.37	4.98
0.25	1.83	2.08	18.49	16.22	2.56	2.92
0.50	1.69	1.92	20.03	17.57	2.36	2.69
1.00	1.46	1.66	23.19	20.34	2.04	2.32
2.00	1.21	1.38	27.88	24.46	1.70	1.93
3.00	1.10	1.26	30.63	26.87	1.54	1.76
4.00	1.05	1.19	32.28	28.31	1.47	1.67
5.00	1.01	1.15	33.39	29.29	1.42	1.61
6.00	0.99	1.12	34.28	30.07	1.38	1.57
7.00	0.96	1.10	35.05	30.74	1.35	1.54
8.00	0.94	1.08	35.77	31.37	1.32	1.51
9.00	0.93	1.06	36.45	31.97	1.30	1.48
10.00	0.91	1.04	37.11	32.55	1.27	1.45
20.00	0.79	0.90	42.75	37.50	1.11	1.26
30.00	0.71	0.81	47.34	41.52	1.00	1.14

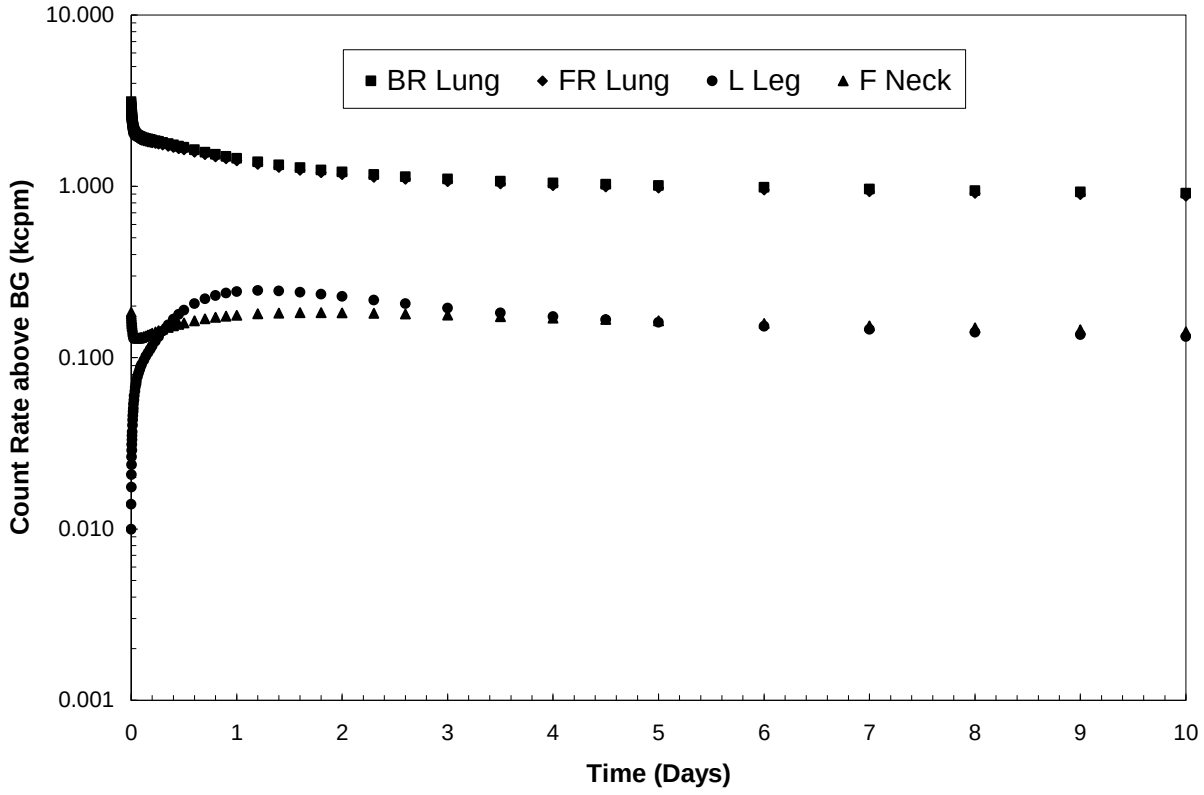

Reference Male – Cs-137

Cs-137 F	Total Count Rate above BG (kcpm)		MDA (µCi)		Background Limit (kcpm)	
Time (days)	Ludlum 2	Ludlum 3	Ludlum 2	Ludlum 3	Ludlum 2	Ludlum 3
0.00	1.51	1.72	48.70	42.72	2.11	2.41
0.25	1.26	1.44	58.21	51.06	1.77	2.01
0.50	1.42	1.62	51.74	45.38	1.99	2.27
1.00	1.48	1.69	49.62	43.53	2.07	2.36
2.00	1.39	1.59	52.75	46.27	1.95	2.22
3.00	1.33	1.51	55.43	48.62	1.86	2.11
4.00	1.29	1.47	57.11	50.10	1.80	2.05
5.00	1.26	1.44	58.25	51.09	1.77	2.01
6.00	1.24	1.42	59.10	51.84	1.74	1.98
7.00	1.23	1.40	59.79	52.45	1.72	1.96
8.00	1.22	1.39	60.39	52.98	1.70	1.94
9.00	1.21	1.37	60.93	53.45	1.69	1.92
10.00	1.20	1.36	61.43	53.88	1.67	1.91
20.00	1.12	1.27	65.73	57.66	1.56	1.78
30.00	1.05	1.19	70.06	61.46	1.47	1.67

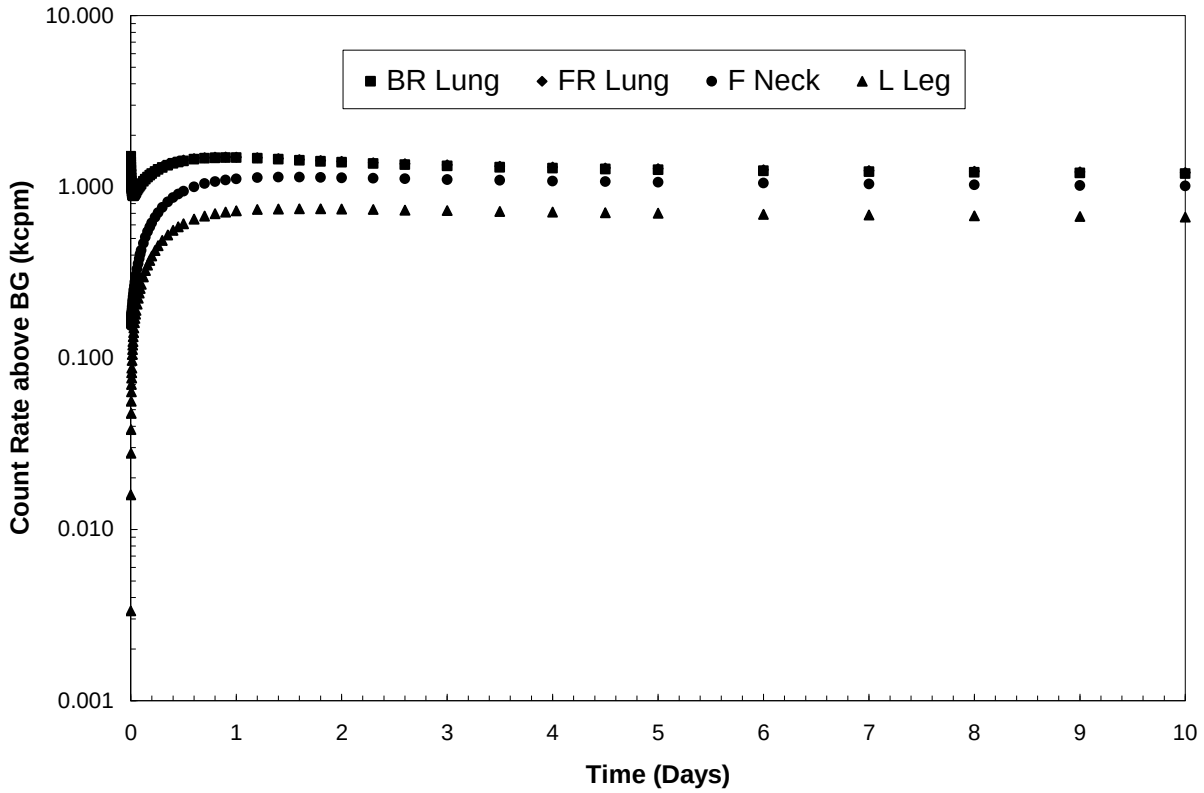

Reference Male – I-131

I-131 F	Total Count Rate above BG (kcpm)		MDA (µCi)		Background Limit (kcpm)	
Time (days)	Ludlum 2	Ludlum 3	Ludlum 2	Ludlum 3	Ludlum 2	Ludlum 3
0.00	5.05	5.76	9.03	7.93	7.07	8.07
0.25	1.50	1.71	30.41	26.68	2.10	2.40
0.50	1.07	1.22	42.73	37.48	1.50	1.71
1.00	0.56	0.64	80.88	70.95	0.79	0.90
2.00	0.18	0.21	251.28	220.42	0.25	0.29
3.00	0.06	0.07	715.80	627.89	0.09	0.10
4.00	0.03	0.03	1821.13	1597.48	0.04	0.04
5.00	0.01	0.01	3691.37	3238.04	0.02	0.02
6.00	0.01	0.01	5504.19	4828.24	0.01	0.01
7.00	0.01	0.01	6488.34	5691.53	0.01	0.01
8.00	0.01	0.01	6862.41	6019.66	0.01	0.01
9.00	0.01	0.01	7019.23	6157.22	0.01	0.01
10.00	0.01	0.01	7147.18	6269.45	0.01	0.01
20.00	0.00	0.00	11305.41	9917.03	0.01	0.01
30.00	0.00	0.00	23388.03	20515.82	0.00	0.00

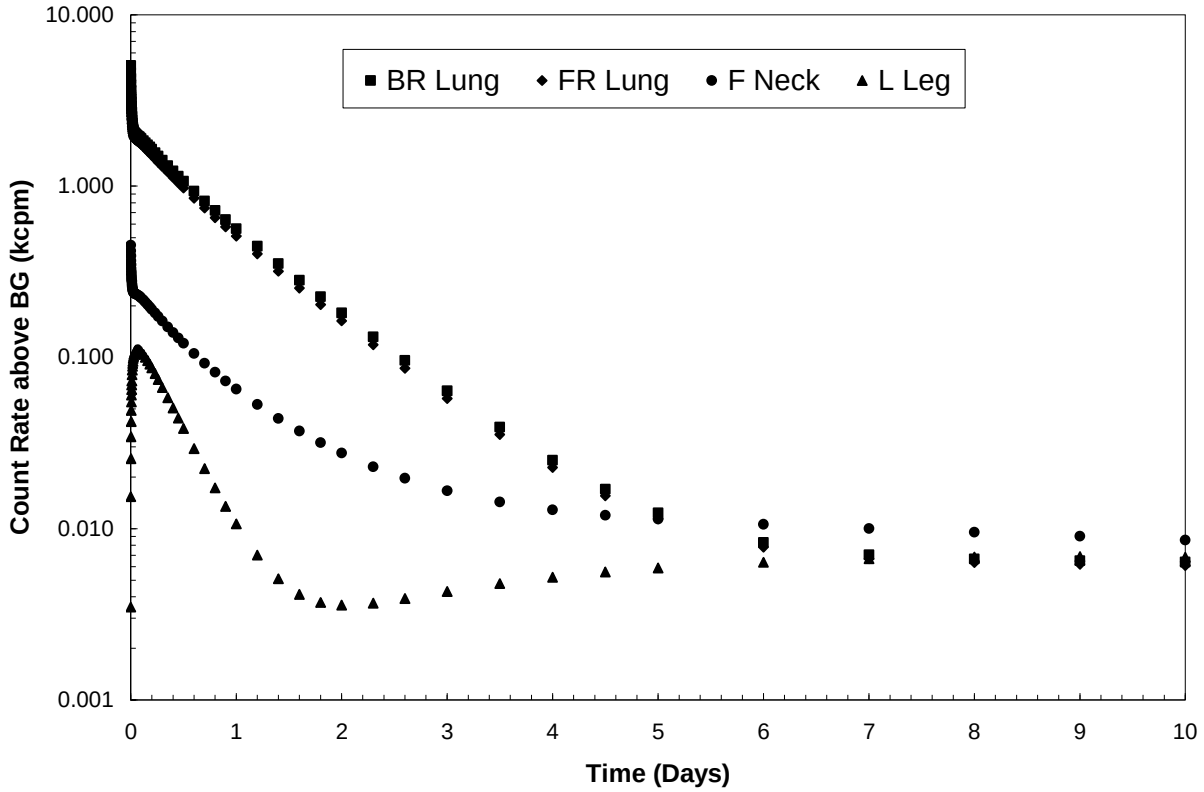

Reference Male – Ir-192

Ir-192 M	Total Count Rate above BG (kcpm)		MDA (µCi)		Background Limit (kcpm)	
Time (days)	Ludlum 2	Ludlum 3	Ludlum 2	Ludlum 3	Ludlum 2	Ludlum 3
0.00	3.76	4.29	17.3	15.1	5.27	6.01
0.25	2.12	2.42	30.6	26.9	2.97	3.38
0.50	1.95	2.22	33.3	29.2	2.73	3.11
1.00	1.67	1.90	38.9	34.1	2.34	2.66
2.00	1.36	1.55	47.9	42.0	1.90	2.17
3.00	1.22	1.40	53.0	46.5	1.71	1.96
4.00	1.16	1.33	55.9	49.0	1.63	1.86
5.00	1.13	1.29	57.6	50.5	1.58	1.80
6.00	1.10	1.26	58.9	51.7	1.54	1.76
7.00	1.08	1.23	60.1	52.7	1.51	1.73
8.00	1.06	1.21	61.2	53.7	1.49	1.69
9.00	1.04	1.19	62.3	54.6	1.46	1.67
10.00	1.03	1.17	63.3	55.6	1.44	1.64
20.00	0.87	1.00	74.3	65.2	1.22	1.40
30.00	0.76	0.86	86.0	75.4	1.06	1.21

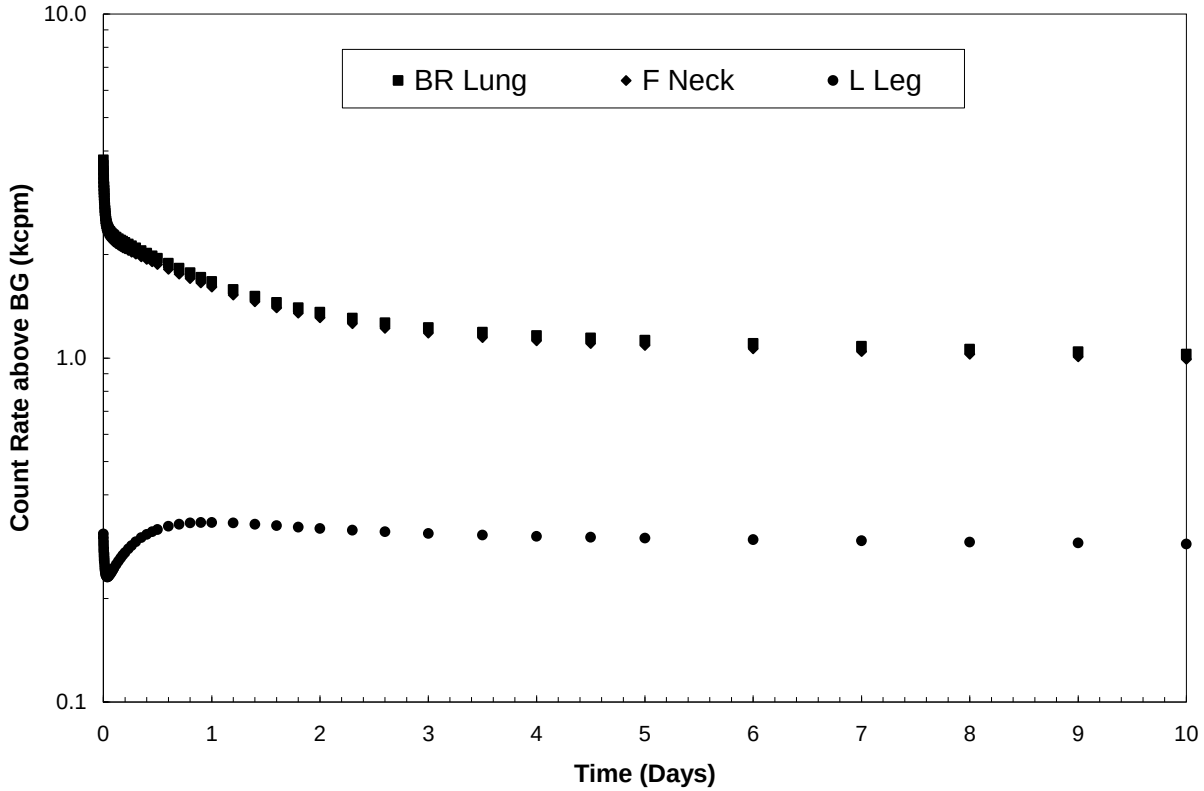

Reference Female – Co-60

Co-60 M	Total Count Rate above BG (kcpm)		MDA (µCi)		Background Limit (kcpm)	
Time (days)	Ludlum 2	Ludlum 3	Ludlum 2	Ludlum 3	Ludlum 2	Ludlum 3
0.00	3.13	3.56	10.81	9.48	4.38	4.99
0.25	1.77	2.02	19.04	16.71	2.48	2.83
0.50	1.65	1.88	20.46	17.95	2.31	2.63
1.00	1.46	1.66	23.19	20.34	2.04	2.33
2.00	1.24	1.42	27.19	23.85	1.74	1.98
3.00	1.14	1.30	29.61	25.97	1.60	1.82
4.00	1.09	1.24	31.12	27.29	1.52	1.73
5.00	1.05	1.20	32.18	28.23	1.47	1.68
6.00	1.02	1.17	33.04	28.98	1.43	1.63
7.00	1.00	1.14	33.80	29.65	1.40	1.60
8.00	0.98	1.12	34.50	30.27	1.37	1.56
9.00	0.96	1.09	35.18	30.86	1.34	1.53
10.00	0.94	1.08	35.82	31.42	1.32	1.51
20.00	0.82	0.93	41.31	36.23	1.15	1.31
30.00	0.74	0.84	45.67	40.06	1.04	1.18

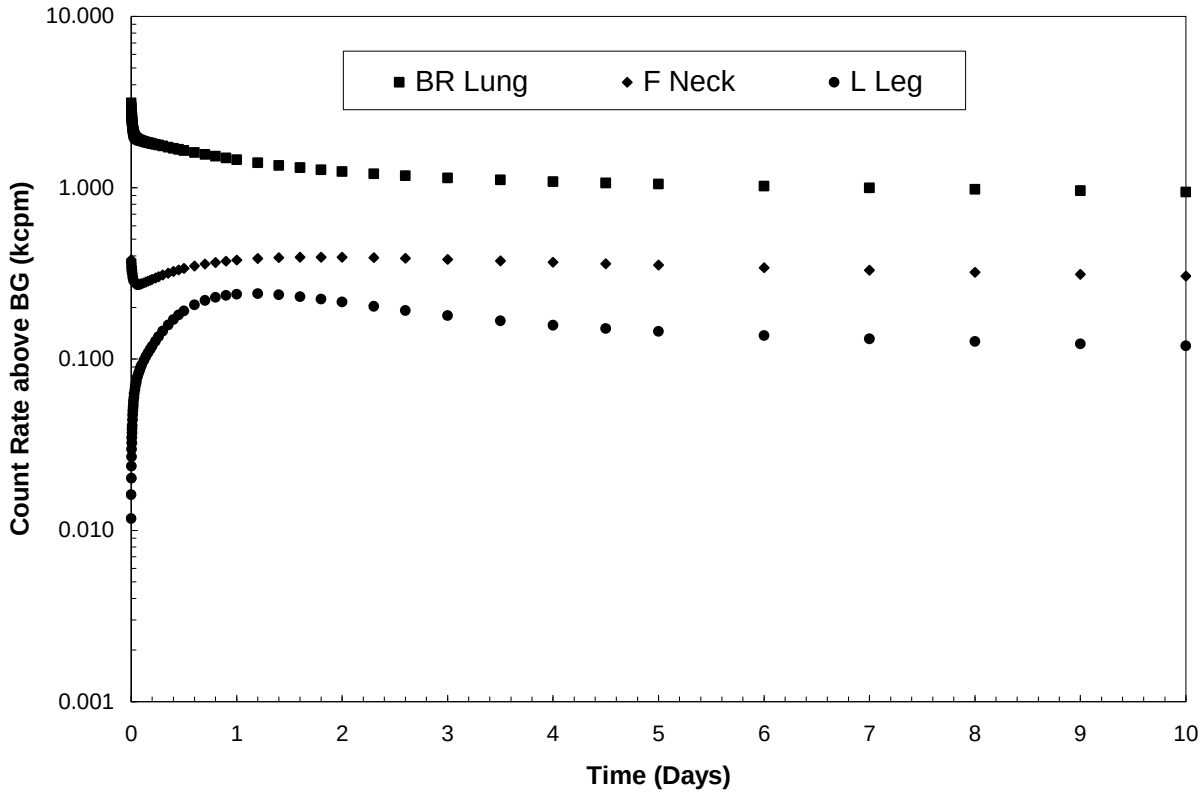

Reference Female – Cs-137

Cs-137 F	Total Count Rate above BG (kcpm)		MDA (µCi)		Background Limit (kcpm)	
Time (days)	Ludlum 2	Ludlum 3	Ludlum 2	Ludlum 3	Ludlum 2	Ludlum 3
0.00	2.07	2.36	35.52	31.16	2.90	3.31
0.25	1.56	1.78	47.27	41.46	2.18	2.49
0.50	1.61	1.83	45.81	40.19	2.25	2.57
1.00	1.56	1.78	47.09	41.31	2.19	2.50
2.00	1.42	1.62	51.97	45.59	1.98	2.26
3.00	1.33	1.52	55.22	48.44	1.87	2.13
4.00	1.29	1.47	57.15	50.13	1.80	2.06
5.00	1.26	1.44	58.40	51.23	1.77	2.01
6.00	1.24	1.42	59.31	52.03	1.74	1.98
7.00	1.23	1.40	60.04	52.67	1.72	1.96
8.00	1.21	1.38	60.66	53.21	1.70	1.94
9.00	1.20	1.37	61.22	53.70	1.68	1.92
10.00	1.19	1.36	61.72	54.14	1.67	1.90
20.00	1.11	1.27	66.07	57.96	1.56	1.78
30.00	1.05	1.19	70.42	61.78	1.46	1.67

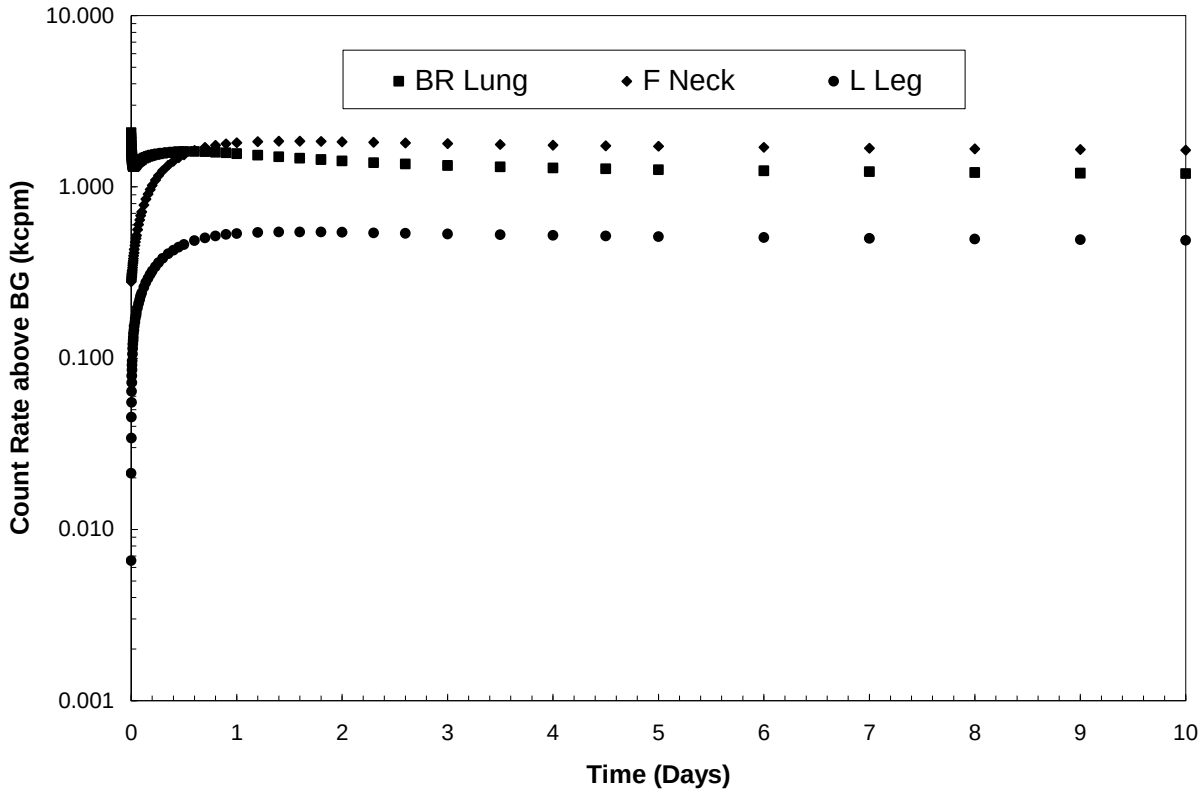

Reference Female – I-131

I-131 F	Total Count Rate above BG (kcpm)		MDA (µCi)		Background Limit (kcpm)	
Time (days)	Ludlum 2	Ludlum 3	Ludlum 2	Ludlum 3	Ludlum 2	Ludlum 3
0.00	1.35	1.54	33.71	29.57	1.90	2.16
0.25	0.53	0.60	86.87	76.21	0.74	0.84
0.50	0.36	0.41	127.28	111.65	0.50	0.57
1.00	0.18	0.21	247.46	217.07	0.26	0.29
2.00	0.07	0.08	645.74	566.44	0.10	0.11
3.00	0.04	0.04	1182.93	1037.66	0.05	0.06
4.00	0.03	0.03	1627.30	1427.45	0.04	0.04
5.00	0.02	0.03	1879.20	1648.42	0.03	0.04
6.00	0.02	0.03	2013.75	1766.45	0.03	0.04
7.00	0.02	0.02	2106.88	1848.14	0.03	0.03
8.00	0.02	0.02	2194.38	1924.89	0.03	0.03
9.00	0.02	0.02	2289.96	2008.73	0.03	0.03
10.00	0.02	0.02	2398.52	2103.97	0.03	0.03
20.00	0.01	0.01	4499.60	3947.02	0.01	0.02
30.00	0.00	0.01	9871.98	8659.64	0.01	0.01

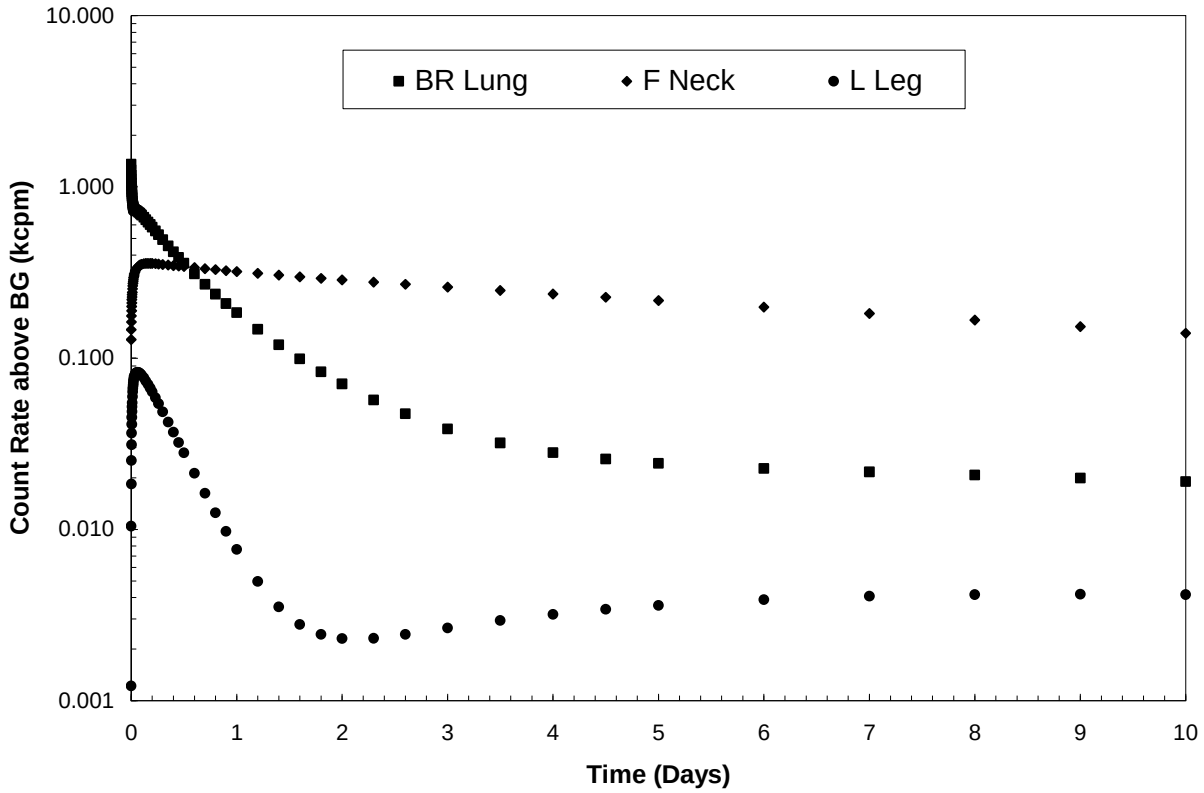

Reference Female – Ir-192

Ir-192 M	Total Count Rate above BG (kcpm)		MDA (µCi)		Background Limit (kcpm)	
Time (days)	Ludlum 2	Ludlum 3	Ludlum 2	Ludlum 3	Ludlum 2	Ludlum 3
0.00	3.77	4.29	17.24	15.13	5.27	6.01
0.25	2.97	3.39	21.84	19.16	4.16	4.75
0.50	3.03	3.45	21.46	18.82	4.24	4.83
1.00	2.59	2.96	25.04	21.96	3.63	4.14
2.00	1.81	2.06	35.87	31.47	2.54	2.89
3.00	1.43	1.63	45.53	39.94	2.00	2.28
4.00	1.26	1.44	51.59	45.25	1.76	2.01
5.00	1.18	1.35	54.92	48.18	1.66	1.89
6.00	1.14	1.30	56.90	49.91	1.60	1.82
7.00	1.11	1.27	58.29	51.13	1.56	1.78
8.00	1.09	1.25	59.45	52.15	1.53	1.74
9.00	1.07	1.22	60.54	53.10	1.50	1.71
10.00	1.05	1.20	61.59	54.02	1.48	1.68
20.00	0.90	1.03	72.19	63.32	1.26	1.44
30.00	0.78	0.89	83.45	73.20	1.09	1.24

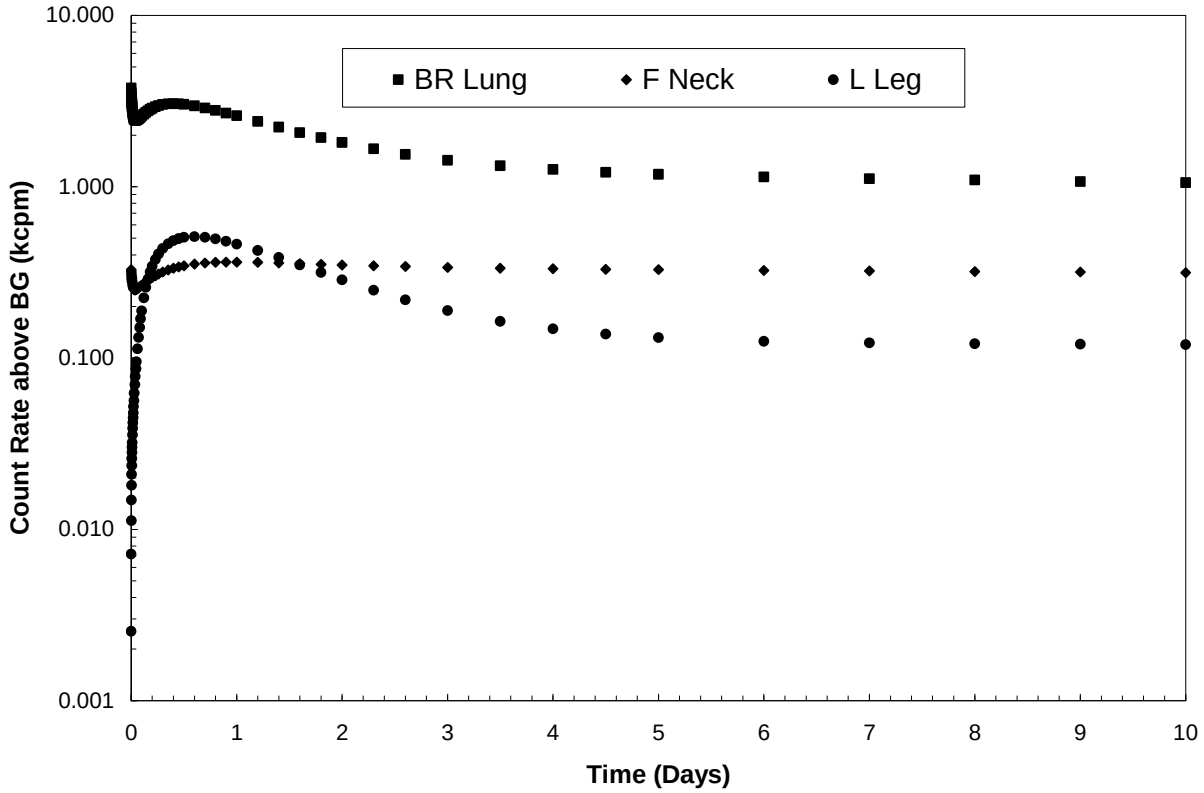

Adipose Male – Co-60

Co-60 M	Total Count Rate above BG (kcpm)		MDA (µCi)		Background Limit (kcpm)	
Time (days)	Ludlum 2	Ludlum 3	Ludlum 2	Ludlum 3	Ludlum 2	Ludlum 3
0.00	2.05	2.34	16.45	14.43	2.87	3.28
0.25	1.21	1.38	27.93	24.50	1.69	1.93
0.50	1.13	1.29	29.79	26.13	1.59	1.81
1.00	1.01	1.15	33.56	29.43	1.41	1.61
2.00	0.86	0.98	39.18	34.37	1.21	1.38
3.00	0.79	0.90	42.64	37.40	1.11	1.26
4.00	0.75	0.86	44.83	39.33	1.06	1.20
5.00	0.73	0.83	46.40	40.70	1.02	1.16
6.00	0.71	0.81	47.68	41.82	0.99	1.13
7.00	0.69	0.79	48.81	42.82	0.97	1.10
8.00	0.68	0.77	49.87	43.74	0.95	1.08
9.00	0.66	0.76	50.87	44.63	0.93	1.06
10.00	0.65	0.74	51.84	45.47	0.91	1.04
20.00	0.56	0.64	59.85	52.50	0.79	0.90
30.00	0.51	0.58	66.03	57.92	0.72	0.82

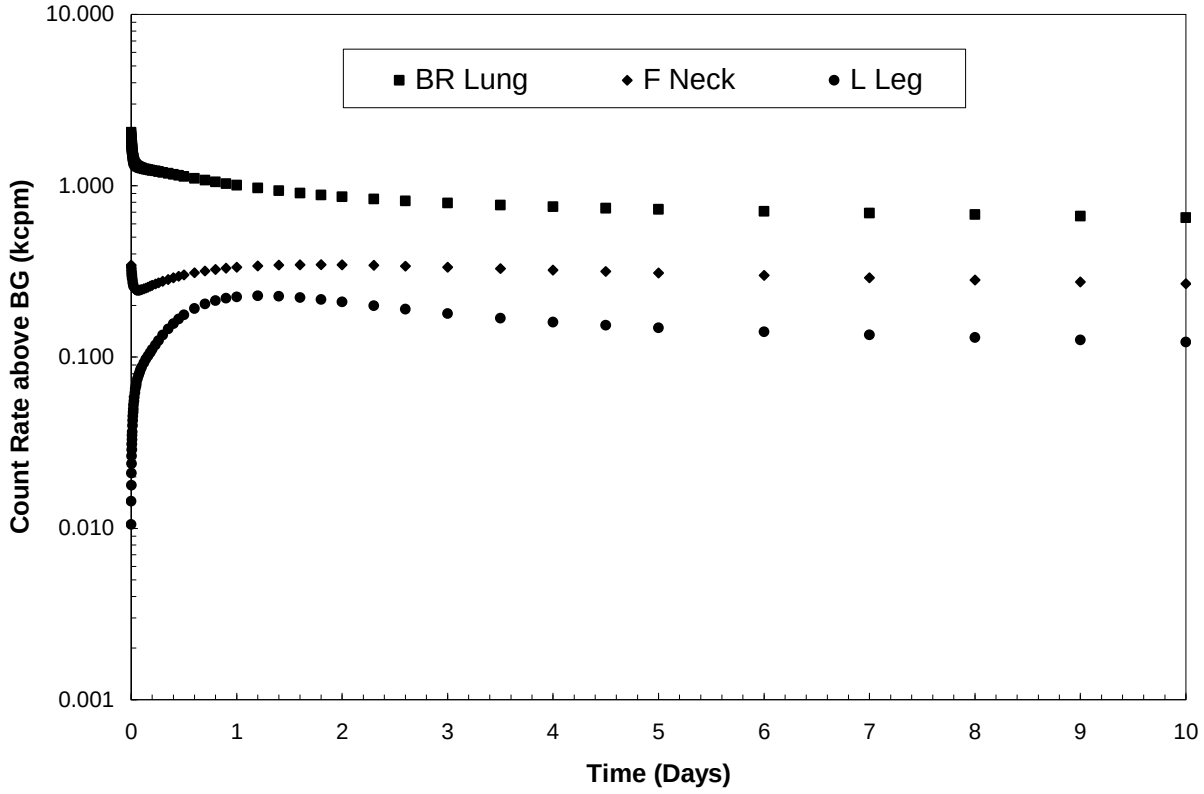

Adipose Male – Cs-137

Cs-137 F	Total Count Rate above BG (kcpm)		MDA (µCi)		Background Limit (kcpm)	
Time (days)	Ludlum 2	Ludlum 3	Ludlum 2	Ludlum 3	Ludlum 2	Ludlum 3
0.00	0.97	1.11	75.85	66.53	1.36	1.55
0.25	0.98	1.11	75.34	66.09	1.37	1.56
0.50	1.14	1.30	64.46	56.54	1.60	1.82
1.00	1.23	1.40	59.94	52.58	1.72	1.96
2.00	1.18	1.34	62.43	54.76	1.65	1.88
3.00	1.13	1.29	65.14	57.14	1.58	1.80
4.00	1.10	1.25	66.93	58.71	1.54	1.76
5.00	1.08	1.23	68.19	59.82	1.51	1.72
6.00	1.06	1.21	69.16	60.67	1.49	1.70
7.00	1.05	1.20	69.96	61.37	1.47	1.68
8.00	1.04	1.19	70.66	61.98	1.46	1.66
9.00	1.03	1.18	71.29	62.53	1.45	1.65
10.00	1.02	1.17	71.87	63.04	1.43	1.64
20.00	0.96	1.09	76.91	67.46	1.34	1.53
30.00	0.90	1.02	81.97	71.91	1.26	1.43

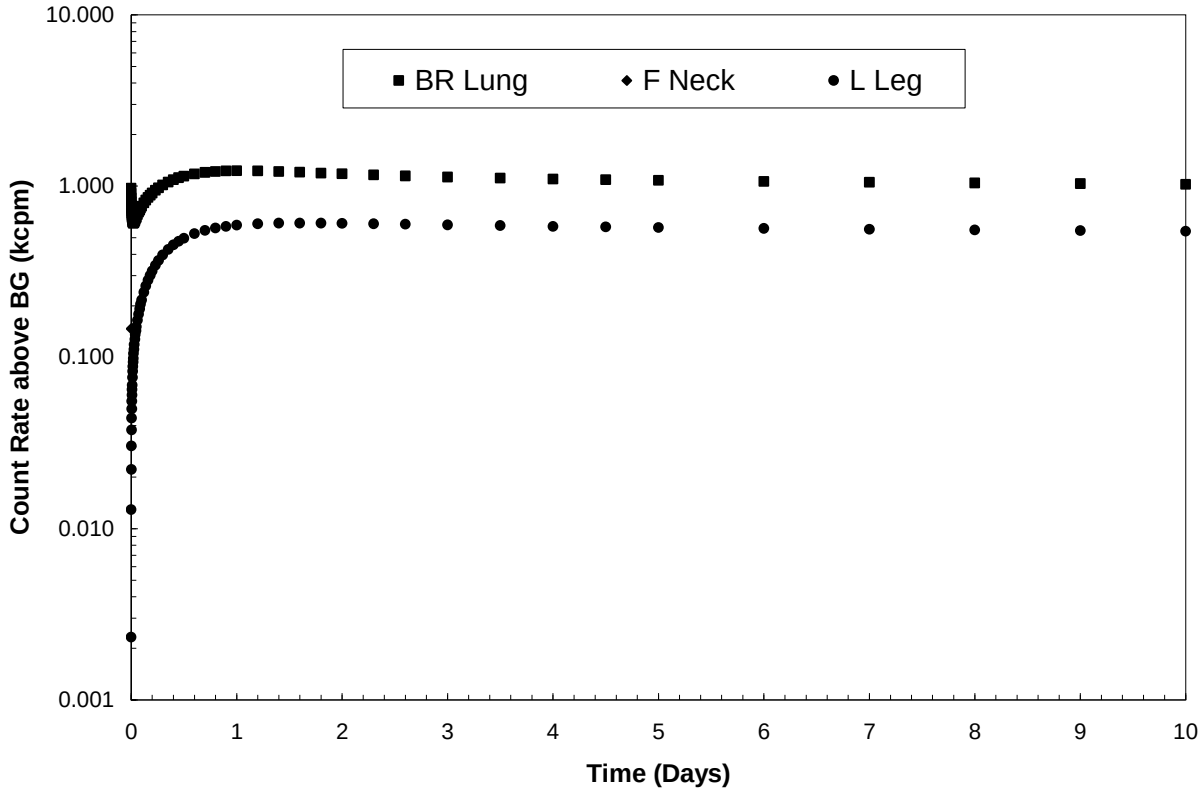

Adipose Male – I-131

I-131 F	Total Count Rate above BG (kcpm)		MDA (µCi)		Background Limit (kcpm)	
Time (days)	Ludlum 2	Ludlum 3	Ludlum 2	Ludlum 3	Ludlum 2	Ludlum 3
0.00	0.87	0.99	52.58	46.12	1.22	1.39
0.25	0.35	0.40	130.58	114.54	0.49	0.56
0.50	0.24	0.27	193.61	169.84	0.33	0.38
1.00	0.12	0.14	383.90	336.75	0.17	0.19
2.00	0.04	0.05	1020.57	895.23	0.06	0.07
3.00	0.02	0.03	1873.76	1643.65	0.03	0.04
4.00	0.02	0.02	2557.61	2243.52	0.02	0.03
5.00	0.02	0.02	2919.83	2561.26	0.02	0.02
6.00	0.01	0.02	3095.27	2715.15	0.02	0.02
7.00	0.01	0.02	3209.13	2815.03	0.02	0.02
8.00	0.01	0.02	3317.36	2909.97	0.02	0.02
9.00	0.01	0.02	3440.11	3017.64	0.02	0.02
10.00	0.01	0.01	3583.98	3143.85	0.02	0.02
20.00	0.01	0.01	6538.10	5735.18	0.01	0.01
30.00	0.00	0.00	14196.73	12453.28	0.00	0.01

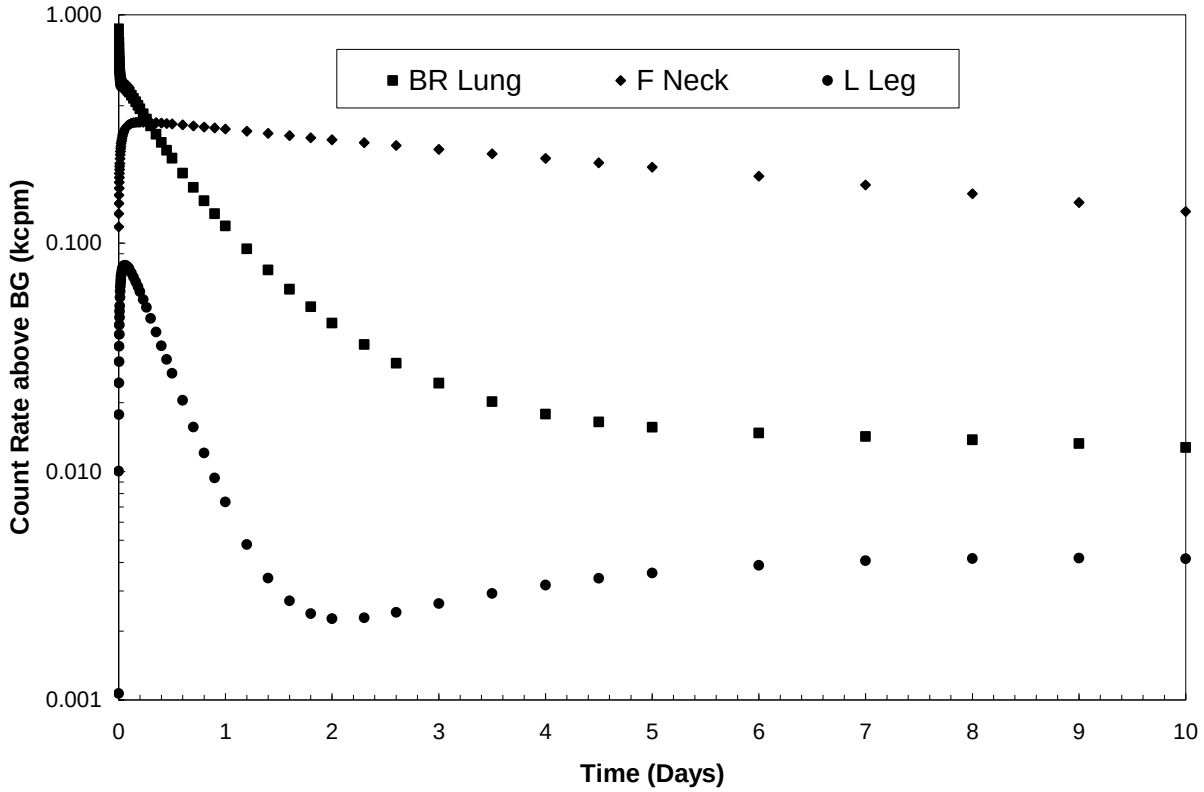

Adipose Male – Ir-192

Ir-192 M	Total Count Rate above BG (kcpm)		MDA (µCi)		Background Limit (kcpm)	
Time (days)	Ludlum 2	Ludlum 3	Ludlum 2	Ludlum 3	Ludlum 2	Ludlum 3
0.00	2.41	2.75	26.95	23.64	3.37	3.85
0.25	1.37	1.56	47.37	41.55	1.92	2.19
0.50	1.27	1.45	50.98	44.72	1.78	2.03
1.00	1.11	1.26	58.70	51.49	1.55	1.77
2.00	0.91	1.04	71.10	62.37	1.28	1.46
3.00	0.83	0.95	78.21	68.61	1.16	1.33
4.00	0.79	0.90	82.09	72.01	1.11	1.26
5.00	0.77	0.88	84.50	74.13	1.08	1.23
6.00	0.75	0.86	86.33	75.73	1.05	1.20
7.00	0.74	0.84	87.93	77.13	1.03	1.18
8.00	0.73	0.83	89.44	78.46	1.02	1.16
9.00	0.71	0.81	90.93	79.76	1.00	1.14
10.00	0.70	0.80	92.40	81.05	0.98	1.12
20.00	0.61	0.69	107.35	94.17	0.85	0.97
30.00	0.53	0.60	123.11	107.99	0.74	0.84

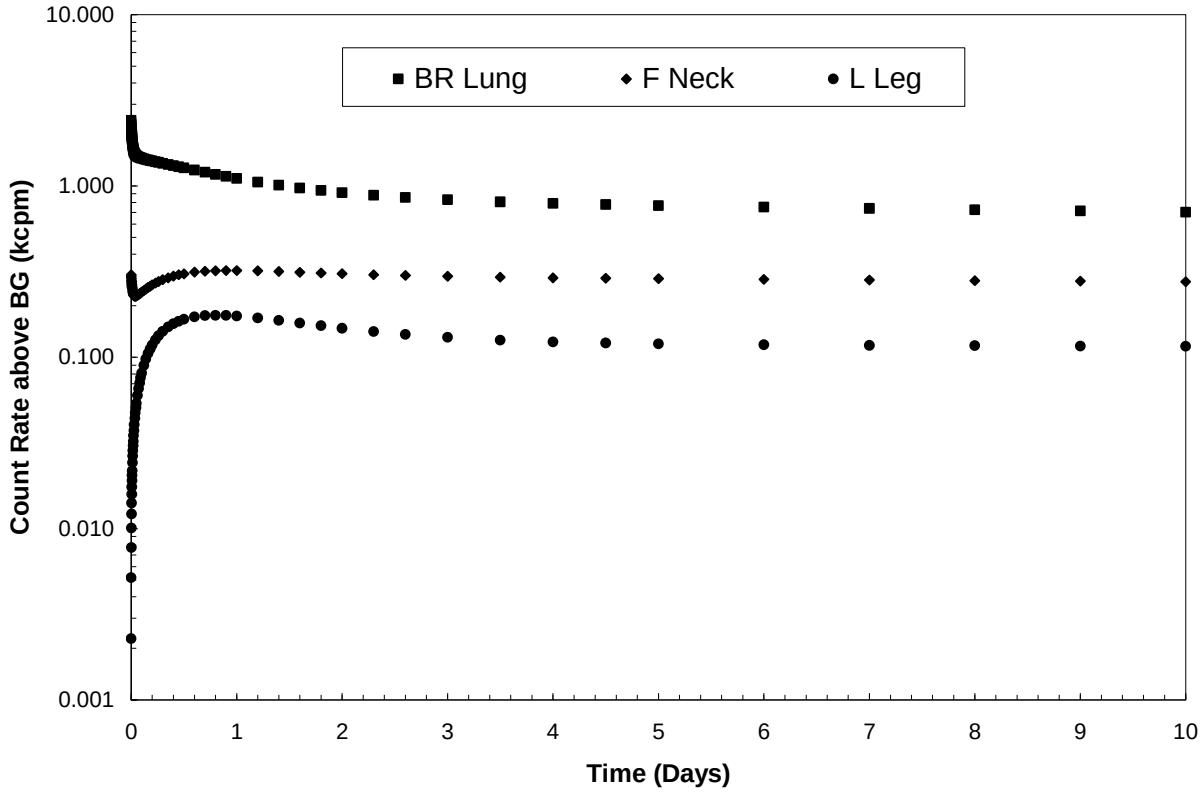

Adipose Female – Co-60

Co-60 M	Total Count Rate above BG (kcpm)		MDA (µCi)		Background Limit (kcpm)	
Time (days)	Ludlum 2	Ludlum 3	Ludlum 2	Ludlum 3	Ludlum 2	Ludlum 3
0.00	2.30	2.62	14.71	12.90	3.22	3.67
0.25	1.34	1.53	25.15	22.06	1.88	2.14
0.50	1.26	1.44	26.80	23.50	1.77	2.01
1.00	1.13	1.28	30.02	26.33	1.58	1.80
2.00	0.97	1.11	34.81	30.54	1.36	1.55
3.00	0.89	1.02	37.79	33.15	1.25	1.43
4.00	0.85	0.97	39.70	34.82	1.19	1.36
5.00	0.82	0.94	41.08	36.03	1.15	1.31
6.00	0.80	0.91	42.21	37.03	1.12	1.28
7.00	0.78	0.89	43.22	37.91	1.09	1.25
8.00	0.77	0.87	44.16	38.74	1.07	1.22
9.00	0.75	0.85	45.05	39.52	1.05	1.20
10.00	0.74	0.84	45.91	40.27	1.03	1.17
20.00	0.64	0.73	53.02	46.51	0.89	1.02
30.00	0.58	0.66	58.47	51.29	0.81	0.92

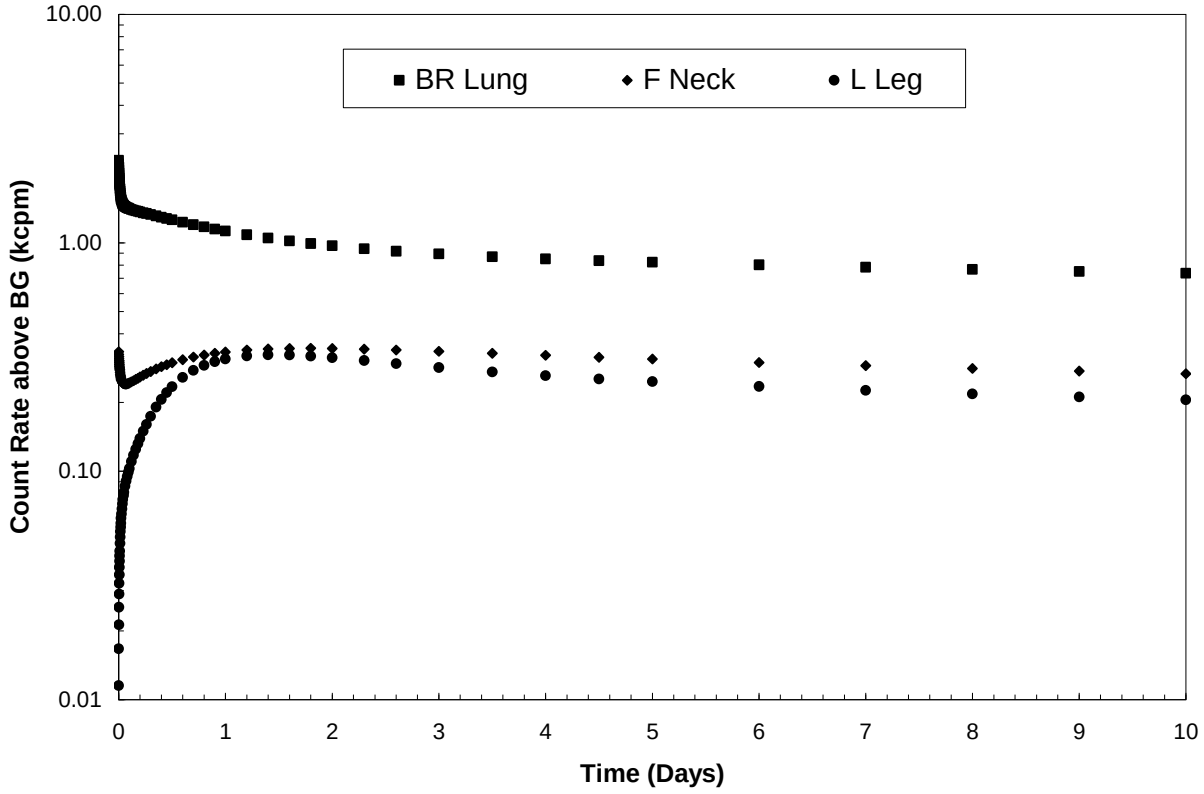

Adipose Female – Cs-137

Cs-137 F	Total Count Rate above BG (kcpm)		MDA (µCi)		Background Limit (kcpm)	
Time (days)	Ludlum 2	Ludlum 3	Ludlum 2	Ludlum 3	Ludlum 2	Ludlum 3
0.00	1.09	1.24	67.46	59.17	1.53	1.74
0.25	1.11	1.26	66.42	58.26	1.55	1.77
0.50	1.31	1.49	56.27	49.36	1.83	2.09
1.00	1.42	1.61	51.99	45.61	1.98	2.26
2.00	1.36	1.56	53.98	47.35	1.91	2.18
3.00	1.31	1.49	56.28	49.37	1.83	2.09
4.00	1.27	1.45	57.82	50.72	1.78	2.03
5.00	1.25	1.43	58.91	51.67	1.75	2.00
6.00	1.23	1.41	59.75	52.41	1.73	1.97
7.00	1.22	1.39	60.45	53.02	1.71	1.94
8.00	1.21	1.38	61.05	53.56	1.69	1.93
9.00	1.20	1.36	61.60	54.03	1.67	1.91
10.00	1.19	1.35	62.10	54.47	1.66	1.89
20.00	1.11	1.26	66.46	58.30	1.55	1.77
30.00	1.04	1.19	70.84	62.14	1.46	1.66

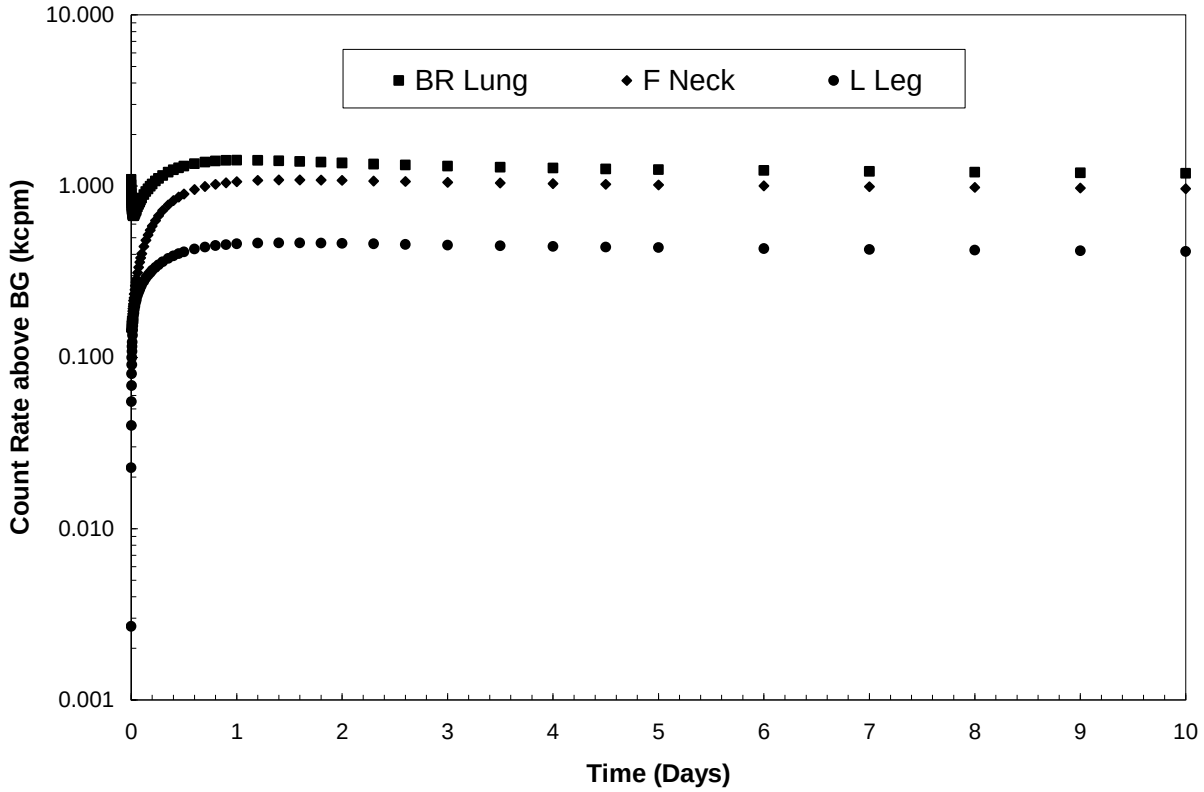

Adipose Female – I-131

I-131 F	Total Count Rate above BG (kcpm)		MDA (µCi)		Background Limit (kcpm)	
Time (days)	Ludlum 2	Ludlum 3	Ludlum 2	Ludlum 3	Ludlum 2	Ludlum 3
0.00	0.99	1.13	46.21	40.53	1.38	1.58
0.25	0.40	0.46	114.16	100.14	0.56	0.64
0.50	0.27	0.31	168.60	147.90	0.38	0.43
1.00	0.14	0.16	330.76	290.14	0.19	0.22
2.00	0.05	0.06	852.87	748.13	0.07	0.09
3.00	0.03	0.03	1512.58	1326.83	0.04	0.05
4.00	0.02	0.03	2019.87	1771.82	0.03	0.04
5.00	0.02	0.02	2291.55	2010.13	0.03	0.03
6.00	0.02	0.02	2433.23	2134.41	0.03	0.03
7.00	0.02	0.02	2532.96	2221.89	0.03	0.03
8.00	0.02	0.02	2629.69	2306.75	0.02	0.03
9.00	0.02	0.02	2737.80	2401.58	0.02	0.03
10.00	0.02	0.02	2862.22	2510.72	0.02	0.03
20.00	0.01	0.01	5318.78	4665.59	0.01	0.01
30.00	0.00	0.00	11628.01	10200.01	0.01	0.01

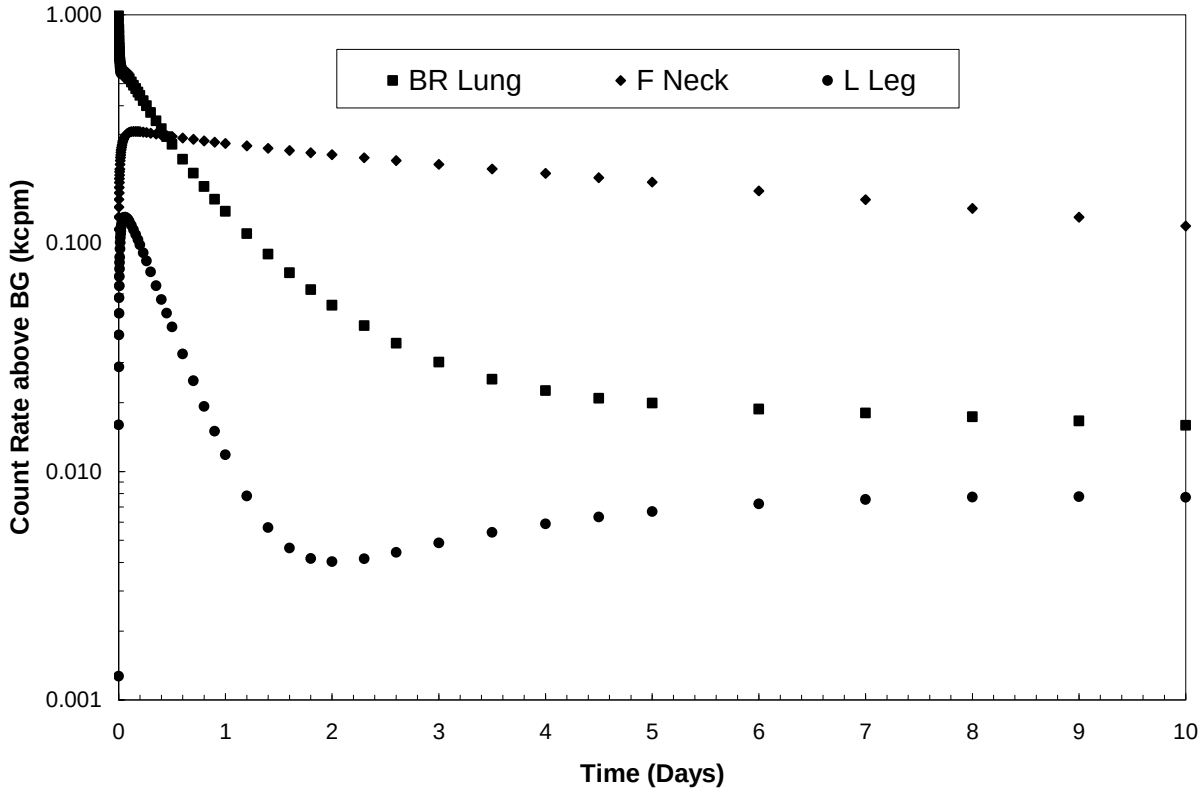

Adipose Female – Ir-192

Ir-192 M	Total Count Rate above BG (kcpm)		MDA (µCi)		Background Limit (kcpm)	
Time (days)	Ludlum 2	Ludlum 3	Ludlum 2	Ludlum 3	Ludlum 2	Ludlum 3
0.00	2.50	2.85	25.98	22.79	3.50	3.99
0.25	2.32	2.64	28.05	24.61	3.24	3.70
0.50	2.42	2.76	26.84	23.54	3.39	3.86
1.00	2.10	2.39	31.01	27.20	2.93	3.34
2.00	1.43	1.64	45.28	39.72	2.01	2.29
3.00	1.10	1.26	58.89	51.66	1.54	1.76
4.00	0.96	1.09	67.72	59.40	1.34	1.53
5.00	0.90	1.02	72.54	63.63	1.25	1.43
6.00	0.86	0.98	75.26	66.02	1.21	1.38
7.00	0.84	0.96	77.07	67.61	1.18	1.35
8.00	0.83	0.94	78.52	68.88	1.16	1.32
9.00	0.81	0.93	79.84	70.03	1.14	1.30
10.00	0.80	0.91	81.10	71.14	1.12	1.28
20.00	0.69	0.79	93.50	82.01	0.97	1.11
30.00	0.61	0.70	106.36	93.30	0.86	0.97

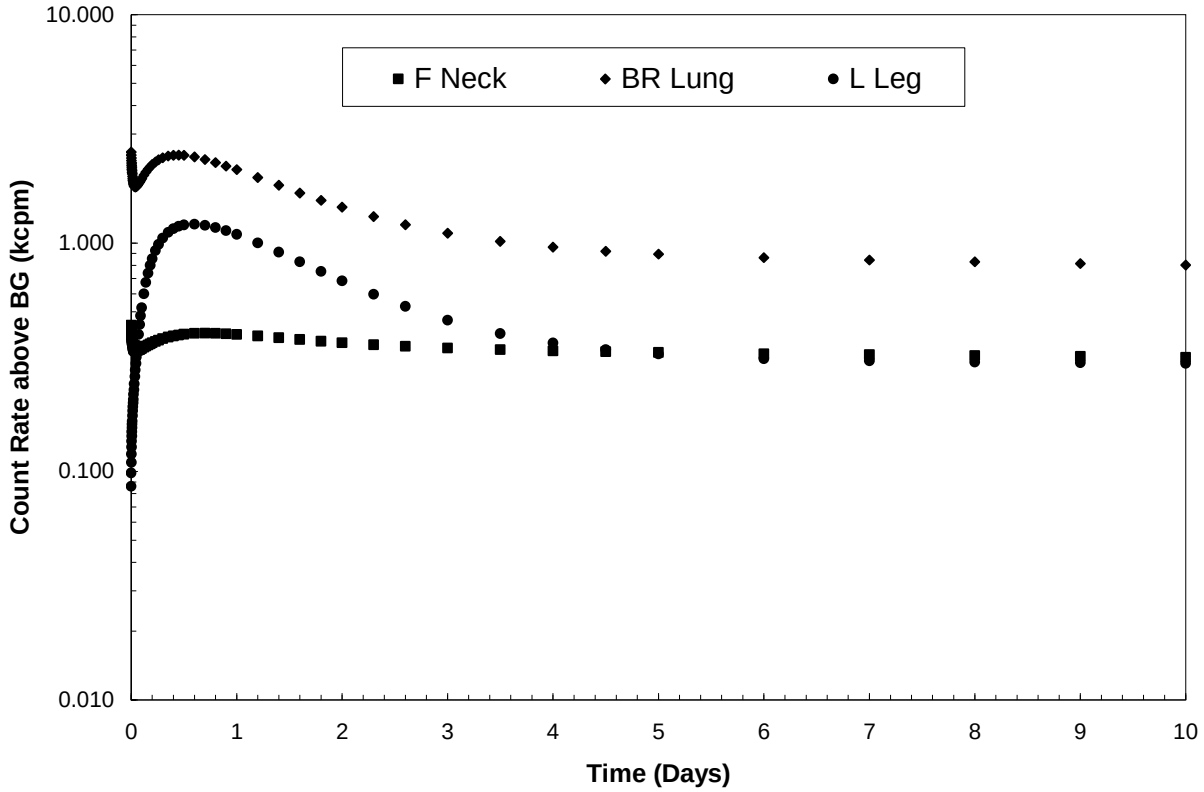

Post Menopausal Adipose Female – Co-60

Co-60 M	Total Count Rate above BG (kcpm)		MDA (µCi)		Background Limit (kcpm)	
Time (days)	Ludlum 2	Ludlum 3	Ludlum 2	Ludlum 3	Ludlum 2	Ludlum 3
0.00	2.29	2.61	14.74	12.93	3.21	3.66
0.25	1.34	1.53	25.14	22.05	1.88	2.15
0.50	1.26	1.43	26.87	23.57	1.76	2.01
1.00	1.12	1.27	30.28	26.57	1.56	1.78
2.00	0.96	1.09	35.35	31.01	1.34	1.53
3.00	0.88	1.00	38.45	33.73	1.23	1.40
4.00	0.84	0.95	40.42	35.46	1.17	1.33
5.00	0.81	0.92	41.83	36.69	1.13	1.29
6.00	0.79	0.90	42.98	37.70	1.10	1.25
7.00	0.77	0.88	43.99	38.59	1.08	1.23
8.00	0.75	0.86	44.94	39.42	1.05	1.20
9.00	0.74	0.84	45.84	40.21	1.03	1.18
10.00	0.72	0.82	46.71	40.97	1.01	1.15
20.00	0.63	0.71	53.93	47.30	0.88	1.00
30.00	0.57	0.65	59.50	52.20	0.79	0.91

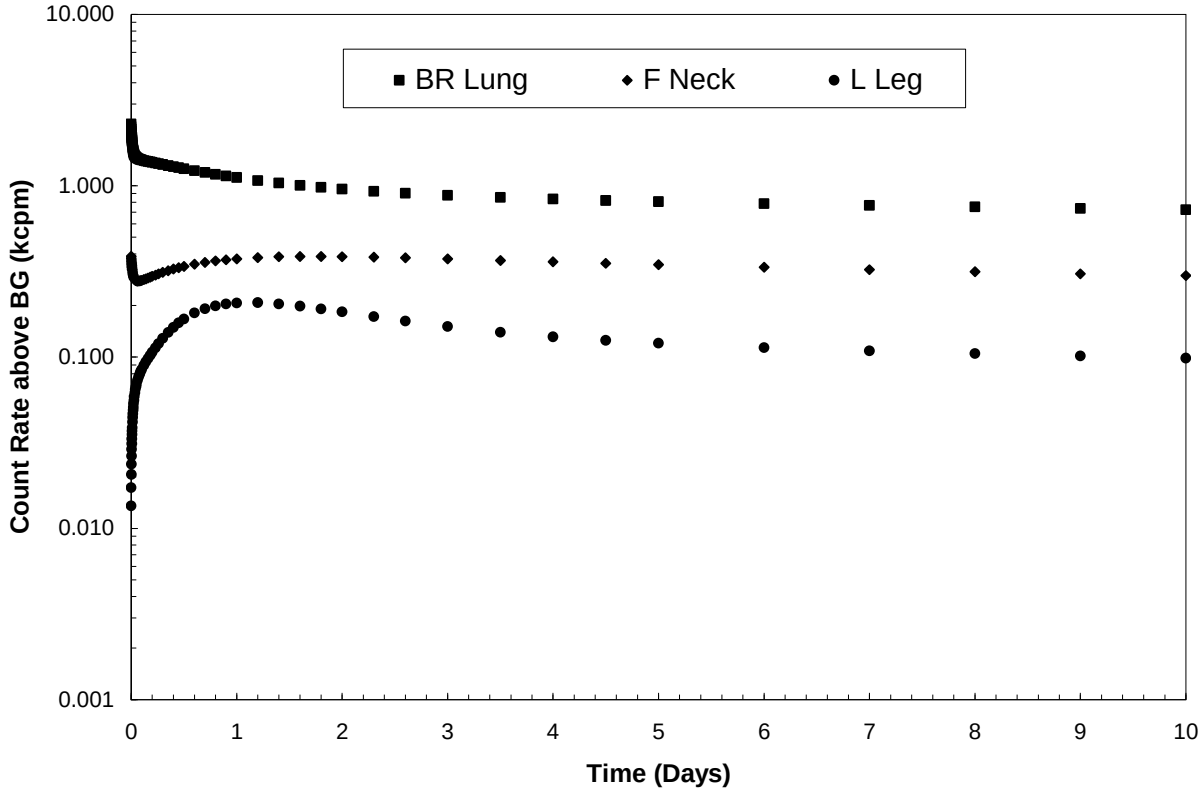

Post Menopausal Adipose Female – Cs-137

Cs-137 F	Total Count Rate above BG (kcpm)		MDA (µCi)		Background Limit (kcpm)	
Time (days)	Ludlum 2	Ludlum 3	Ludlum 2	Ludlum 3	Ludlum 2	Ludlum 3
0.00	1.13	1.29	64.90	56.93	1.59	1.81
0.25	1.27	1.45	58.10	50.97	1.77	2.02
0.50	1.53	1.75	48.11	42.20	2.14	2.44
1.00	1.68	1.92	43.72	38.35	2.36	2.69
2.00	1.64	1.87	44.97	39.45	2.29	2.61
3.00	1.58	1.80	46.75	41.01	2.21	2.51
4.00	1.54	1.75	47.98	42.08	2.15	2.45
5.00	1.51	1.72	48.85	42.85	2.11	2.41
6.00	1.49	1.69	49.54	43.46	2.08	2.37
7.00	1.47	1.68	50.11	43.96	2.06	2.35
8.00	1.46	1.66	50.61	44.39	2.04	2.32
9.00	1.44	1.64	51.06	44.79	2.02	2.30
10.00	1.43	1.63	51.47	45.15	2.00	2.28
20.00	1.34	1.52	55.08	48.32	1.87	2.13
30.00	1.25	1.43	58.71	51.50	1.76	2.00

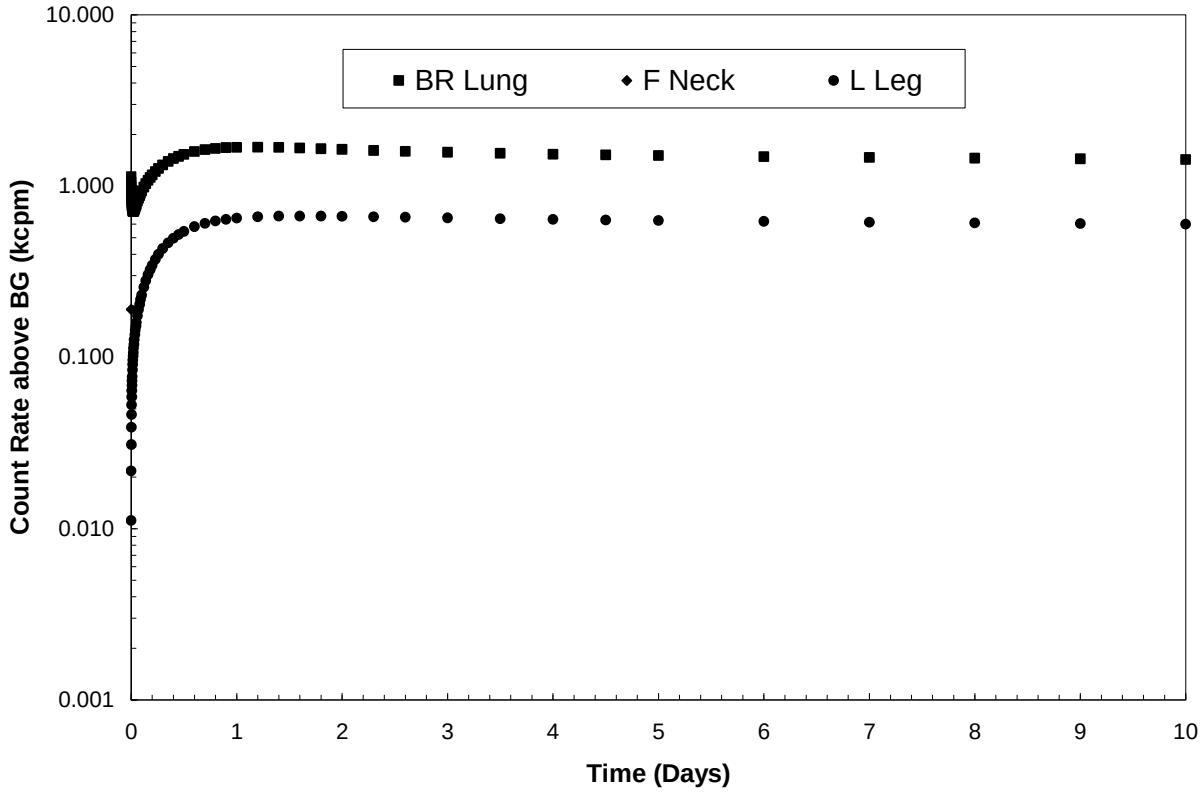

Post Menopausal Adipose Female – I-131

I-131 F	Total Count Rate above BG (kcpm)		MDA (µCi)		Background Limit (kcpm)	
Time (days)	Ludlum 2	Ludlum 3	Ludlum 2	Ludlum 3	Ludlum 2	Ludlum 3
0.00	0.97	1.11	46.98	41.21	1.36	1.55
0.25	0.38	0.43	121.02	106.16	0.53	0.60
0.50	0.25	0.29	182.14	159.77	0.35	0.40
1.00	0.12	0.14	377.26	330.93	0.17	0.19
2.00	0.04	0.05	1152.57	1011.03	0.06	0.06
3.00	0.02	0.02	2515.40	2206.49	0.03	0.03
4.00	0.01	0.01	3799.19	3332.63	0.02	0.02
5.00	0.01	0.01	4329.17	3797.52	0.01	0.02
6.00	0.01	0.01	4376.85	3839.35	0.01	0.02
7.00	0.01	0.01	4303.49	3774.99	0.01	0.02
8.00	0.01	0.01	4245.19	3723.85	0.02	0.02
9.00	0.01	0.01	4233.29	3713.41	0.02	0.02
10.00	0.01	0.01	4269.16	3744.88	0.01	0.02
20.00	0.01	0.01	6676.19	5856.31	0.01	0.01
30.00	0.00	0.00	13781.36	12088.91	0.00	0.01

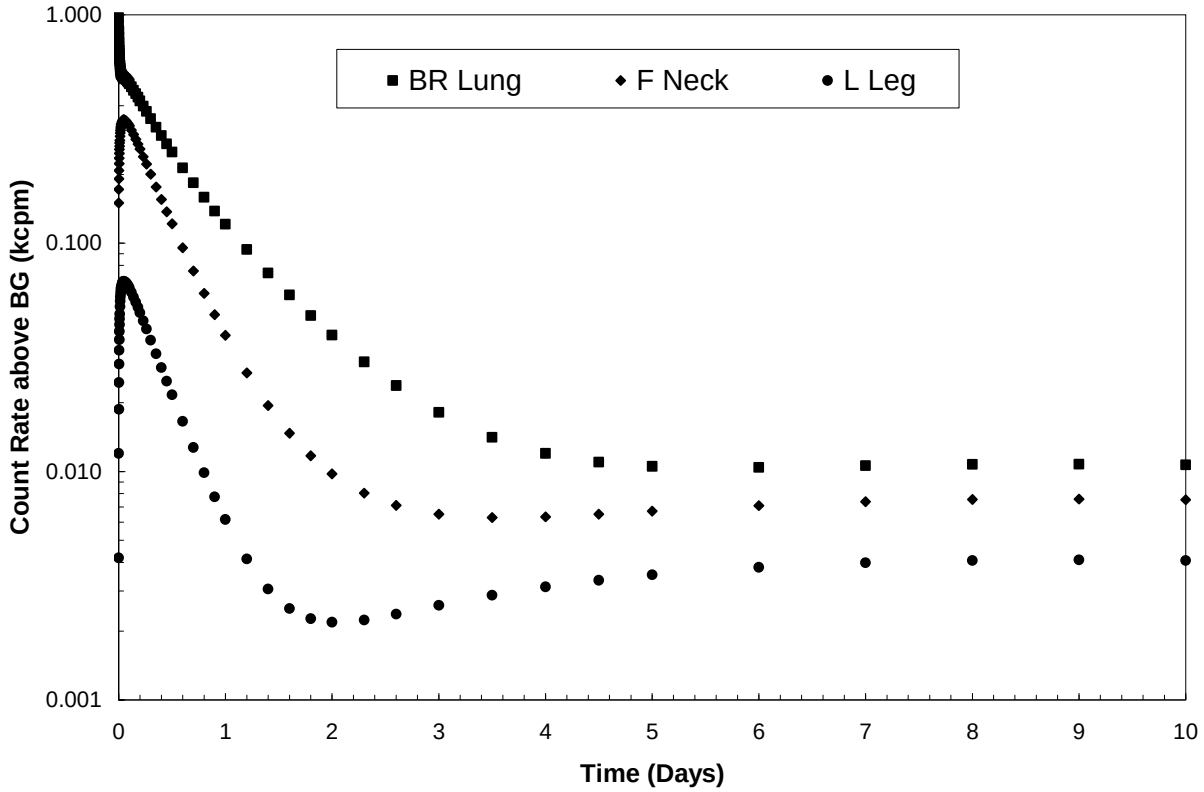

Post Menopausal Adipose Female – Ir-192

Ir-192 M	Total Count Rate above BG (kcpm)		MDA (µCi)		Background Limit (kcpm)	
Time (days)	Ludlum 2	Ludlum 3	Ludlum 2	Ludlum 3	Ludlum 2	Ludlum 3
0.00	2.69	3.06	24.18	21.21	3.76	4.29
0.25	1.52	1.74	42.61	37.38	2.13	2.43
0.50	1.41	1.61	45.98	40.33	1.98	2.26
1.00	1.23	1.40	53.02	46.51	1.72	1.96
2.00	1.01	1.15	64.26	56.37	1.42	1.61
3.00	0.92	1.05	70.70	62.02	1.29	1.47
4.00	0.88	1.00	74.21	65.10	1.23	1.40
5.00	0.85	0.97	76.40	67.02	1.19	1.36
6.00	0.83	0.95	78.06	68.47	1.17	1.33
7.00	0.82	0.93	79.51	69.75	1.14	1.30
8.00	0.80	0.92	80.89	70.95	1.12	1.28
9.00	0.79	0.90	82.24	72.14	1.11	1.26
10.00	0.78	0.89	83.58	73.32	1.09	1.24
20.00	0.67	0.76	97.21	85.27	0.94	1.07
30.00	0.58	0.66	111.59	97.88	0.82	0.93

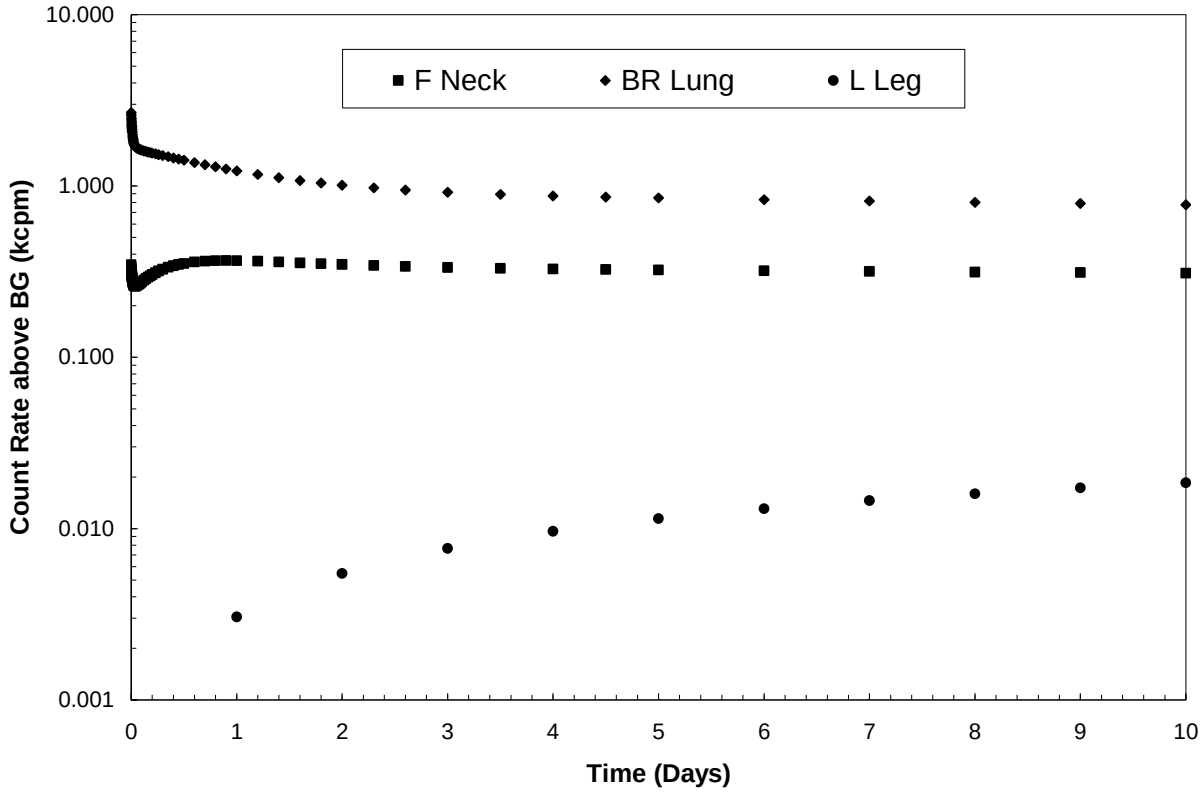

10-year-old Child – Co-60

Co-60 M	Total Count Rate above BG (kcpm)		MDA (µCi)		Background Limit (kcpm)	
Time (days)	Ludlum 2	Ludlum 3	Ludlum 2	Ludlum 3	Ludlum 2	Ludlum 3
0.00	4.32	4.92	7.82	6.86	6.05	6.89
0.25	2.56	2.92	13.18	11.56	3.59	4.09
0.50	2.41	2.75	14.00	12.28	3.38	3.85
1.00	2.17	2.47	15.60	13.69	3.03	3.46
2.00	1.87	2.14	18.03	15.82	2.62	2.99
3.00	1.73	1.97	19.57	17.17	2.42	2.76
4.00	1.64	1.87	20.57	18.04	2.30	2.62
5.00	1.59	1.81	21.29	18.68	2.22	2.53
6.00	1.54	1.76	21.89	19.20	2.16	2.46
7.00	1.51	1.72	22.42	19.67	2.11	2.41
8.00	1.47	1.68	22.91	20.10	2.06	2.35
9.00	1.44	1.65	23.38	20.51	2.02	2.31
10.00	1.42	1.62	23.83	20.91	1.98	2.26
20.00	1.23	1.40	27.54	24.16	1.72	1.96
30.00	1.11	1.27	30.34	26.62	1.56	1.78

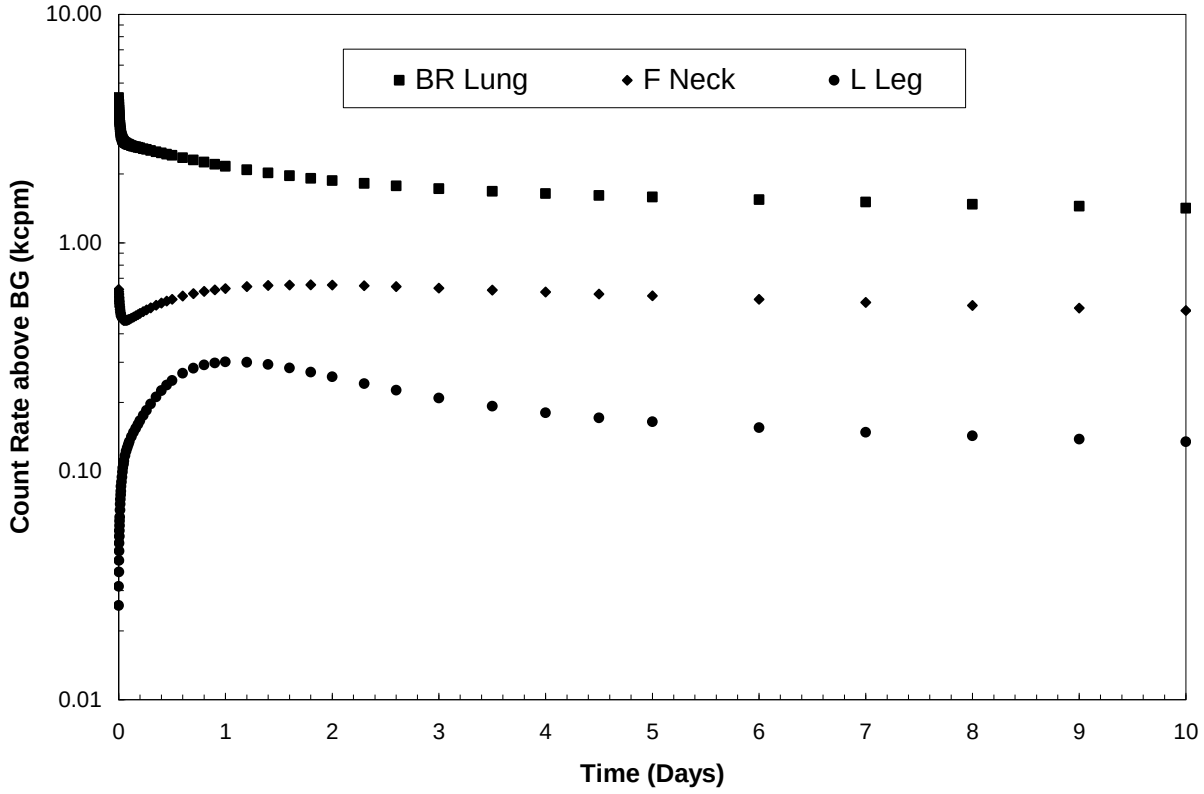

10-year-old Child – Cs-137

Cs-137 F	Total Count Rate above BG (kcpm)		MDA (µCi)		Background Limit (kcpm)	
Time (days)	Ludlum 2	Ludlum 3	Ludlum 2	Ludlum 3	Ludlum 2	Ludlum 3
0.00	2.07	2.36	35.52	31.16	2.89	3.30
0.25	2.25	2.56	32.68	28.67	3.15	3.59
0.50	2.66	3.04	27.57	24.18	3.73	4.25
1.00	2.90	3.30	25.36	22.25	4.05	4.62
2.00	2.80	3.19	26.23	23.01	3.92	4.47
3.00	2.69	3.07	27.31	23.95	3.77	4.29
4.00	2.62	2.99	28.04	24.59	3.67	4.18
5.00	2.57	2.93	28.55	25.05	3.60	4.10
6.00	2.54	2.89	28.96	25.40	3.55	4.05
7.00	2.51	2.86	29.29	25.69	3.51	4.00
8.00	2.48	2.83	29.58	25.95	3.48	3.96
9.00	2.46	2.81	29.85	26.18	3.45	3.93
10.00	2.44	2.78	30.09	26.39	3.42	3.90
20.00	2.28	2.60	32.20	28.24	3.19	3.64
30.00	2.14	2.44	34.32	30.10	3.00	3.42

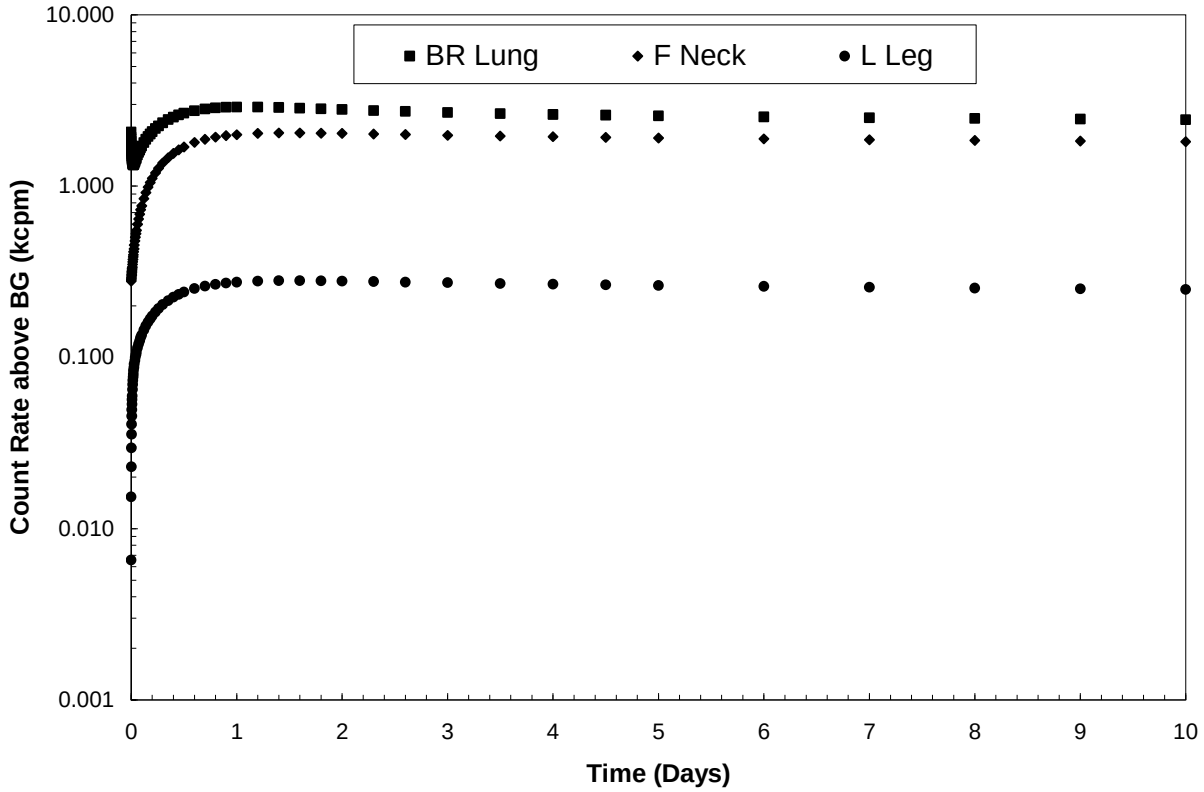

10-year-old Child – I-131

I-131 F	Total Count Rate above BG (kcpm)		MDA (µCi)		Background Limit (kcpm)	
Time (days)	Ludlum 2	Ludlum 3	Ludlum 2	Ludlum 3	Ludlum 2	Ludlum 3
0.00	1.87	2.13	24.43	21.43	2.62	2.98
0.25	0.78	0.89	58.23	51.08	1.10	1.25
0.50	0.53	0.61	86.01	75.44	0.74	0.85
1.00	0.27	0.31	167.42	146.86	0.38	0.44
2.00	0.11	0.13	413.33	362.57	0.15	0.18
3.00	0.07	0.07	694.08	608.84	0.09	0.10
4.00	0.05	0.06	894.95	785.04	0.07	0.08
5.00	0.05	0.05	1003.04	879.86	0.06	0.07
6.00	0.04	0.05	1064.44	933.72	0.06	0.07
7.00	0.04	0.05	1111.78	975.25	0.06	0.07
8.00	0.04	0.04	1159.08	1016.74	0.06	0.06
9.00	0.04	0.04	1211.60	1062.81	0.05	0.06
10.00	0.04	0.04	1271.27	1115.15	0.05	0.06
20.00	0.02	0.02	2409.84	2113.89	0.03	0.03
30.00	0.01	0.01	5308.29	4656.39	0.01	0.01

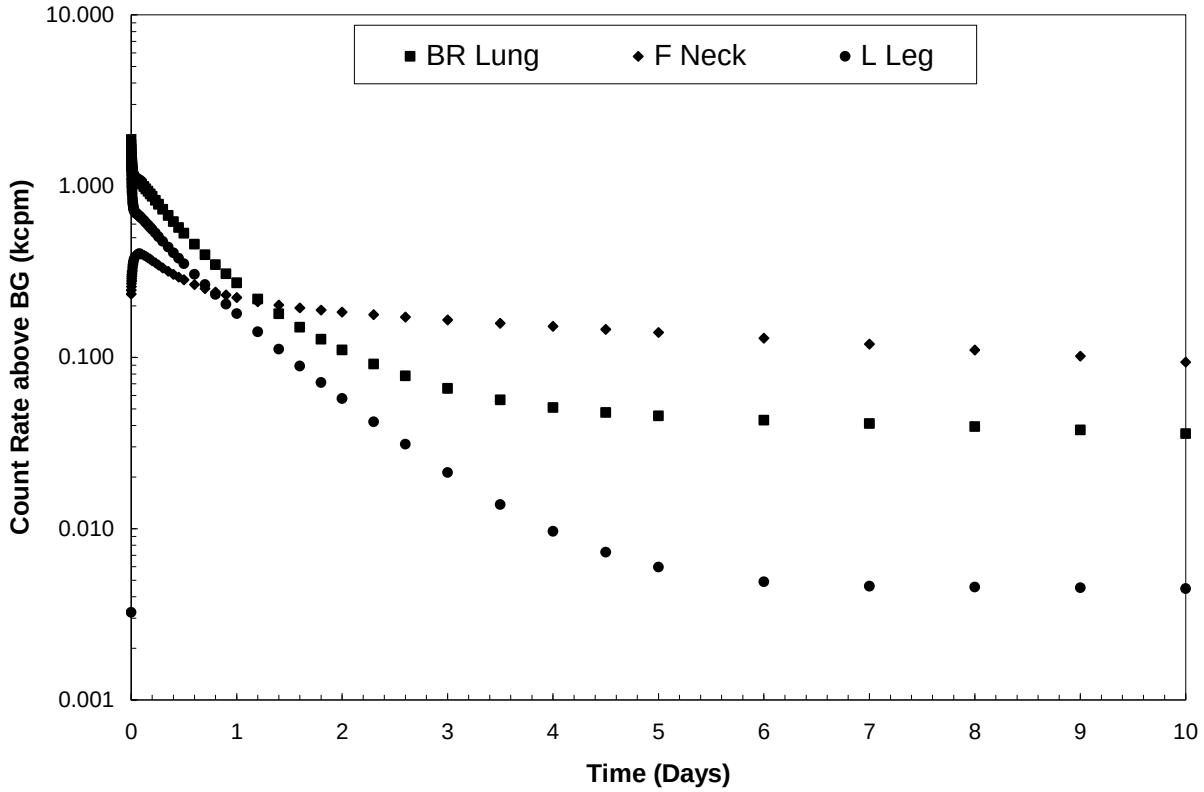

10-year-old Child – Ir-192

Ir-192 M	Total Count Rate above BG (kcpm)		MDA (µCi)		Background Limit (kcpm)	
Time (days)	Ludlum 2	Ludlum 3	Ludlum 2	Ludlum 3	Ludlum 2	Ludlum 3
0.00	5.43	6.18	11.98	10.50	7.60	8.66
0.25	3.12	3.56	20.81	18.26	4.37	4.98
0.50	2.91	3.32	22.31	19.57	4.08	4.65
1.00	2.54	2.90	25.54	22.40	3.56	4.06
2.00	2.11	2.40	30.80	27.02	2.95	3.37
3.00	1.92	2.19	33.84	29.68	2.69	3.06
4.00	1.83	2.09	35.49	31.13	2.56	2.92
5.00	1.78	2.03	36.52	32.03	2.49	2.84
6.00	1.74	1.99	37.29	32.71	2.44	2.78
7.00	1.71	1.95	37.97	33.30	2.40	2.73
8.00	1.68	1.92	38.61	33.86	2.36	2.69
9.00	1.66	1.89	39.23	34.41	2.32	2.64
10.00	1.63	1.86	39.85	34.96	2.28	2.60
20.00	1.41	1.61	46.12	40.46	1.97	2.25
30.00	1.23	1.41	52.69	46.22	1.73	1.97

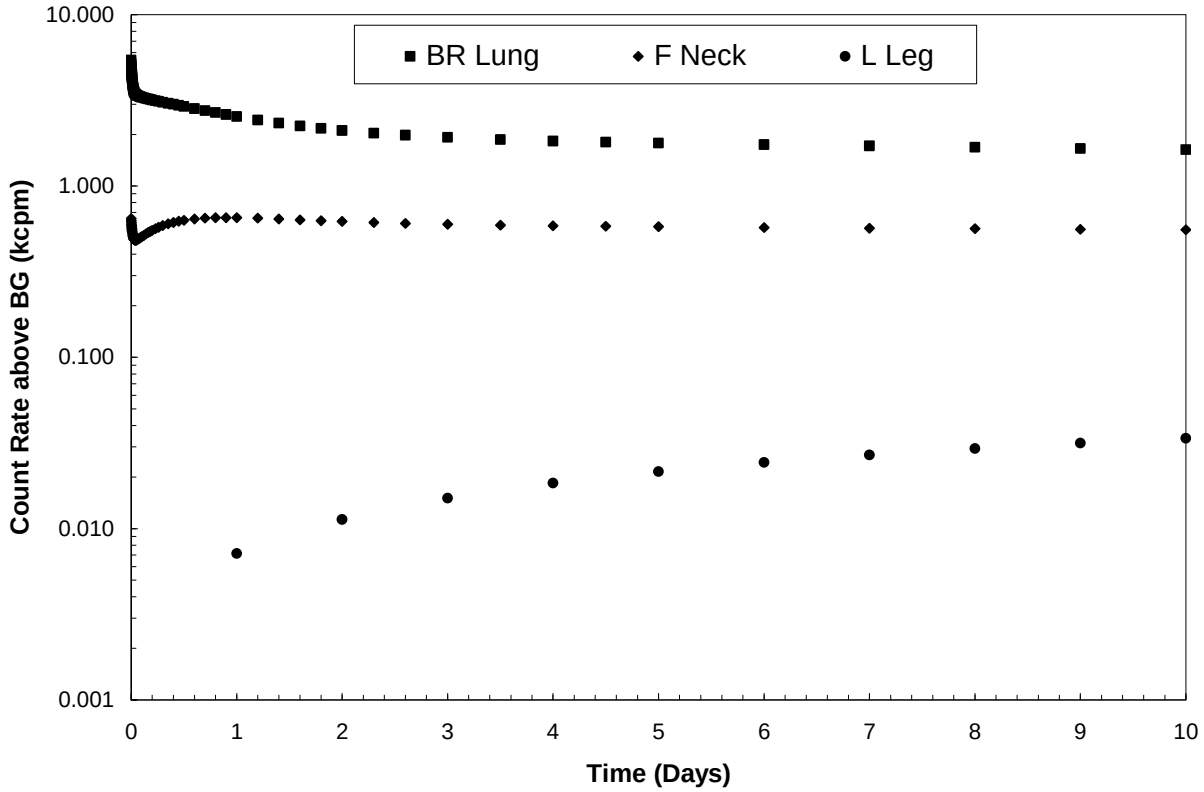

APPENDIX D: TRIAGE PROCEDURE SHEET FOR FIRST RESPONDERS

Ludlum Model 3 Survey Meter (Male)

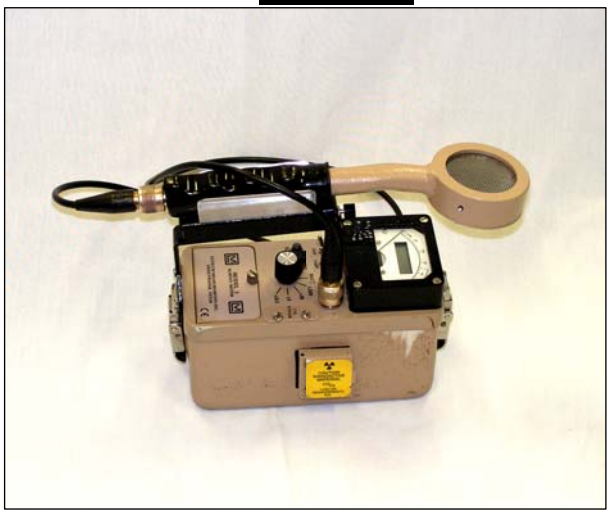

Basic Operation

How to operate:

- Rotate the center dial from the OFF position to BAT.
- Ensure the needle moves to the right to show that the battery is working.
- Turn the dial to the proper scale (start at ×0.1)
- Set the detector to Slow (S) Mode
- Remove the probe from the holder, wrap the probe in plastic wrap and place the wire mesh side against object of interest.
- Press RESET and wait until the needle settles on a value to determine the output
- NOTE: If the needle slides to the far right of the scale, turn the dial up a scale (e.g. ×0.1 to ×1) and press RESET and repeat if necessary.

Background Levels

How to determine background:

- Turn the dial to ×0.1, put in Slow (S) Mode, and keep the pancake probe in its holder.
- Set the probe away from the object to be measured as well as anything radioactive or suspected to be radioactive.
- Press RESET, wait until the needle settles at a particular value, and record that datum
- Repeat the process 4 times and average the 5 numbers to determine background.

Warning Levels

Notes about the table:

- All values in the table are above background. Ex: If table says 1200 cpm and background is 700 cpm, then detector should read 1900 cpm.
- Values less than 40 CPM can be considered undetectable.
- All values are in cpm (counts per minute)

Ludlum Model 3 Survey Meter (Male)

Screening Levels

Time (days)	Co-60 (cpm)	Cs-137 (cpm)	I-131 (cpm)	Ir-192 (cpm)
0.00	1100	1700	5700	4200
0.25	640	1400	1700	2400
0.50	570	1600	1200	2200
1.00	470	1600	640	1900
2.00	370	1500	210	1500
3.00	330	1500	70	1400
4.00	310	1400	30	1300
5.00	300	1400	10	1200
6.00	300	1400	10	1200
7.00	300	1400	10	1200
10.00	290	1300	10	1100

APPENDIX E: CONDENSED TRIAGE PROCEDURE SHEET

G-M Survey Meter

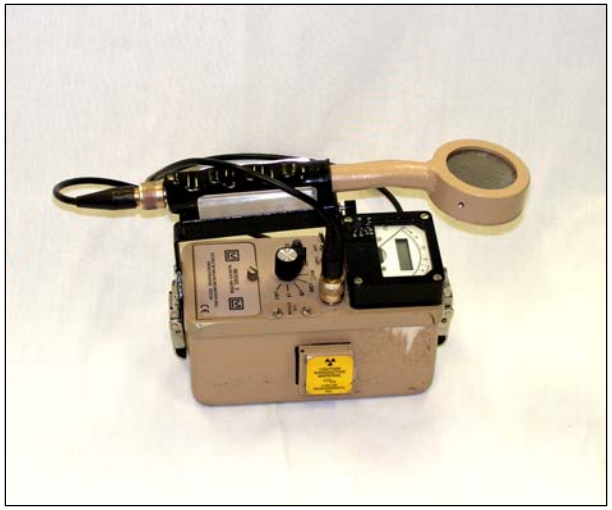

Basic Operation

How to operate:

- Rotate the center dial from the OFF position to BAT.
- Ensure the needle moves to the right to show that the battery is working.
- Turn the dial to the proper scale (start at ×0.1)
- Set the detector to Slow (S) Mode
- Remove the probe from the holder, wrap the probe in plastic wrap and place the wire mesh side against object of interest.
- Press RESET and wait until the needle settles on a value to determine the output
- NOTE: If the needle slides to the far right of the scale, turn the dial up a scale (e.g. ×0.1 to ×1) and press RESET and repeat if necessary.

Background Levels

How to determine background:

- Turn the dial to ×0.1, put in Slow (S) Mode, and keep the pancake probe in its holder.
- Set the probe away from the object to be measured as well as anything radioactive or suspected to be radioactive.
- Press RESET, wait until the needle settles at a particular value, and record that datum
- Repeat the process 4 times and average the 5 numbers to determine background.

Warning Levels

Notes about the table:

- All values in the table are above background. Ex: If table says 1200 cpm and background is 700 cpm, then detector should read 1900 cpm.
- Values less than 40 CPM can be considered undetectable.
- All values are in cpm (counts per minute)

G-M Survey Meter

ADULT

Time (days)	Co-60 (cpm)	Cs-137 (cpm)	I-131 (cpm)	Ir-192 (cpm)
0.00	660	970	870	2400
0.25	371	980	350	1300
0.50	330	1100	240	1200
1.00	270	1200	120	1100
2.00	210	1100	40	910
3.00	190	1100	20	830
4.00	180	1100	10	790
5.00	180	1000	10	770
6.00	170	1000	10	750
7.00	170	1000	10	740
10.00	170	1000	10	700

CHILD

Time (days)	Co-60 (cpm)	Cs-137 (cpm)	I-131 (cpm)	Ir-192 (cpm)
0.00	1300	2000	1800	5400
0.25	770	2200	780	3100
0.50	690	2600	530	2900
1.00	570	2900	270	2500
2.00	450	2800	110	2100
3.00	400	2600	70	1900
4.00	380	2600	50	1800
5.00	370	2500	50	1700
6.00	370	2500	40	1700
7.00	360	2500	40	1700
10.00	350	2400	40	1600

REFERENCES

1. Anigstein, R., et al. 2007. "Use of Radiation Detection, Measuring, and Imaging Instruments to Assess Internal Contamination from Inhaled Radionuclides. Part II: Field Tests and Monte Carlo Simulations Using Anthropomorphic Phantoms." http://emergency.cdc.gov/radiation/clinicians/evaluation/pdf/Part_II.pdf. Accessed May 2008.

2. Ansari, Armin. Discussion during a meeting on handheld detector project. 10 Mar. 2008.

3. Attix, F.H. (1986) Introduction to Radiological Physics and Radiation Dosimetry. (John Wiley and Sons, New York).

4. Berger, M.J., et al. 2005. ESTAR, PSTAR, and ASTAR: Computer Programs for Calculating Stopping-Power and Range Tables for Electrons, Protons, and Helium Ions (version 1.2.3). Available: http://physics.nist.gov/Star. Accessed May 2008.

5. Coursey, J.S., D.J. Schwab, and R.A. Dragoset. 2001. Atomic Weights and Isotopic Compositions (version 2.31), National Institute of Standards and Technology, Gaithersburg, MD. January 31, 2003 http://physics.nist.gov/Comp. Accessed May 2008.

6. Currie, L. A. Anal. Chem. 40 (3), 586 (1968).

7. DOE/NRC Interagency Working Group on Radiological Dispersal Devices. Radiological Dispersal Devices: An Initial Study To Identify Radioactive Materials of Greatest Concern And Approaches To Their Tracking, Tagging, And Disposition. Report to the Nuclear Regulatory Commission and the Secretary of Energy, May 2003.

8. Eckerman, K.F., Cristy, M., Ryman, J.C., The ORNL Mathematical Phantom Series, Oak Ridge National Laboratory, http://homer.hsr.gov/VLab/VLabPhan.html. (1996)

9. Eckerman, K.F., Sjoreen, A.L., Radiological Toolbox. ORNL/TM-2004/27R1.

10. Eckerman, K.F., et al, Dose and Risk Calculation Software. ORML/TM-2001/190.

11. Ferguson, C.D., et al., 2003, *Commercial Radioactive Sources: Surveying the Security Risks,* Occasional Paper No.11, Center for Nonproliferation Studies, Monterey Institute of International Studies, Monterey, CA, Jan.

12. GAO (U.S. Government Accountability Office), 2003a, DOE Action Needed to Ensure Continued Recovery of Unwanted Sealed Radioactive Sources, GAO-03-483, report to the Ranking Minority Member, Subcommittee on Financial Management, the Budget,

and International Security, Committee on Governmental Affairs, U.S. Senate, Apr. Available at http://www.gao.gov/highlights/d03483high.pdf. Accessed May. 2008.

13. GAO, 2003b, U.S. and International Assistance Efforts to Control Sealed Radioactive Sources Need Strengthening, GAO-03-638, report to the Ranking Minority Member, Subcommittee on Financial Management, the Budget, and International Security, Committee on Governmental Affairs, U.S. Senate, May. Available at http://www.gao.gov/highlights/d03638high.pdf. Accessed May 2008.

14. Harper, FT; Musolino, SV; Wente, WB. Realistic radiological dispersal device hazard boundaries and ramifications for early consequence management decisions. Health Phys. 2007 July;93(1):1-16.

15. International Commission on Radiological Protection (ICRP). (1994). Human Respiratory Tract Model for Radiological Protection. ICRP Publication 66, Pergamon Press, Oxford.

16. International Commission on Radiological Protection (ICRP) (1996) 91 Age-dependent dose to members of the public from intake of radionuclides: Part 5 compilation of ingestion and inhalation dose coefficients. Annals of the ICRP, Volume 26, Issue 1

17. International Commission on Radiological Protection (ICRP) (2002) Basic Anatomical and Physiological Data for Use in Radiological Protection: Reference Values. ICRP Publication 89. International Commission on Radiological Protection, Pergamon Press, New York.

18. Knoll, G.F. (2000). Radiation Detection and Measurement, Third Edition. (John Wiley and Sons, New York).

19. Kramer, Gary H.; Barry M. Hauck. Fundamental Uncertainties in Lung Counting, Health Physics. The Radiation Safety Journal. 93(4):318-324, October 2007.

20. Kramer, Gary H.; Kevin Capello. Effect of lung volume on counting efficiency: A Monte Carlo Investigation., Health Physics. 88(4):357-363, April 2005.

21. Kramer, Gary H; Kevin Capello; Barry M. Hauck. Evaluation of Two Commercially Available Portal Monitors for Emergency Response, Health Physics. Operational Radiation Safety. 92(2) Supplement 1: S50-S56, February 2007.

22. Kramer, Gary H.; Kevin Capello; Barry M. Hauck. The HML's New Field Deployable, High resolution Whole Body Counter

23. Kramer, Gary H.; Kevin Capello; Barry M. Hauck; Jason T. Brown. Sensitivity of Portable Personnel Portal Monitors: Potential Problems when Dealing with Contaminated Persons, Health Physics. 91(4):367-372, October 2006.

24. Kramer, Gary H.; Paul Crowley; Linda C. Burns. The Uncertainty in the Activity Estimate from a Lung Count Due to the Variability in Chest Wall Thickness Profile, Health Physics. 78(6):739-743, June 2000.

25. LND, Inc., "7311 Pancake Mica Window Alpha-Beta-Gamma Detector Specification Sheet," Oceanside, NY.

26. Lorio, R. A. Feasibility of Determining Radioactivity in Lungs Using A Thyroid Uptake Counter: A Thesis Presented to the Faculty. Georgia Institute of Technology (2005).

27. Ludlum Measurements Inc., "Model 44-9 Alpha, Beta, Gamma Detector Manual," Serial Number PR090405, Sweetwater, TX, August 2004.

28. MCNP A General Monte Carlo N-Particle Transport Code Version 5, Volumes I, II, and III: User's Guide. LA-CP-03-0245. LANL x-5 Monte Carlo Team, April 2003.

29. NIST Standard Reference Materials. http://nist.gov/srm. Accessed May 2008.

30. Office of Biological and Environmental Research (BER), Office of Science, U.S. Department of Energy. http://www.science.doe.gov/ober Accessed May 2008.

31. Oliveira, C., Lourenco, M., Dantas, B., Lucena, E., Design and Operation of a Whole-body Monitoring System for the Goiania Radiation Accident. Health Physics. 60(1):51-55, January 1991.

32. Radiation Event Medical Management. Radiological Dispersal Devices (RDDs), U.S. Department of Health and Human Services, Mar. 2008. Available at http://www.remm.nlm.gov/rdd.htm#top. Accessed May. 2008.

33. Scarboro, S. B. The Use of a Thyroid Uptake System for Assaying Internal Contamination Following a Radioactive Dispersal Event. A Thesis Presented to the Faculty. Georgia Institute of Technology, May 2008.

34. Sohier, A., Hardeman, F. (2006) Radiological Dispersion Devices: are we prepared? Journal of Environmental Radioactivity 85 pp 171-181.

35. Turner, J.E. (1995). Atoms, Radiation, and Radiation Protection, Second Edition. (John Wiley and Sons, New York).

36. Van Riper, K. A. 2004. "BodyBuilder: A Product of White Rock Science." http://www.whiterockscience.com/bodybuilder/oakridge.html. Accessed May 2008.

37. Visual Editor Consultants (2005). VisEd Version 19k. http://www. mcnpvised.com.

38. White Rock Science (2004). Bodybuilder, http://www.whiterockscience.com/bodybuilder/bodybuilder.html.

39. X-5 Monte Carlo Team. MCNP A General Monte Carlo N-Particle Transport Code, Version 5. Los Alamos, NM: Los Alamos National Laboratory; LA-UR-03-1987; 2003.